

---

# Demonstrating the Capabilities of UAS Topobathymetric Sonar Mapping in Support of DOT Project Planning, Monitoring and Modeling



**NCDOT Project 2024-32**  
**FHWA/NC/2024-32**  
**April 2025**

---

Narcisa G. Pricope, PhD  
Md Salman Bashit, MSc  
Department of Geosciences  
Mississippi State University



**RESEARCH &  
DEVELOPMENT**

Title Page for RP2024-32

# Demonstrating the Capabilities of UAS Topobathymetric Sonar Mapping in Support of DOT Project Planning, Monitoring and Modeling

## FINAL REPORT

Submitted to:  
North Carolina Department of Transportation  
Office of Research  
(Research Project No. RP2024-32)

Submitted by:  
Narcisa G. Pricope, Ph.D., and Md Salman Bashit, M.Sc. (Mississippi State University)  
Ok-Youn Yu and Song Shu (Appalachian State University)

Lead Organization: Department of Geosciences & Office of Research and Economic  
Development

Mississippi State University  
75 B. S. Hood Rd, Mississippi State, MS 39762

1. Report No. <b>FHWA/NC/2024-32</b>	2. Government Accession No.	3. Recipient's Catalog No.	
4. Title and Subtitle <b>Demonstrating the Capabilities of UAS Topobathymetric Sonar Mapping in Support of DOT Project Planning, Monitoring and Modeling</b>		5. Report Date <b>April 1 2025</b>	
		6. Performing Organization Code	
7. Author(s) <b>Narcisa G. Pricope, PhD Md Salman Bashit, MSc</b>		8. Performing Organization Report No.	
9. Performing Organization Name and Address <b>Mississippi State University 75 B. S. Hood Rd, Mississippi State, MS 39762</b>		10. Work Unit No. (TRAIS)	
		11. Contract or Grant No.	
12. Sponsoring Agency Name and Address <b>NC Department of Transportation Research and Development Unit 1549 Mail Service Center Raleigh, NC 27699-1549</b>		13. Type of Report and Period Covered <b>Final Report January 1 2024 – March 31 2025</b>	
		14. Sponsoring Agency Code <b>RP2024-32</b>	
Supplementary Notes: All raw and processed data produced by Mississippi State University is available for download here at this <a href="#">OneDrive Link</a> . <p>This collaborative project between Mississippi State University and Appalachian State University evaluated the performance, feasibility, and accuracy of advanced bathymetric surveying technologies across diverse aquatic environments in the southeastern United States. Motivated by the limitations of traditional topographic LiDAR in water-covered or inundated zones, the project focused on integrating unmanned aerial systems (UAS) with sonar-based and optical survey methods to improve underwater terrain mapping for planning, monitoring, and inspection applications.</p> <p>Mississippi State University led efforts to test UAS-echo sounder systems across a gradient of waterbody types in Mississippi, including catfish ponds, lakes, rivers, irrigation reservoirs, and coastal bays. Field campaigns demonstrated that UAS-mounted sonar provides reliable and high-resolution bathymetric data in both turbid and clear water conditions, with an RMSE as low as 6.6 cm and <math>R^2</math> values up to 86.6% when benchmarked against LiDAR and GNSS reference datasets. Multiple interpolation methods were assessed, with Topo to Raster and Universal Kriging identified as top performers. The study emphasized the operational value of UAS-echo sounders in supporting flood modeling, sediment monitoring, drainage assessments, and infrastructure inspections.</p> <p>Appalachian State University conducted complementary surveys at three North Carolina sites—Wards Mill reach of the Watauga River, Rhodhiss Lake, and Price Lake—to assess post-dam removal changes, evaluate method performance in various hydrological settings, and compare Structure-from-Motion (SfM) photogrammetry to sonar-based approaches. SfM achieved high accuracy in shallow, clear waters (RMSE ~0.1 m), while sonar methods proved superior in deeper, turbid environments, though at higher cost. The integration of both technologies at Price Lake delivered comprehensive depth coverage and demonstrated the benefits of hybrid survey designs.</p> <p>Together, these efforts offer a replicable, cost-effective framework for high-resolution bathymetric mapping in inland and nearshore environments. The project advances the use of UAS-borne sonar and photogrammetry as complementary tools tailored to site-specific water clarity, depth, and operational constraints. Recommendations support hybrid workflows to optimize data accuracy, inform infrastructure planning, and enable responsive water resource management across dynamic and sensitive aquatic systems.</p>			
17. Key Words Unmanned Aerial Systems, UAS-borne sonar technology		18. Distribution Statement	
19. Security Classif. (of this report) Unclassified	20. Security Classif. (of this page) Unclassified	21. No. of Pages 113	22. Price

## DISCLAIMER

The contents of this report reflect the views of the author(s) and not necessarily the views of the University. The author(s) are responsible for the facts and the accuracy of the data presented herein. The contents do not necessarily reflect the official views or policies of either the North Carolina Department of Transportation or the Federal Highway Administration at the time of publication. This report does not constitute a standard, specification, or regulation.



## Acknowledgments

We are deeply grateful to our NCDOT collaborators, especially John Kirby and Timothy Albrecht for their ongoing -going support. We are also deeply grateful to the entire team at Mississippi State University that made this project possible: Dr. Adam Skarke and Dr. Volkan Senyurek for their support throughout, as well as Daniel McCraine and Sean Carpenter at the Geosystems Research Institute (GRI) at Mississippi State for purchasing the sonar device needed to complete this project and leading the data collection campaigns.

## Executive Summary

Topographic LiDAR has well-documented limitations in water-covered, partially inundated, or tidally influenced zones due to null return values. To address these deficiencies, Mississippi State University (MSU) conducted advanced research and field testing on UAS-based bathymetric surveying technologies—particularly echo-sounder-equipped drones—across a range of aquatic environments in Mississippi, including ponds, lakes, rivers, irrigation reservoirs, and nearshore coastal zones.

The project evaluated and improved data acquisition and processing workflows for generating high-resolution bathymetric surfaces. MSU deployed custom-built drones integrating UAS-borne sonar systems and collaborated with the Information Processing and Sensing (IMPRESS) Laboratory and Dr. Adam Skarke's research group to expand sensor capability through additional sonar and ground-penetrating radar (GPR) systems. Use cases included flood modeling, sediment transport monitoring, drainage capacity evaluation, aquatic habitat assessment, and infrastructure inspection.

Key tasks included: (1) conducting a comprehensive technical review of UAS-based topobathymetric surveying technologies; (2) designing a replicable project sampling framework for safe, reliable mission execution; (3) performing multi-site data collection under varied hydrologic and geomorphic conditions; (4) implementing rigorous end-to-end data pre- and post-processing pipelines; and (5) defining the operational envelope of UAS-echo sounder technology concerning with respect to feasibility, data quality, and environmental constraints.

The study produced detailed bathymetric datasets across seven field sites. Comparative accuracy analysis using LiDAR and GNSS ground truth data revealed that the UAS-echo sounder system achieved an RMSE as low as 6.6 cm and an  $R^2$  value of up to 86.6% in optimal conditions. Multiple interpolation techniques were tested, with the Topo to Raster and Universal Kriging methods yielding the best performance in surface generation. Variability in flight line spacing and sampling density was analyzed to determine optimal configurations for balancing accuracy and operational efficiency.

The results demonstrate that UAS-echo sounders are a robust and cost-effective alternative to traditional boat-based or LiDAR bathymetry, particularly for small, shallow, or difficult-to-access water bodies. The integration of sonar with UAV platforms offers a flexible solution for a broad range of geospatial and engineering applications, with the potential for significant time and cost savings in inspection, planning, and monitoring workflows.

# Table of Contents

## Contents

Title Page for RP2024-32.....	i
DISCLAIMER .....	iii
Acknowledgments.....	iv
Executive Summary .....	v
Table of Contents .....	vi
List of Tables.....	vii
List of Figures .....	viii
Introduction.....	1
<b>Chapter 1 – Mississippi State University Work.....</b>	<b>2</b>
Literature Review.....	2
Report Body .....	5
PROPOSED TASK BREAKDOWN AND SUMMARY OF PROJECT STAGES .....	5
Task 1: Create a replicable and easy-to-implement project design and sampling strategy that articulates pre- and mission criteria and considerations to ensure safe and successful project execution. ....	5
Task 2: Design and conduct field data collections across a gradient of use cases, bathymetric sensor technology (including UAS-borne sonar and GPR sensors) and conditions and conduct outreach to public schools in the region during this process. ....	20
Task 3: implement end-to-end data pre- and post-processing workflows for site data collected and construct an implementation practicality envelope that defines what is and is not feasible and accomplishable with the request technology from an applied perspective by area of application (planning, modeling and mapping, and monitoring).....	39
Real-life Use of the UAS-echo Sounder Technology for Water Volume Calculation:.....	65
References:.....	69
Mississippi State University Appendices .....	71
APPENDIX 1:.....	71
APPENDIX 2:.....	75
<b>Chapter 2 – Appalachian State University Work.....</b>	<b>80</b>
Executive Summary .....	80
Introduction.....	81
Research Objectives.....	82
Significance of Proposed Work.....	84
Ward Mill Dam Results.....	85

Rhodhiss Lake near Huffman Bridge in Morganton, NC Results..... 87

Findings and Conclusions ..... 100

Recommendations..... 101

Implementation and Technology Transfer Plan ..... 102

List of Tables

Table 1: Bathymetric data collection locations ..... 21

Table 2: Collected UAS-echo sounder data of each location and flight line coverage length ..... 35



## List of Figures

Figure 1: UAS-echosounder system setup and different elements and components of the technology.....	5
Figure 2: Echo-sounder and its mandatory hardware components .....	6
Figure 3: Different variants of echo-sounder sensor.....	7
Figure 4: An interface of UgCS ground control software and mission planning.....	8
Figure 5: UAS-echo-sounder technology data collection mechanism and water depth calculations .....	9
Figure 6: After primary cleaning the exported sounding datasets in .csv format.....	11
Figure 7: Proposed field data collection workflow showing the three major stages of pre and post-field work. ....	12
Figure 8: Pixhawk autopilot-based drone interaction diagram .....	14
Figure 9: Geocue Trueview 515 3D Imaging System.....	16
Figure 10: Geo7X GNSS rover.....	17
Figure 11: Schematic diagram of a GPR survey. Reflected waves penetrating the subsurface travel at different velocities based on the dielectric permittivity ( $\epsilon$ ) of the media in which they encounter. All subsurface anomalies can be observed by the GPR. ....	18
Figure 12: (a) UAV-based GPR system. (b) Components of developed GPR system. ....	19
Figure 13: Simplified flowchart of GPR processing steps.....	19
Figure 14: Study area in Mississippi showing bathymetric data collection locations .....	22
Figure 15: The study area at Pond D1, Delta Research and Extension Center (DREC), Stoneville, MS...	23
Figure 16: UAS-echo sounder data collection day at the catfish pond, DREC .....	24
Figure 17: LiDAR data collection at the drained catfish pond .....	24
Figure 18: LiDAR data collection at the catfish pond, DREC.....	25
Figure 19: GNSS data collection at the puddles of the catfish pond.....	25
Figure 20: GNSS data collection day at the catfish pond remaining puddles.....	26
Figure 21: UAS-echo sounder data collection at Bay Springs Lake.....	28
Figure 22: Filed data collection day at Bay Springs Lake .....	29
Figure 23 UAS-echo sounder data collection at Grand Bay (A) and Middle Bay (B) .....	29
Figure 24: Data collection day at Grand Bay and Middle Bay .....	30
Figure 25: UAS-echo sounder data collection at North Farm, Starkville .....	31
Figure 26: Data collection day at North Farm, Starkville.....	32
Figure 27: UAS-echo sounder data collection at Tombigbee River.....	32
Figure 28: Data collection day at Tombigbee River .....	33
Figure 29: UAS-echo sounder data collection at White's Creek Lake.....	34
Figure 30: Data collection day at White's Creek Lake.....	35
Figure 31: Initial UAS-echo sounder data cleaning workflow using Eye4hydromagic software.....	40
Figure 32: Editing the echogram to eliminate any spikes and errors .....	40
Figure 33: Flowchart of UAS-echo sounder and LiDAR data integration process for field surveys using geospatial techniques. ....	42
Figure 34: Workflow of integrating LiDAR and GNSS values with interpolated raster surface using Echo-sounder data and accuracy assessment.....	43
Figure 35: Data sampling workflow and accuracy assessment.....	45
Figure 36: Location of UAS-bathymetry data outliers plotted by (a)3 standard deviations (SD) (left) and (b)2SD (right), respectively.....	47
Figure 37: Scatterplots illustrating the correlation between UAS-echo sounder bathymetric measurements and LiDAR-derived elevation data, highlighting data distribution and accuracy assessment. ....	47

Figure 38: 1-meter resolution bathymetric surfaces generated using the top-performing interpolation methods for two different flight path spacing scenarios: (a)Topo to Raster (5-meter flight line spacing), (b)Topo to raster (10-meter flight line spacing), (c) Universal Kriging (UK) (5-meter flight line spacing), (d) Radial basis function - Completely regularized spline (RBF-CRS) (10-meter flight line spacing).....	49
Figure 39: 3D of the Catfish Pond's bathymetric surface. ....	49
Figure 40: Comparison of RMSE across various interpolation methods for a 5-meter flight line spacing, evaluated at four different point sampling intervals along the flight lines.....	50
Figure 41: Comparison of R-squared values for various interpolation methods at a 5-meter flight line spacing, assessed across four different point sampling intervals along the flight lines. ....	51
Figure 42: Comparison of RMSE across various interpolation methods at a 10-meter flight line spacing, evaluated at four different point sampling intervals along the flight lines.....	52
Figure 43: Comparison of R-squared values for various interpolation methods at a 10-meter flight line spacing, assessed across four different point sampling intervals along the flight lines. ....	52
Figure 44: Bathymetric surface of Bay Springs Lake using UAS-echo sounder's continuous mode data collection.....	55
Figure 45: Bathymetric surface of Middle Bay using UAS-echo sounder's continuous mode data collection.....	56
Figure 46: Bathymetric surface of Grand Bay using UAS-echo sounder's continuous mode data collection .....	57
Figure 47: Bathymetric surface of Tombigbee River using UAS-echo sounder's continuous mode data collection.....	59
Figure 48: Bathymetric surface of Tombigbee River using UAS-echo sounder's continuous mode data collection.....	60
Figure 49: River types based on their sinuosity, number of channels and lateral movement (Nichols, G., 1999. Sedimentology and Stratigraphy. Wiley- Blackwell, Oxford.) .....	61
Figure 50: Google earth image of the Tombigbee River where the data has been collected .....	61
Figure 51: Bathymetric surface of White's Creek Lake using UAS-echo sounder's continuous mode data collection.....	62
Figure 52: Bathymetric surface of White's Creek Lake using UAS-echo sounder's grasshopper mode data collection.....	63
Figure 53: 3D of the White's Creek Lake bathymetric surface. ....	64
Figure 54: Bathymetric elevation map generated using 5-meter flight spacing UAS-echo sounder data and using topoR (Topo to raster) interpolation method. ....	65
Figure 55: water volume calculation steps in ArcGIS pro-environment.....	66
Figure 56: Surface volume calculation tool in ArcGIS pro.....	66
Figure 57: Ward's Mill Dam – facing upstream (left: pre-removal, right: post-removal). ....	82
Figure 58: Two more testing sites (left: Price Lake, right: Rhodhiss Lake). ....	83
Figure 59: Cross-section data analysis.....	85
Figure 60: Storm damage overview .....	86
Figure 61: Bank erosion and GCP collection (left), Erosion and deposition from Helene (right).....	86
Figure 62: (a) test flights and training scenarios at App State Duck Pond. (b) collect echo sounder data at Rhodhiss Lake. (c) collect ground truth data with a canoe at Rhodhiss Lake. ....	88
Figure 63: Study Location .....	89
Figure 64: (a) Bathymetric data collected by drone-based echo sounder, (b) ground truth depth measurements.....	90
Figure 65: Interpolated depth matrix from UAV based echo sounder.....	90
Figure 66: Delaunay triangulation algorithm interpolation compared to the ground truth data. ....	91

Figure 67: Comparison between the UAV-interpolated depth and traditional survey depth.....	92
Figure 68: M600 Pro (left), ECT 400s Echologger (right) .....	92
Figure 69: Flight paths .....	93
Figure 70: Example Echogram as seen in Hydromagic Software.....	93
Figure 71: Post Helene interpolated depth map. ....	94
Figure 72: Depth change after Helene, red indicates erosion and blue indicates deposition. ....	95
Figure 73: Visualization of Rhodhiss bathymetry, with Huffman bridge SfM model included.....	96
Figure 74: Map of collected data points.....	97
Figure 75: Price Lake bathymetric map.....	98
Figure 76: Accuracy assessment .....	99
Figure 77: 3D Visualization .....	99

## Introduction

This report advances the state of practice for bathymetric and topobathymetric mapping by demonstrating the feasibility, precision, and operational benefits of integrating UAS-based echo sounders and ground-penetrating radar (GPR) across diverse aquatic environments. The findings support transportation agencies like NCDOT in making more informed decisions for infrastructure planning, floodplain management, and water resource monitoring. By assessing sensor performance across varied site conditions, this work contributes to the evolving national priority of employing agile, cost-effective, and resilient remote sensing technologies for transportation and environmental stewardship. The methodologies and lessons learned herein are intended to guide future survey design and the application of UAS platforms for precision bathymetric and subsurface assessments across the United States and beyond. The methods outlined in this report also align with national efforts such as the USDOT's National Roadway Flooding Framework and advancing state-level climate adaptation and transportation resilience planning.



# Chapter 1 – Mississippi State University Work

## Literature Review

Bathymetry is the scientific study of the depth of underwater topography (Jagalingam et al., 2015), is of utmost importance for a range of purposes, especially in inland bodies of water like lakes and rivers, where it facilitates navigation, environmental surveillance, and resource administration (Bandini et al., 2018). For inland waters, bathymetric mapping aids in evaluating sedimentation rates, which can impact water depth and quality, and guides maintenance operations such as dredging to recover lost depths (Bandini et al., 2023; Yao et al., 2023). Overall, bathymetry offers essential information for efficiently managing aquatic resources, guaranteeing safety, and advancing environmental sustainability (Hell et al., 2012). Remote sensing provides various technologies for acquiring or assisting in the derivation of topographic bathymetric data. The methods encompass LiDAR, radar altimetry, multi-beam sonar, single-beam sonar, photogrammetry, satellite imagery, and InSAR (Erena et al., 2019; Genchi et al., 2020). Each of these techniques offers distinct capabilities for acquiring data regarding the Earth's surface and subaqueous topography. Specially for bathymetric data collection techniques utilizing single-beam and multi-beam echo-sounders aboard ships and boats continues to be the prevailing approach for conducting extensive, deep-water surveys (Jawak et al., 2015). These methods provide exceptional precision and comprehensive coverage (Wölfl et al., 2019).

However, these techniques are costly, challenging to implement, and unsuitable for shallow water conditions and small water bodies (Ferreira & Andrade, 2022; Jagalingam et al., 2015). Furthermore, the integration of sonar/echo-sounder into Unmanned Surface Vehicles (USVs) has significantly enhanced their capabilities in shallow or inaccessible regions (Sotelo-Torres et al., 2023). Nevertheless, unoccupied aerial systems (UAS) echo-sounder bathymetry is becoming recognized as a versatile and economical option for both inland and coastal waters, especially in regions that are not reachable by traditional boats (Alvarez et al., 2018) and not feasible for small area coverage. UAS-Echo-sounder bathymetry is a developing technology that integrates UAS with a sonar sensor to perform bathymetric surveys (Bashit & Pricope, 2024). This novel technique entails affixing a sonar device to a drone or UAS, enabling underwater cartography and depth analyses in regions that may have challenges for conventional means of access (Bashit & Pricope, 2024). UAS-Echo-sounder systems provide several benefits, including the production of high-quality data, enhanced water penetration capabilities in comparison to UAS-green band Lidar, and the capability to effectively survey shallow water environments that create difficulties for traditional boat-based techniques. Their depth measuring capabilities range from 0.5 to 200 meters, making them advantageous for surveying remote, hazardous, or unnavigable areas. Although UAS bathymetry encounters constraints in deep-ocean water settings and spatial resolution when compared to multi-beam systems, it exhibits potential for conducting small-scale surveys, particularly in shallow waters and locations with limited accessibility (Pricope & Bashit,

2023). The technology is subject to continuous development, with current research concentrated on enhancing precision, and coverage. However, this technology is still in the developmental stage and necessitates additional study, assessment of accuracy, and improvement before it can be widely adopted.

UAS-Echo-sounder surveys using bathymetric single-beam technology provide precise depth measurements along designated flight paths over bodies of water. Although it provides point-based depth measurements and is useful, it does not offer a comprehensive representation of the underwater topography. As a result, interpolation is an essential procedure in bathymetry that overcomes this constraint by approximating numerical values of depth between observed locations (Parente & Vallario, 2019). More specifically interpolation methods are statistical procedures employed to predict values within a given set of known data points (Arun, 2013). Using this interpolation method, it is possible to generate a continuous surface or map from the individual depth measurements, converting discrete data into a complete representation of the underwater topography (Li et al., 2019). To produce precise and comprehensive bathymetric maps from UAS-Echo-sounder data, such interpolation is essential (Udoh et al., 2022). The significant research gap in interpolation methods and UAS-bathymetric sensors mostly concerns the necessity to enhance the precision, effectiveness, and suitability of these technologies in diverse underwater settings. Some well-known interpolation techniques such as Inverse Distance Weighted (IDW), Kriging, Radial Basis Function (RBF) and Topo Raster(TopoR) are frequently employed to bridge the gaps between known data points to ensure a more comprehensive and precise representation of the seafloor (Parente & Vallario, 2019). Every technique possesses distinct merits and drawbacks, including variations in precision, computational expense, and the level of smoothness in the resultant interpolated surface (Siljeg et al., 2015). Existing interpolation techniques exhibit distinct advantages and disadvantages based on data density and terrain properties. However, no universally ideal be applied to all situations.

The primary objective of this study is to assess the accuracy of the UAS-echo-sounding data relative to in situ measurements. It refers valuation of the accuracy and dependability of UAS-echo-sounding technology in mapping underwater topography. The second objective is to assess and determine the most effective interpolation method for generating continuous underwater surfaces from UAS-echo-sounding data. Here the main goal was to compare different interpolation techniques to ascertain which interpolation method produces the most accurate and representative underwater digital elevation models (DEMs).

Finally, our last objective was to explore sample data collection methods for producing comparable underwater elevation models to meet both industrial and research requirements. This represents the assessment of a range of survey techniques and mission planning strategies to ascertain the efficient and cost-effective methods for collecting UAS-Echo-sounding bathymetric

data according to the detailing needs of Industry and research. The research seeks to enhance data acquisition techniques and strengthen post-processing methodologies to contribute to more accurate and dependable bathymetric mapping solutions using UAS-echo-sounding technology. Future work may also explore the feasibility of integrating GPR to detect salt wedge dynamics within estuarine and tidal environments. The sensitivity of GPR to variations in subsurface dielectric properties suggests that it may be applicable for identifying saline–freshwater interfaces, a technique that could further expand the operational range of the presented methods. Pilot studies and site-adapted testing will be required to assess the efficacy and limitations of this approach.

# Report Body

## PROPOSED TASK BREAKDOWN AND SUMMARY OF PROJECT STAGES

**Task 1: Create a replicable and easy-to-implement project design and sampling strategy that articulates pre- and mission criteria and considerations to ensure safe and successful project execution.**

For our project, we have utilized a cutting-edge UAS-echo-sounder system manufactured by SPH Engineering. We received significant technology support from the Geosystems Research Institute (GRI) of Mississippi State University.

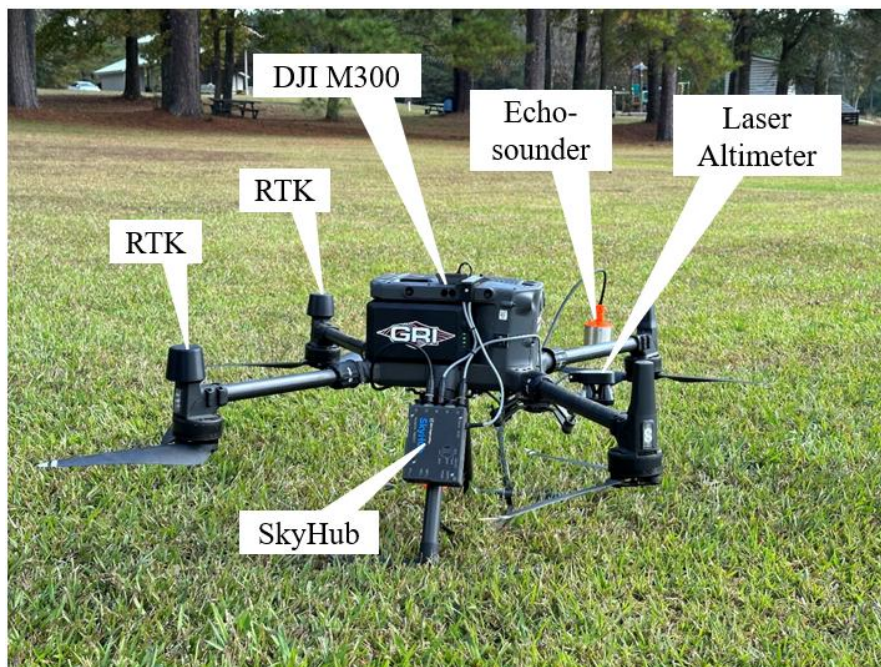


**Figure 1:** UAS-echosounder system setup and different elements and components of the technology

### **Integrated System for Bathymetry with Echo Sounder:**

The comprehensive drone-based bathymetry system comprises the following components:

- A commercially available drone, such as the DJI M300 RTK, M210, M600 Pro, or any drone equipped with a Pixhawk autopilot system. For this project, we specifically used the DJI M300 RTK drone.
- An echo sounder sensor is attached to a cable for underwater depth measurement.
- A radar/laser altimeter to accurately determine the drone's height above the water surface.
- The heart of the integrated system is UgCS SkyHub – a small and powerful onboard computer with special software responsible for mission control and the storage of geotagged data.
- Mission control software to manage and execute the survey operations.





- 1 – echo sounder with stainless steel protection housing, cable, hook and carabiner to attach the sensor to the drone
- 2 – cables set
- 3 – UgCS SkyHub onboard computer
- 4 – radar altimeter with mountings for the drone (for our project we have used laser altimeter).

**Figure 2:** Echo-sounder and its mandatory hardware components

*In addition to the DJI platforms used for echo-sounder data collection, GPR deployments were conducted using a custom-built mid-size hexacopter UAV configured to carry a frequency-domain GPR sensor. This expands MSU's range of airborne platforms for subsurface and shallow-water survey applications, complementing the capabilities of the Wingtra Gen 1 and other DJI Matrice platforms and allowing sensor and mission profiles to be matched to site-specific constraints.*

### **The sensor:**

There are three single-beam echo-sounder options available (refer to the table below), all manufactured by the Korean company EofE Ultrasonics Ltd. (<https://www.echologger.com/>), which specializes in high-precision sonar equipment for surveying. Each echo sounder features an integrated tilt sensor to discard data when the sensor is not near vertical, as well as a temperature sensor. All models boast a nominal accuracy of 0.2% of the depth and a resolution of less than 1mm. The measurement range starts from the transducer's base, with a practical minimum depth of approximately 15cm deeper, as the sensor must be fully submerged during operation. The sensors utilize the RS232 interface for reliable data transmission over long cables.

Sensor	ECT 400S	ECT D052S	ECT D032S
Type	Single frequency	Dual frequency	Dual frequency
Acoustic frequency	450 kHz	50/200 kHz	30/200 kHz
Measurement range*	0.15 ... 100m	1.0 ... 200m (50 kHz) 0.5 ... 200m (200 kHz)	1.0 ... 200m (30 kHz) 0.5 ... 200m (200 kHz)
Beam width Conical (-3dB)	5°	27° / 7° (50 kHz/200 kHz)	26° / 5° (30 kHz/200 kHz)
Weight of the echo sounder (in the air)	275g	460g	460g
Weight of all components in the air (echo sounder, SkyHub, altimeter, housing, cables, mountings)	1.6 kg (light housing) 2.6 kg (heavy housing)	2.7 kg	4.2 kg
Suitable DJI drones (or Pixhawk drones of comparable size)	M210 (light housing) M300 RTK M600 Pro	M300 RTK M600 Pro	M600 Pro

**Figure 3:** Different variants of echo-sounder sensor

For this project, we used an ECT D052S dual-frequency sensor. The minimum measurement range is 0.5m and the maximum is 200m.

### **Altimeter:**

To ensure accurate depth measurements and the safety of the drone, maintaining precise altitude above the water's surface is crucial. We employ a laser altimeter along with a specialized terrain (surface) tracking algorithm to maintain the drone's altitude consistently during automated survey operations.

### **UgCS SkyHub:**

The core of the integrated system is the UgCS SkyHub, a compact yet powerful onboard computer equipped with specialized software. Its primary function is to maintain a consistent drone altitude above the water surface using data from a radar altimeter. Unlike standard DJI drones, which rely on less precise barometric altimeters and can experience altitude drifts of several meters during a single flight, the radar altimeter ensures altitude stability with a drift of only about 5 cm. The onboard computer's second function is to store echo sounder measurements in a geotagged format. It uses the drone's GPS receiver for geotagging, and if the drone is equipped with an RTK/PPK receiver, the data points can achieve centimeter-level precision.

Measurements are saved in three formats:

- A simple CSV text format containing coordinates, depth, and additional information, compatible with various XYZ data processing software like Surfer, Oasis Montaj, and Excel.
- NMEA 0183, which works with popular hydrographic software such as HydroMagic and Reefmaster.
- SEG-Y, which includes full echo sounder data.

In addition to depth measurements, the system logs water temperature and the tilt angles of the sensor. Data logging starts automatically once the echo sounder is submerged and ceases when the sensor is no longer in the water. The onboard software simultaneously transmits real-time depth data to the ground station, enabling the operator to verify proper functionality and perform manual measurements, particularly when the drone is not engaged in an automated mission.

### Ground Control Software:

The ground control software used is UgCS, which includes an additional companion application for managing the echo sounder. Throughout the flight, the ground operator can monitor the real-time depth measurements provided by the echo sounder.

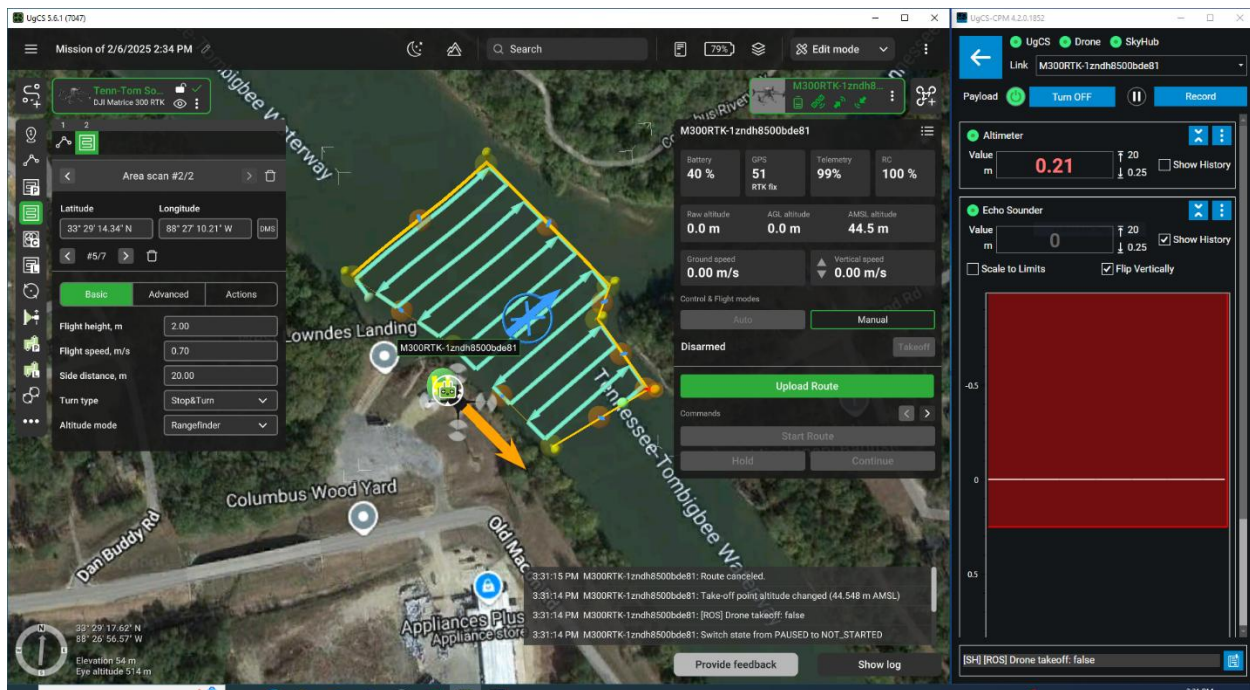


Figure 4: An interface of UgCS ground control software and mission planning

### Modes of operations:

The integrated system offers three operational modes:

- Continuous measurements along survey lines.
- Measurements at designated waypoints. Also known as Grass-hopper mode.
- Manual measurements.

In the first mode, the drone operator needs to plan missions with a survey grid or individual lines over water. Once the sensors are submerged, data logging will initiate automatically. The drone will then tow the submerged sensor at a low speed (0.5–0.7 m/s) while conducting measurements at a constant depth.

## UAS-echo-sounder technology data collection mechanism:

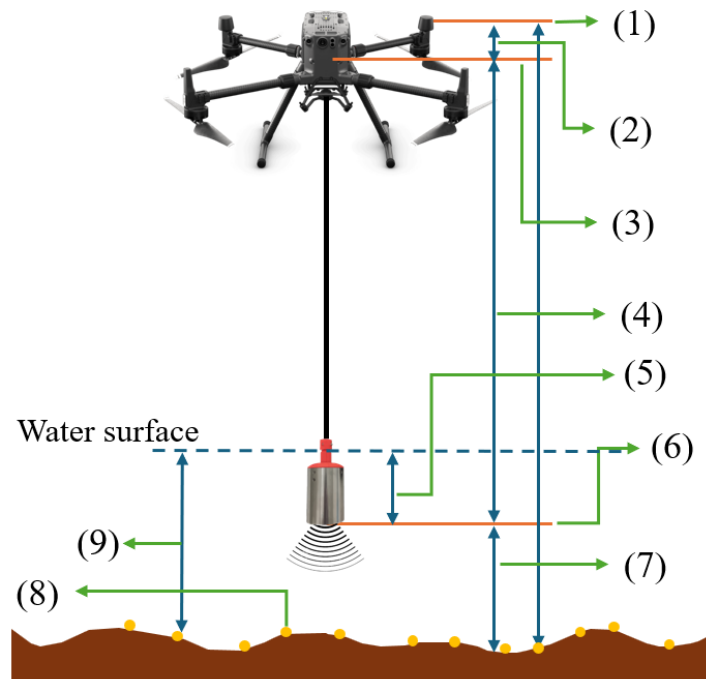


**Figure 5: UAS-echo-sounder technology data collection mechanism and water depth calculations**

In the following, the UAS-echo-sounder technology data collection mechanism is described with the proper serial number.

**(1) Drone's Ellipsoidal height /Orthometric height:** The drone's RTK stores the drone's ellipsoidal height /orthometric height data using a GNSS receiver and sends it to the SkyHub computer.

Ellipsoidal Height: The drone's altitude above a reference ellipsoid (a mathematical model of Earth's shape).

Orthometric Height: The drone's elevation above the geoid (closely related to sea level, accounting for gravity). These measurements provide precise vertical positioning for the drone.

**(2) Distance between the drone's RTK and the laser Altimeter:** This is the vertical distance between the drone's RTK and the laser/radar altimeter, which is about 20cm.

**(3) Placement of the Radar/Laser Altimeter:** This indicates where the radar or laser altimeter is mounted on the drone. It measures the distance from the drone to the water surface.

**(4) Cable length:** This refers to the length of the cable connecting the drone to the echo-sounder sensor submerged in the water. It is the length from the altimeter to the bottom of the echo sounder.



**(5) Height of the sensor:** This is the vertical height of the echo-sounder sensor.

**(6) Bottom of the echo-sounder sensor:** This is the lowest point of the echo-sounder sensor, which emits sound waves to measure the distance to the underwater surface.

**(7) Distance between the bottom of the echo-sounder sensor and the underwater surface:** This is the measured depth from the sensor's bottom of the water body, calculated using the echo-sounder.

**(8) Elevation of the bathymetric surface point:** This represents the height of the underwater surface point relative to a reference datum, such as sea level.

Equation:

Elevation = Orthometric Height – ((( 4) Cable length + (2) Distance between the drone's RTK and the leaser Altimeter) - (5) sensor height) - (9)water depth) **(1)**

**(9) Water depth:** This is the total depth of the water, calculated as the distance from the water surface to the bottom of the water body, derived from the echo-sounder measurements.

Equation:

water depth = (7) distance from the bottom of the sensor to the surface + (5)sensor height **(2)**

After data collection and primary data cleaning the exported final data in CSV format must contain the following information.

**Longitude and Latitude:** UgCS SkyHub computer identifies and calculates the exact locations and stores Longitude and Latitude values for each of the bathymetric point locations.

**Raw depth (Hi):** Unprocessed depth readings from the echosounder using the high frequency of the sensor. When the waterbody is very shallow high frequency works the best.

**Corrected depth (Hi):** Corrected for water temperature, salinity, and pressure. Ensures depth accuracy by compensating for environmental and sensor errors.

**Elevation (Hi):** UgCS SkyHub computer calculates the elevation considering the **Equation 1**. The most important data of the entire data collection because water depth can be changed but accurate underwater elevation remains the same for a long period . So, knowing the depth and change of the elevation of any water body elevation data is crucial for regular and long-term monitoring of a water body. Elevation (Hi) is the value generated using the high frequency of the sensor.

**Raw depth (Lo):** Unprocessed depth readings from the echosounder using the low frequency of the sensor. When the waterbody is deep low frequency works the best.

**Corrected depth (Lo):** Corrected for water temperature, salinity, and pressure. Ensures depth accuracy by compensating for environmental and sensor errors.

**Elevation (Lo):** Elevation (Lo) is the value generated using the Low frequency of the sensor.

**Ellipsoidal height / Orthometric height:** The drone's RTK stores the drone's ellipsoidal height /orthometric height data using a GNSS receiver. The final output data looks like the following CSV tabular datasets.

1	Easting	Northing	Longitude	Latitude	Raw Depth (Hi)	Corrected Depth (Hi)	Elevation (Hi)	Raw Depth (Lo)	Corrected Depth (Lo)	Elevation (Lo)	Ellipsoidal Height	Orthometric Height	Date (short)	Date (full)
725	647542.332	438186.896	-90.89757068	33.45089115	0.64	0.64	35.157	1.82	1.82	33.977	11.671	38.297	6/18/2024	Tuesd
726	647542.332	438186.896	-90.89757068	33.45089115	0.63	0.63	35.169	1.58	1.58	34.219	11.673	38.299	6/18/2024	Tuesd
727	647542.191	438186.893	-90.8975722	33.45089112	0.65	0.65	35.149	1.53	1.53	34.269	11.673	38.299	6/18/2024	Tuesd
728	647542.191	438186.893	-90.8975722	33.45089112	0.62	0.62	35.187	1.57	1.57	34.237	11.681	38.307	6/18/2024	Tuesd
729	647542.04	438186.9	-90.89757382	33.45089117	0.64	0.64	35.167	1.53	1.53	34.277	11.681	38.307	6/18/2024	Tuesd
730	647542.042	438186.9	-90.8975738	33.45089117	0.63	0.63	35.182	1.54	1.54	34.272	11.686	38.312	6/18/2024	Tuesd
731	647541.885	438186.915	-90.89757548	33.4508913	0.62	0.62	35.192	1.48	1.48	34.332	11.686	38.312	6/18/2024	Tuesd
732	647541.885	438186.915	-90.89757548	33.4508913	0.63	0.63	35.174	1.5	1.5	34.304	11.678	38.304	6/18/2024	Tuesd
733	647541.729	438186.924	-90.89757717	33.45089137	0.63	0.63	35.174	1.5	1.5	34.304	11.678	38.304	6/18/2024	Tuesd
734	647541.729	438186.924	-90.89757717	33.45089137	0.63	0.63	35.165	1.47	1.47	34.325	11.669	38.295	6/18/2024	Tuesd
735	647541.576	438186.928	-90.89757882	33.4508914	0.63	0.63	35.165	1.45	1.45	34.345	11.669	38.295	6/18/2024	Tuesd
736	647541.576	438186.928	-90.89757882	33.4508914	0.62	0.62	35.179	1.45	1.45	34.349	11.673	38.299	6/18/2024	Tuesd
737	647541.43	438186.933	-90.89758038	33.45089143	0.62	0.62	35.179	1.47	1.47	34.329	11.673	38.299	6/18/2024	Tuesd
738	647541.43	438186.933	-90.89758038	33.45089143	0.61	0.61	35.181	1.47	1.47	34.321	11.665	38.291	6/18/2024	Tuesd
739	647541.292	438186.933	-90.89758187	33.45089143	0.63	0.63	35.161	1.5	1.5	34.291	11.665	38.291	6/18/2024	Tuesd
740	647541.292	438186.933	-90.89758187	33.45089143	0.6	0.6	35.177	1.44	1.44	34.337	11.651	38.277	6/18/2024	Tuesd
741	647541.16	438186.93	-90.89758328	33.4508914	0.6	0.6	35.177	1.44	1.44	34.337	11.651	38.277	6/18/2024	Tuesd
742	647541.16	438186.93	-90.89758328	33.4508914	0.6	0.6	35.176	1.46	1.46	34.316	11.65	38.276	6/18/2024	Tuesd
743	647541.03	438186.929	-90.89758468	33.45089138	0.6	0.6	35.176	1.5	1.5	34.276	11.65	38.276	6/18/2024	Tuesd
744	647541.03	438186.929	-90.89758468	33.45089138	0.6	0.6	35.179	1.5	1.5	34.279	11.653	38.279	6/18/2024	Tuesd
745	647540.9	438186.928	-90.89758608	33.45089137	0.62	0.62	35.159	1.57	1.57	34.209	11.653	38.279	6/18/2024	Tuesd
746	647540.9	438186.928	-90.89758608	33.45089137	0.61	0.61	35.169	1.69	1.69	34.089	11.653	38.279	6/18/2024	Tuesd
747	647540.767	438186.932	-90.89758752	33.4508914	0.62	0.62	35.159	1.57	1.57	34.209	11.653	38.279	6/18/2024	Tuesd
748	647540.767	438186.932	-90.89758752	33.4508914	0.63	0.63	35.155	1.63	1.63	34.155	11.659	38.285	6/18/2024	Tuesd
749	647540.632	438186.933	-90.89758897	33.4508914	0.63	0.63	35.155	1.53	1.53	34.255	11.659	38.285	6/18/2024	Tuesd

**Figure 6: After primary cleaning the exported sounding datasets in .csv format**

To ensure a safe and successful data collection and sampling strategy, it is essential to clearly define and address pre-mission and post-mission criteria and considerations. These are outlined below:

There are three basic considerations. They are preparation, fieldwork day, and post-fieldwork day.

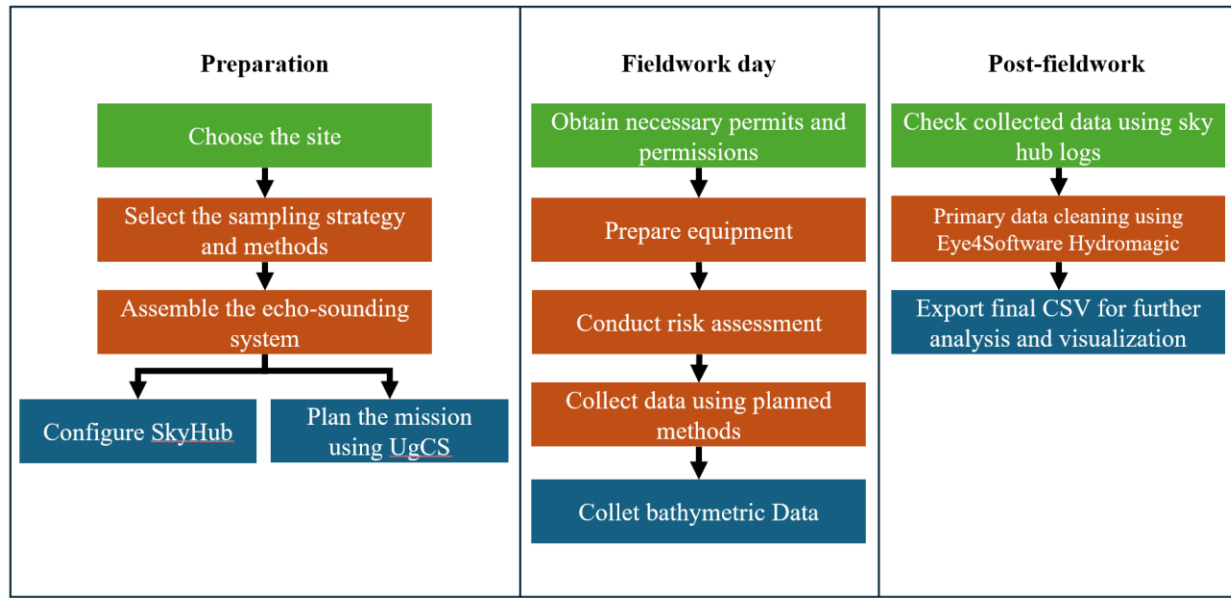


**Figure 7: Proposed field data collection workflow showing the three major stages of pre and post-field work.**

## Preparation:

### 1. Choose the Site:

Selecting an appropriate site is critical for effective UAS-echo-sounder operations. The site must align with the survey objectives, such as mapping bathymetry and monitoring underwater elevation. Factors like water depth, and flow velocity influence echo-sounder performance, while aerial restrictions (e.g., no-fly zones, obstacles) impact UAS deployment. Additionally, accessibility for takeoff/landing must be evaluated. Pre-survey reconnaissance using satellite imagery or historical data helps identify optimal locations, ensuring the site supports both safe UAS flight and high-quality acoustic data collection.

### 2. Select the Sampling Strategy and Methods

The sampling strategy defines how the UAS-echo-sounder system will collect data. For bathymetric surveys, Continuous measurements along survey lines and measurements at designated waypoints, Also, known as Grass-hopper mode, are manual measurements. The choice between single-beam (focused depth profiling) or multi-beam (wide-area 3D mapping) echo-sounders depends on resolution requirements and survey scale. Methods must account for waterbody type (e.g., rivers, lakes) and environmental variables like wave action, and seaweed in the water.

### **3. Assemble the Echo-Sounding System**

This step involves mounting the echo-sounder hardware onto the UAS (NCDOT deliverables 2025\SPH Documentation and training\Video recordings).

### **4. Configure SkyHub Using UGCS**

SkyHub, a telemetry and payload management system, is configured via UGCS to integrate the echo sounder with the UAS. This step establishes communication protocols between the drone's autopilot, the echo sounder's data stream, and the ground station. Parameters such as ping rate (acoustic pulse frequency), data storage paths, and real-time telemetry feeds are set. UGCS enables operators to monitor sensor health, adjust flight paths mid-mission, and visualize bathymetric data in real-time. Pre-launch validation ensures all components function cohesively, minimizing risks of data loss or system failure during execution.

#### **Field day work:**

##### **1. Obtain Necessary Permits and Permissions**

Fieldwork days involving the use of a UAS (Unmanned Aerial System) equipped with an echosounder sensor for bathymetric data collection require careful planning and execution. The first step is to obtain the necessary permits and permissions. This ensures compliance with local regulations and secures access to the study area. It is crucial to coordinate with relevant authorities and stakeholders to avoid legal issues and ensure smooth operations.

##### **2. Prepare Equipment**

Next, preparing the equipment is essential. This involves checking the UAS, echosounder sensor, and other related tools to ensure they are in optimal working condition. Calibration of the echosounder sensor is particularly important to ensure accurate depth measurements. Additionally, battery and power sources should be prepared to handle any unforeseen technical issues during the fieldwork.

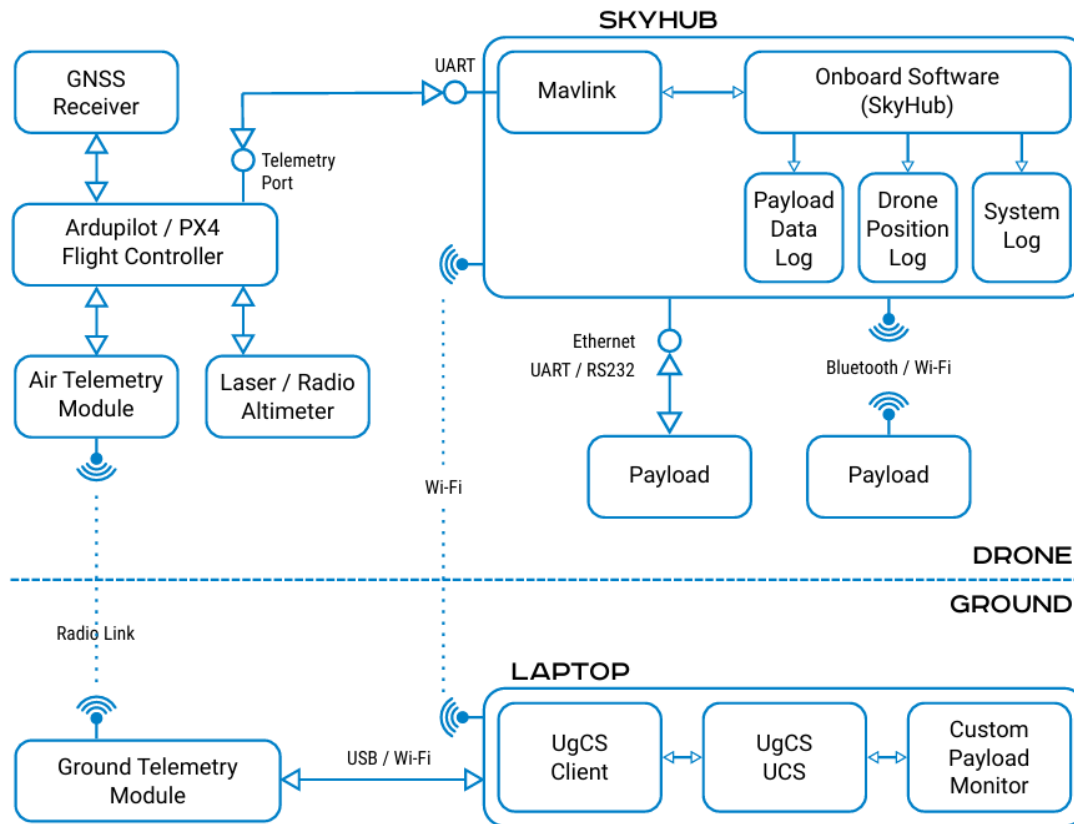


**Figure 8: Pixhawk autopilot-based drone interaction diagram**

The flowchart shows the UAS-echo sounder hardware and software interaction mechanism the source of the diagram is NCDOT deliverables 2025\SPH Documentation and training\Documents\skyhub-user-manual-2024.pdf.

### 3. Conduct Risk Assessment

Conducting a risk assessment is a critical step to ensure the safety of the team and the equipment. This includes evaluating environmental conditions, such as weather and water currents, and identifying potential hazards. Safety protocols should be established, and all team members should be briefed on emergency procedures. This step helps mitigate risks and ensures a safe working environment.

### 4. Collect Data Using Planned Methods

Once all preparations are complete, the team can proceed to collect data using the planned methods. The UAS is deployed to fly over the water body, and the echosounder sensor is used to measure the depth and map the underwater terrain. The flight path should be carefully planned to cover the study area systematically, ensuring comprehensive data collection. Real-time monitoring of the UAS and sensor data is essential to address any issues promptly. Integrated

system supports three modes (NCDOT deliverables 2025\SPH Documentation and training\Documents\echo-sounder-systemdescription-sph-engineering.pdf) of operations and it should be selected according to the project need.

## **5. Collect Bathymetric Data**

Finally, the collected bathymetric data need to be reviewed and stored securely. Initial data checks should be done on-site to check for quality and consistency. Proper documentation of the fieldwork, including any challenges encountered and how they were addressed, is important for future reference and analysis. This structured approach ensures accurate and reliable bathymetric data collection using UAS technology.

### **Post-fieldwork:**

#### **1. Check collected data using sky hub logs:**

The post-fieldwork processing of UAS echo-sounder data begins with the crucial data verification step. During this initial phase, collected data is meticulously checked using sky hub logs to ensure all raw data from the echo-sounder is properly recorded and complete. This verification process serves as the foundation for all subsequent processing steps.

#### **2. Primary data cleaning is performed using Eye4Software Hydromagic:**

Following verification, the data moves into the cleaning phase, which utilizes Eye4Software Hydromagic, a specialized software platform (Described in Appendix 1). This comprehensive cleaning process is essential for eliminating noise and artifacts from the echo-sounder readings, ensuring the highest possible data quality and accuracy. The software's sophisticated tools help transform raw data into reliable bathymetric measurements.

#### **3. Export final CSV for further analysis and visualization:**

The final phase involves the export process, where the cleaned and processed data is converted into CSV format. This export step is crucial as it makes the data readily available for further analysis, visualization, or integration with other datasets. The CSV format ensures compatibility with various analysis tools and software platforms, making it versatile for different applications in underwater mapping and analysis. This standardized format also facilitates easy sharing and collaboration among project stakeholders.

### **Conclusion:**

By following this structured approach and considering all pre- and post-mission criteria, teams can ensure a safe, successful, and replicable execution of bathymetric surveys using UAS-echo-sounder technology. This methodology not only maximizes data quality and operational

efficiency but also promotes consistency across multiple survey projects, facilitating long-term monitoring and analysis of underwater environments.

### **LiDAR Sensor:**

For the project, LiDAR data was collected with a Geocue Trueview 515 3D Imaging System. This sensor contains a 32-channel laser scanner with two recorded returns, dual true color cameras for point cloud colorization, a Trimble/Applanix APX-15 IMU/GNSS, and weighs 2.25 kg. Overall, the Trueview 515 has a system accuracy of better than 5 centimeters RMSE. This system is currently integrated on a DJI Matrice 300 RTK which allows for roughly 30 minutes of flight time. The data collection to capture the drained catfish pond was flown at a 30-meter altitude, 4 meters per second, and with 13.5-meter transect spacing resulting in 2000 points per square meter on average.



**Figure 9: Geocue Trueview 515 3D Imaging System**

Following data acquisition, the raw LiDAR data was processed into a LAS file using Geocue's LP360 Drone software. Both LiDAR data and base station data were imported into the software and the points were generated by combining the laser reflections and their GNSS location based on the position and orientation of the TV515. The TV515 GNSS locations were then corrected based on the correction factors recorded by the base station. Once the point cloud was generated the points were colorized by the RGB values from the cameras mounted on the TV515. The colorization is beneficial for having additional situational awareness about what each point is reflecting and allows for more information when classifying the point cloud.

Next, isolated noise filtering was performed where each point was evaluated by drawing a vertical cylinder with a 2-meter radius and 30-centimeter height around it. Points with no neighboring points within this cylinder were identified as noise and removed. The remaining point cloud was then classified into ground, water, and other noise classes. Specifically, this



dataset had numerous returns from areas containing shallow water. These points need to be separated into a known class because this system was not designed to be used in a bathymetric role and was not calibrated for dealing with laser returns passing through other mediums such as water. Also present in the scene was a pond aerator that had to be manually classified and separated from the ground surface.

To assess the accuracy of the corrected LAS point cloud, the vertical distances between ground checkpoint reflections and their known GNSS elevations were compared. Since the checkpoints were square ( $40 \times 40$  cm), an inverse distance weighting average was used to calculate a single elevation value representing the point cloud elevation at each of the 4 checkpoints. The mean and standard deviation of the vertical distance differences were then estimated.

If the mean was significantly larger than the standard deviation, an affine shift was applied to the point cloud to align it with the control points. Conversely, if the mean was negligible or small relative to a high standard deviation, the point cloud remained unadjusted as the statistics did not provide a reliable basis for alignment. In our case, we kept it unadjusted.

### **GNSS:**

Even though the pond was drained, some residual puddles did not have time to fully dry. The puddles were manually sampled with a high-accuracy RTK/PPK Geo7X GNSS rover. The Geo7X is accurate to centimeter level in the horizontal and 1.5 cm in the vertical direction.



**Figure 10: Geo7X  
GNSS rover**

### **GPR Sensor:**

#### **Theoretical Background - GPR detection of bathymetry**

GPR is a geophysical tool that utilizes short-range electromagnetic wave-based radar technology. It is designed to locate buried objects and has been widely used in civil engineering, archaeological research, geophysical investigations, soil moisture, and tree root detection.

The detectability of a buried object via GPR is mainly dependent on the dielectric properties of the object and media and the size of the object. Because electromagnetic waves reflect when they encounter a different dielectric permittivity in a geological medium. GPR measures the amplitude and the travel time of the reflected energy. Figure 11: shows the principle of the GPR survey.

Commercial GPRs are very successful in detecting materials such as PVC, steel, other utility materials, and bones since their dielectric permittivity is quite different from that of the soil.

However, using GPR in bathymetry is more challenging because of the high electric conductivity of water. So, the current GPR systems are not designed for bathymetry.

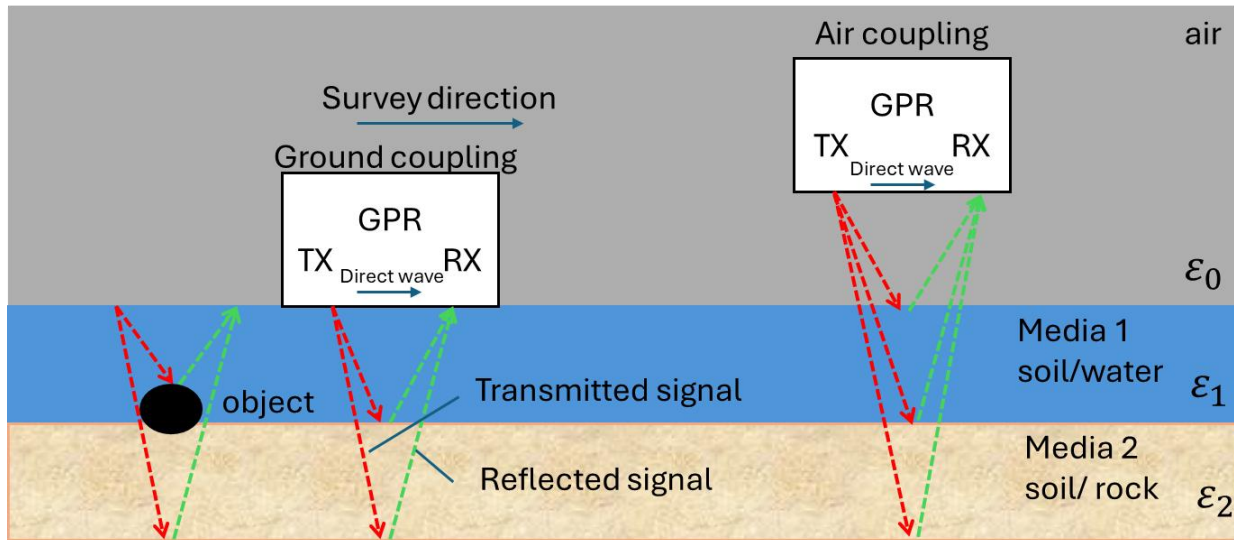


**Figure 11: Schematic diagram of a GPR survey. Reflected waves penetrating the subsurface travel at different velocities based on the dielectric permittivity ( $\epsilon$ ) of the media in which they encounter. All subsurface anomalies can be observed by the GPR.**

## Material and instrumentation

For this project, we used a custom-built frequency-domain GPR system developed by the research group. The developed GPR system attached a custom-made mid-size hexacopter UAV. Figure 12 shows the components of the GPR system and the UAV platform. For the transmitter and receiver antennas, we used the TBMA1 Biconical Measurement Antenna, which can operate between 30 MHz and 1000 MHz. Mini-circuits-vayyar transceiver board is used to generate frequency sweep signals and to acquire the signals from the receiver antenna. To amplify the RF signal power up to a 25dbm level, we used Mini-Circuits' ZHL-10M4G21W0. The onboard computer runs the designed GPR software and records GPR data and location information via a GPS unit.

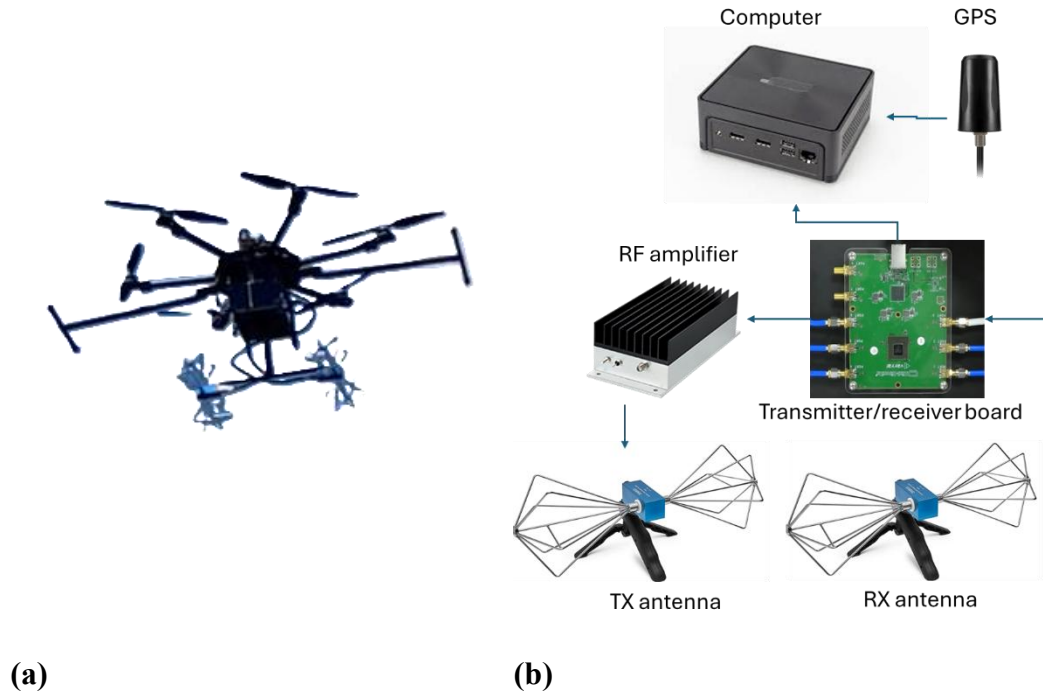


**Figure 12: (a) UAV-based GPR system. (b) Components of developed GPR system.**

### GPR model and processing steps

In the study, we used the stepped frequency sweeping GPR system. This system generates a continuous-wave signal between 200 MHz and 600 MHz with 10Khz IF and 200 frequency points. The reflected signals are received by the receiver antenna and the same transceiver board and recorded to the onboard computer. The received spectral data is converted to the time domain (A-scan) using the inverse Fourier transform. Then by using all sampled frequency responses, we generated B-scan radargram data. For preprocessing mean of B-scan data was removed B-scan data. Figure 13 shows the simplified process of the sweep frequency GPR system.

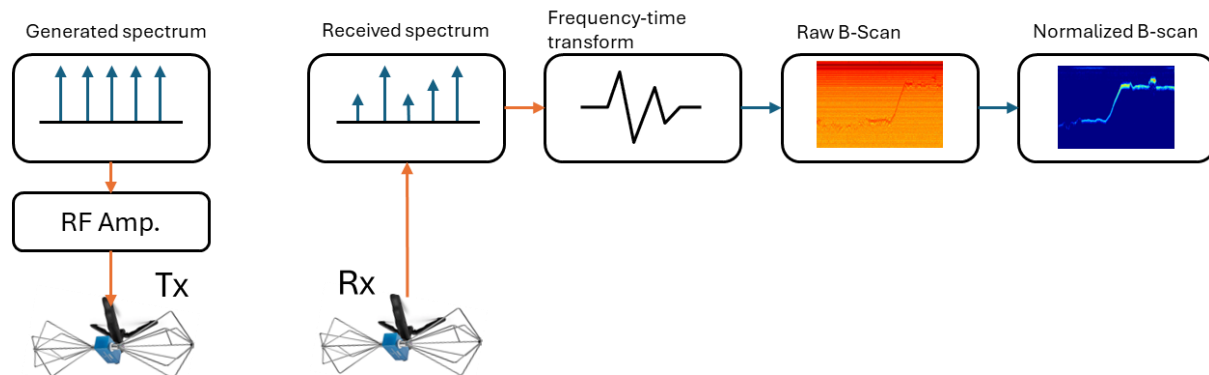


**Figure 13: Simplified flowchart of GPR processing steps.**

**Task 2: Design and conduct field data collections across a gradient of use cases, bathymetric sensor technology (including UAS-borne sonar and GPR sensors) and conditions and conduct outreach to public schools in the region during this process.**

Our objective was to evaluate the performance of UAS-echo-sounder and ground-penetrating radar (GPR) sensor technologies. The UAS-echo sounder was deployed across a variety of aquatic environments, including catfish ponds, lakes, rivers, nearshore coastal zones, and irrigation reservoirs. To assess its precision, we conducted a comprehensive accuracy analysis using data from a catfish pond and compared multiple interpolation techniques to identify the most effective method for generating high-resolution bathymetric models. Additionally, we investigated the technology's adaptability across different operational scenarios to understand its gradient of practical applications. Additionally testing bathymetric technologies like UAS-echo sounders and GPR across diverse aquatic environments is critical for assessing their operational limits, accuracy under variable conditions, and adaptability to real-world challenges. Each waterbody type introduces unique physical and environmental factors that influence sensor performance.

Select a range of waterbodies to capture diverse environmental conditions:

- **Catfish Pond:** Controlled environment with known depth reference data for accuracy assessment.
- **Lake:** Still water with potential vegetation and sediment variability.
- **River:** Flowing water with varying turbidity and depth.
- **Nearshore Coastal Water:** Saline environment with wave action and tidal influences.
- **Irrigation Water Reservoirs:** Shallow water with potential sedimentation and agricultural runoff.

A list of the selected sites is described in detail in Table 1 and locations in figure no.15

**Expected Outcomes**

- A comprehensive evaluation of UAS-echo-sounder and GPR performance across diverse waterbodies for bathymetric data collection.
- Identification of optimal interpolation methods for bathymetric surface generation.
- Insights into the operational limits and adaptability of these technologies for real-world applications.
- High-quality datasets for future research and technology development.

**Table 1:** Bathymetric data collection locations

Serial No.	Location	GPS coordinates	Data Collection Date	Total area covered (Acre)	Total flight time (approx)	Waterbody Type	Operational Mode	Sensor	Flight line spacing (Meter)	Speed
1	Bay Springs Lake	34.553921, -88.307328	02/24/2025	7.04	60min	Lake	Continuous	UAS-echo sounder	20	0.7m/s
2	Delta Research and Extension Center (DREC) of Mississippi State University (MSU)	33.451210, -90.897475	8/21/2024	1.67	60 min	Catfish Pond	Continuous	UAS-echo sounder	5	0.7m/s
3	(DREC), MSU	33.451210, -90.897475	9/10/2024	1.67	10min(LiDAR)/ 60 min(GNSS)	Catfish Pond	-	LiDAR/ GNSS	-	-
4	Grand Bay and Middle Bay, MS	30.426867, -88.371553	8/28/2025- 8/29/2025	15.416	120 min	Nearshore coastal water	Continuous	UAS-echo sounder	10	0.7m/s
5	North Farm, Starkville	33.474346, -88.773817	7/25/2024	1.46	30 min	Irrigation water reservoir	Continuous	UAS-echo sounder	10	0.7m/s
6	Tombigbee River	33.488027, -88.454831	02/06/2025	8.11	70 min	River	Continuous	UAS-echo sounder	20	0.7m/s
7	White's Creek Lake	33.556829, -89.275294	10/29/2025	5.04	40min(continuous)/ 60 min(Grasshopper)	Lake	Continuous/ Grasshopper	UAS-echo sounder	10	0.7m/s
8	North Farm, Starkville	33.474346, -88.773817	-	-	-	Irrigation water reservoir	-	GPR	-	-



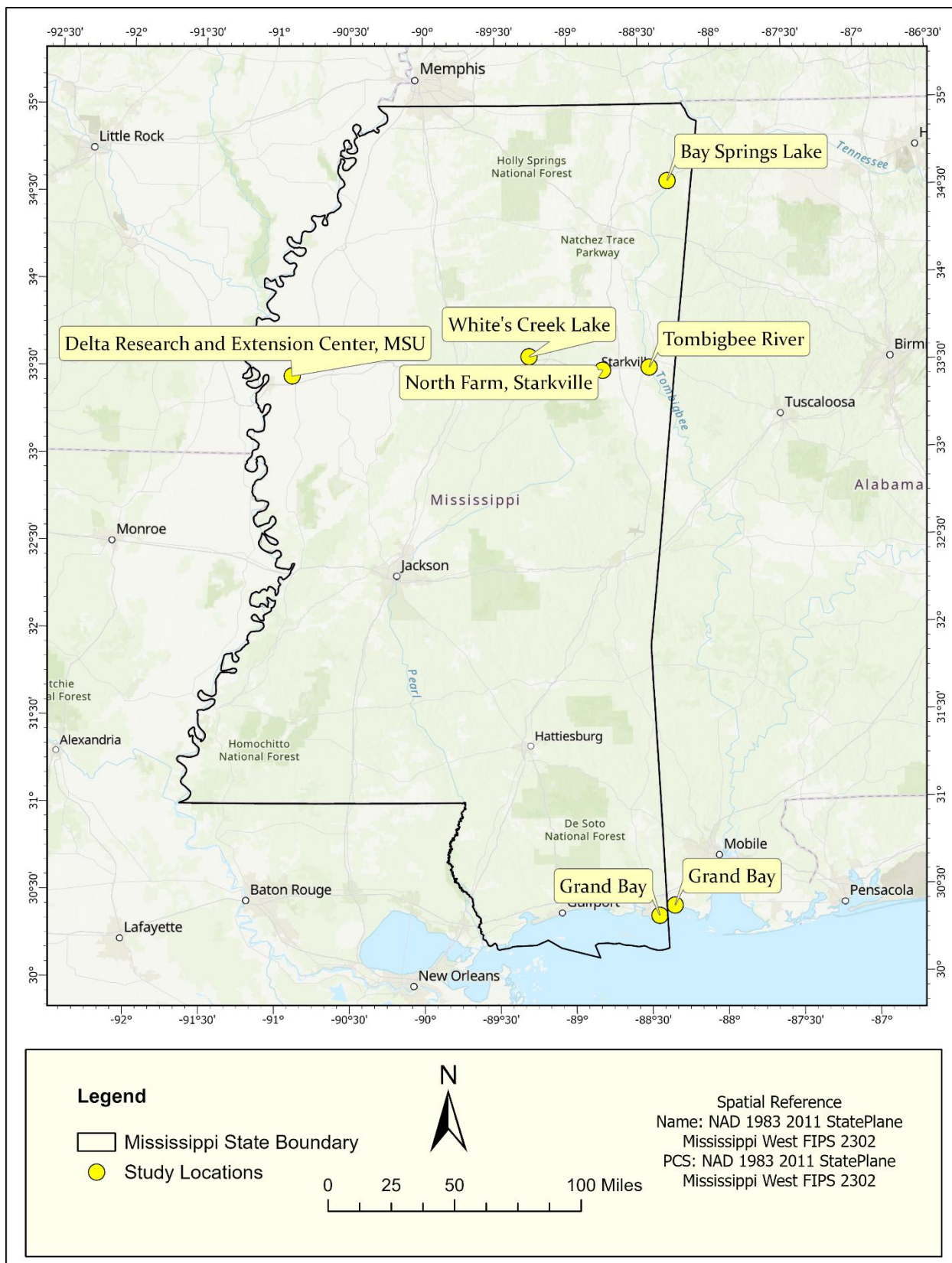


**Figure 14: Study area in Mississippi showing bathymetric data collection locations**

### Design and conduct Field Data Collection for Catfish Pond Studies:

We have selected a catfish pond at the Delta Research and Extension Center (DREC) of Mississippi State University (MSU). DREC of Mississippi State University mostly concentrates its research on cotton, rice, soybean, corn, and catfish production. DREC maintains many ponds as part of its catfish research setup. For our study, one of these catfish ponds was selected, located at 33.451210, -90.897475. The area of the pond is approximately 1.67 Acres.

### UAS-Echosounder data collection:

Our team first collected UAS-Echo-sounder data at the pond while it was full of water. Then the water of the pond was drained with the DREC's help.



**Figure 15: The study area at Pond D1, Delta Research and Extension Center (DREC), Stoneville, MS.**





**Figure 16: UAS-echo sounder data collection day at the catfish pond, DREC**

### **In-situ LiDAR data collection:**

After three weeks of the first sonar data collection, our team conducted a second survey of the empty pond with a LiDAR sensor.

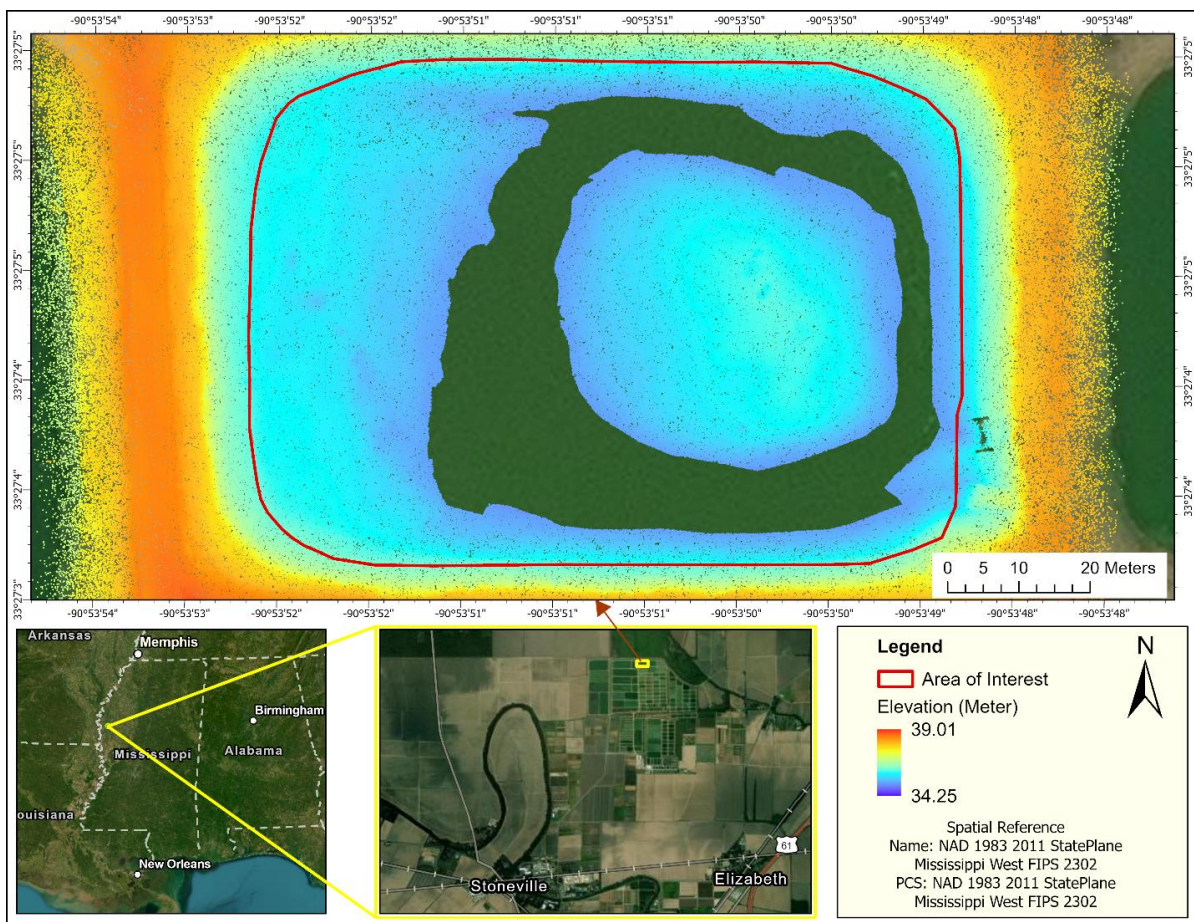


**Figure 17: LiDAR data collection at the drained catfish pond**



Within the area of interest, we have more than 218 million LiDAR points and to be exact it is 21839980 points.



**Figure 18: LiDAR data collection at the catfish pond, DREC**

#### **In-situ GNSS data collection:**

There was some water potholes left in the pond, and we collected the height of those potholes using a Trimble GNSS receiver.

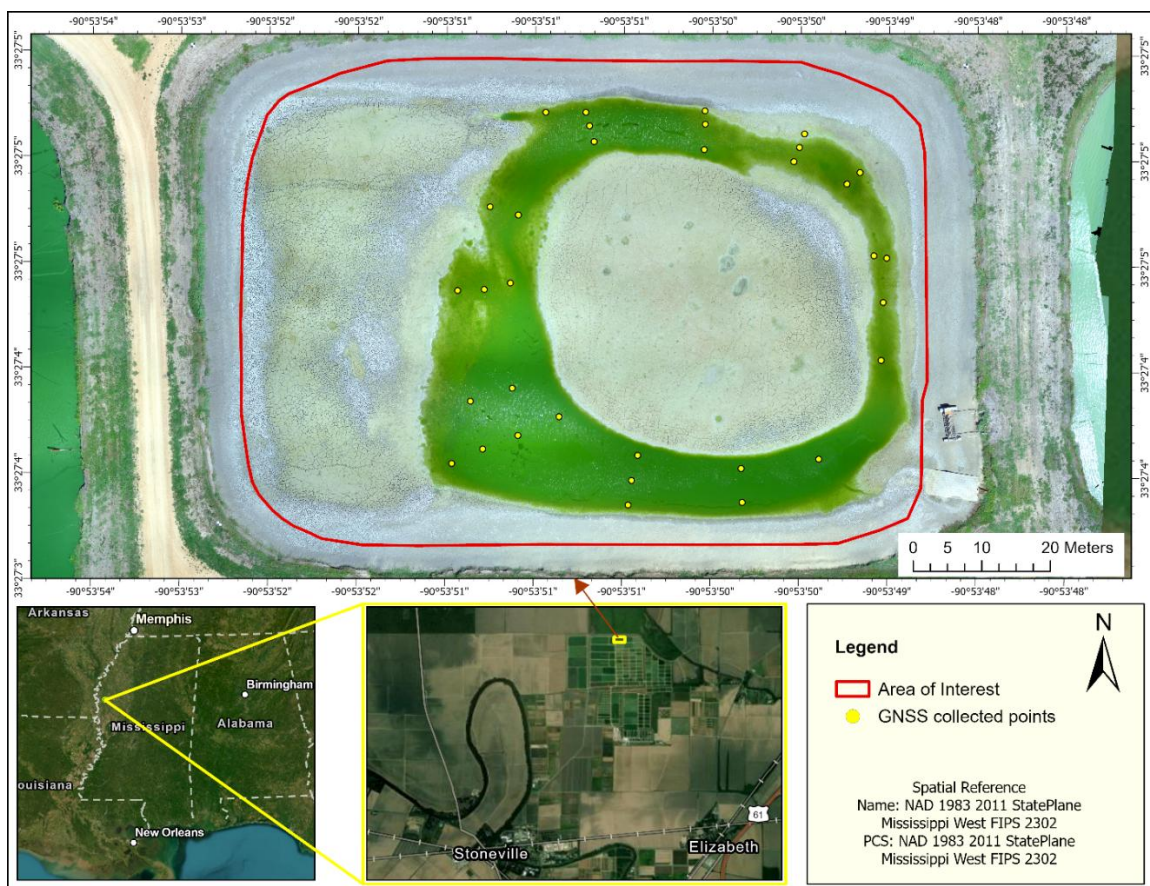


**Figure 19: GNSS data collection at the puddles of the catfish pond**

We covered bathymetry of the areas covered by puddles was manually sampled and we collected 33 reference points using GNSS.



**Figure 20: GNSS data collection day at the catfish pond remaining puddles**

These comparative data sets helped us to evaluate the accuracy and precision of the UAS-echo sounder data where LiDAR and GNSS topography data of the empty pond worked as a ground truth reference. It allowed us to conduct a very high level of accuracy assessment of the UAS-Echo-sounding bathymetric technology. End-to-end data pre- and post-processing workflows are explained in detail in Task 3.

Despite having reference Lidar data only for Catfish Pond, collecting data across diverse environments is critical for the following reasons:

### **1. Spatial Variability and Generalizability**

Bathymetric systems such as our UAS-echo sounder must operate reliably in varied environments. By surveying six distinct water bodies, including lakes, rivers, coastal waters, reservoirs, and ponds, we evaluate how factors such as sediment type, flow dynamics, turbidity, and vegetation affect measurements. This process confirms that our system's accuracy is not confined to the specific conditions of Catfish Pond but extends to broader applications.

### **2. System Validation Across Environmental Challenges**

While only Catfish Pond has reference Lidar data for direct comparison, data from other sites still validate the UAS-echo sounder's consistency through methods such as internal consistency checks (e.g., verifying depth measurements against known reservoir slopes or riverbed profiles),



anomaly detection to identify recurring errors like noise in flowing water, and performance benchmarking across environments. By contrasting results in calm ponds, turbulent rivers, and saline coastal waters, this approach highlights systemic limitations and environment-specific biases, ensuring the system's reliability is confirmed across diverse conditions.

### **3. Characterizing Environmental Influences**

By characterizing environmental influences across diverse sites, the system is uniquely challenged in each setting: lakes and ponds assess performance in calm waters, rivers evaluate noise from currents and uneven beds, coastal waters test turbidity and wave interference, and reservoirs analyze variable water levels and sedimentation. This variety of conditions pinpoints which environments necessitate algorithmic refinements or operational safeguards to ensure consistent and reliable functionality.

### **4. Future-Proofing the Dataset**

Collecting UAS-echo sounder data establishes a baseline for retrospective validation should reference data such as Green band bathymetric LiDAR or multibeam-sonar become available in the future. For instance, hydrological models or dredging projects in reservoirs and rivers may later generate ground truth data for comparison, while long-term monitoring of coastal erosion or lake sedimentation could utilize our dataset as a historical baseline. This proactive approach ensures compatibility with future validation efforts across diverse scenarios.

### **6. Scientific and Operational Relevance**

Our multisite approach advances bathymetric science by highlighting UAS-echo sounder limitations in underrepresented environments, such as turbid coastal zones, while informing best practices for applications like habitat mapping, flood modeling, and dredging operations. Additionally, it supports algorithm development to reduce noise in dynamic conditions, ensuring the system's adaptability and reliability across both research and real-world operational scenarios.

### **7. Mitigating Single-Site Validation Risks**

Relying solely on Catfish Pond risks overfitting validation to its unique conditions (e.g., calm water, uniform substrate). Multi-location data ensures our conclusions reflect real-world complexity, reducing the risk of deploying the system in untested environments.

### **Practical Justification in Our Study**

In our project, we emphasize:

Robustness: Ensuring the UAS-echosounder works in rivers and lakes, not just ponds.

Environmental diagnostics: Pinpointing where the system fails (e.g., high turbidity).

Legacy value: A public dataset for future researchers studying similar environments.

Risk reduction: Avoiding overconfidence in a system validated only in idealized conditions.

While Catfish Pond’s Lidar data provides critical validation, collecting data across six environments strengthens the scientific rigor and practical utility of our work. It ensures our UAS-echosounder is tested against real-world variability, supports future research, and delivers actionable insights for diverse users—from ecologists to engineers.

### Design and conduct Field Data Collection for Bay Springs Lake:



**Figure 21:** UAS-echo sounder data collection at Bay Springs Lake

Field data collection at Bay Springs Lake, a lake on the Tennessee-Tombigbee Waterway in Mississippi. The survey was executed with a flight path interval of 20 meters and required 60 minutes to finalize data collection for 7.04 acres. The total length of the flight path (m) covered using three sets of batteries is 1660.13 meters. The procedure encompassed meticulous planning of flight parameters, real-time monitoring during data collection, and post-processing to produce precise lakebed maps. The environmental conditions were optimal for data collection. The water surface was calm, creating a stable environment for UAS operations. This enabled us to conduct three complete, uninterrupted flight sessions, guaranteeing high-quality echo sounder data. The lack of wind and waves reduced interference, enhancing the mission's success. All equipment functioned as anticipated, and the collected data seems consistent and reliable.



**Figure 22: Filed data collection day at Bay Springs Lake**

We faced a configuration issue on our first flight and lost our first set of battery power. We described it in Task 3's observation section of Bay Springs Lake.

### **Design and conduct Field Data Collection for Grand Bay and Middle Bay, MS:**

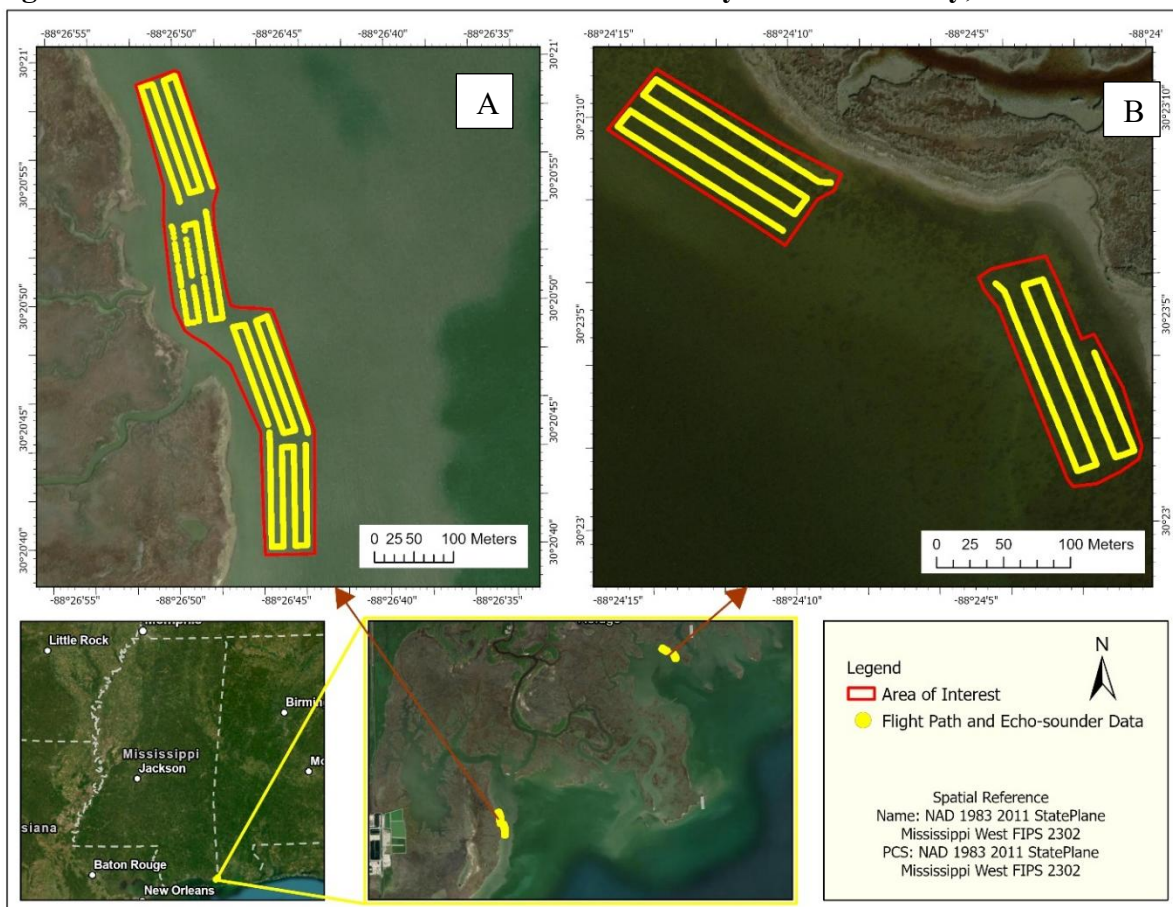


**Figure 23 UAS-echo sounder data collection at Grand Bay (A) and Middle Bay (B)**



Data collection along the Mississippi coast presented greater challenges compared to other locations. The Grand Bay Coastal Resources Center played a crucial role in facilitating our efforts. The process begins by boarding a boat from the docking area and traveling to the selected offshore coastal site. We then deploy our system from one of the boats provided by the Grand Bay Coastal Resources Center.



**Figure 24: Data collection day at Grand Bay and Middle Bay**

Field data collection at Grand Bay and Middle Bay, Mississippi, involved a detailed survey conducted with a flight path interval of 10 meters. The flight time alone totaled 120 minutes, allowing us to cover two distinct areas spanning 15.42 acres over a two days. Including the time spent traveling by boat to the survey location and collecting the data, the entire process required approximately 6 work hours across the two days.

Using six sets of batteries, we achieved a total flight path distance of 3,577.38 meters. Although we initially had only four battery sets, the two-day timeframe allowed us to recharge the additional two sets for use on the second day. The procedure involved careful planning of flight parameters, real-time monitoring during data collection, and thorough post-processing to generate precise maps of the bay areas. This facilitated six comprehensive, uninterrupted flight sessions, guaranteeing the collection of high-quality data. The flights proceeded without any notable issues, and the mission was executed with efficiency. However, we have faced some challenges, and we have some recommendations that we have discussed in task 3.



## Design and conduct Field Data Collection for North Farm, Starkville:

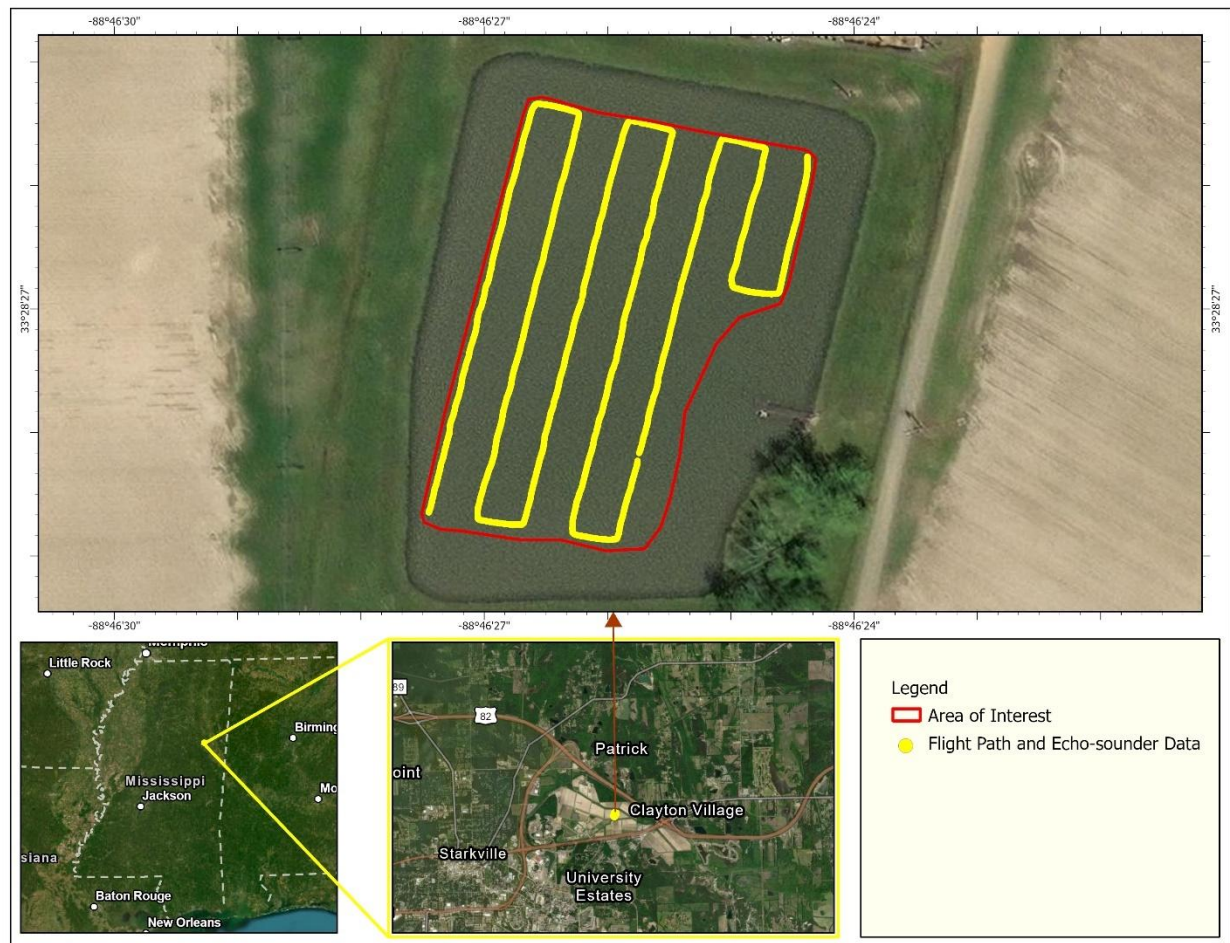


**Figure 25: UAS-echo sounder data collection at North Farm, Starkville**

The survey took place at the North Irrigation Water Reservoir Farm in Starkville, employing a flight path interval of 10 meters. The data collection necessitated 30 minutes to encompass 1.46 acres. The cumulative flight path length of 643.11 meters was attained over 1.25 flight sessions, with 40% battery life remaining to guarantee safe operations.



**Figure 26: Data collection day at North Farm, Starkville**

### Design and conduct Field Data Collection for Tombigbee River:



**Figure 27: UAS-echo sounder data collection at Tombigbee River**



The survey took place at the Tombigbee River in Mississippi, employing a flight path interval of 20 meters. The data collection necessitated 70 minutes to encompass 8.11 acres. The cumulative flight path length of 1,868.49 meters was attained over 3.5 flight sessions, with 40% battery life remaining to guarantee safe operations.



**Figure 28: Data collection day at Tombigbee River**

The procedure encompassed meticulous flight parameter planning, real-time monitoring throughout data acquisition, and post-processing to produce precise riverbed maps. The environmental conditions were ideal: calm water surfaces and minimal wind created a stable operating environment for the UAS, reducing interference and guaranteeing high-quality sonar data. All equipment functioned as anticipated, and the gathered datasets were coherent and dependable.

#### **Design and conduct Field Data Collection for White's Creek Lake:**

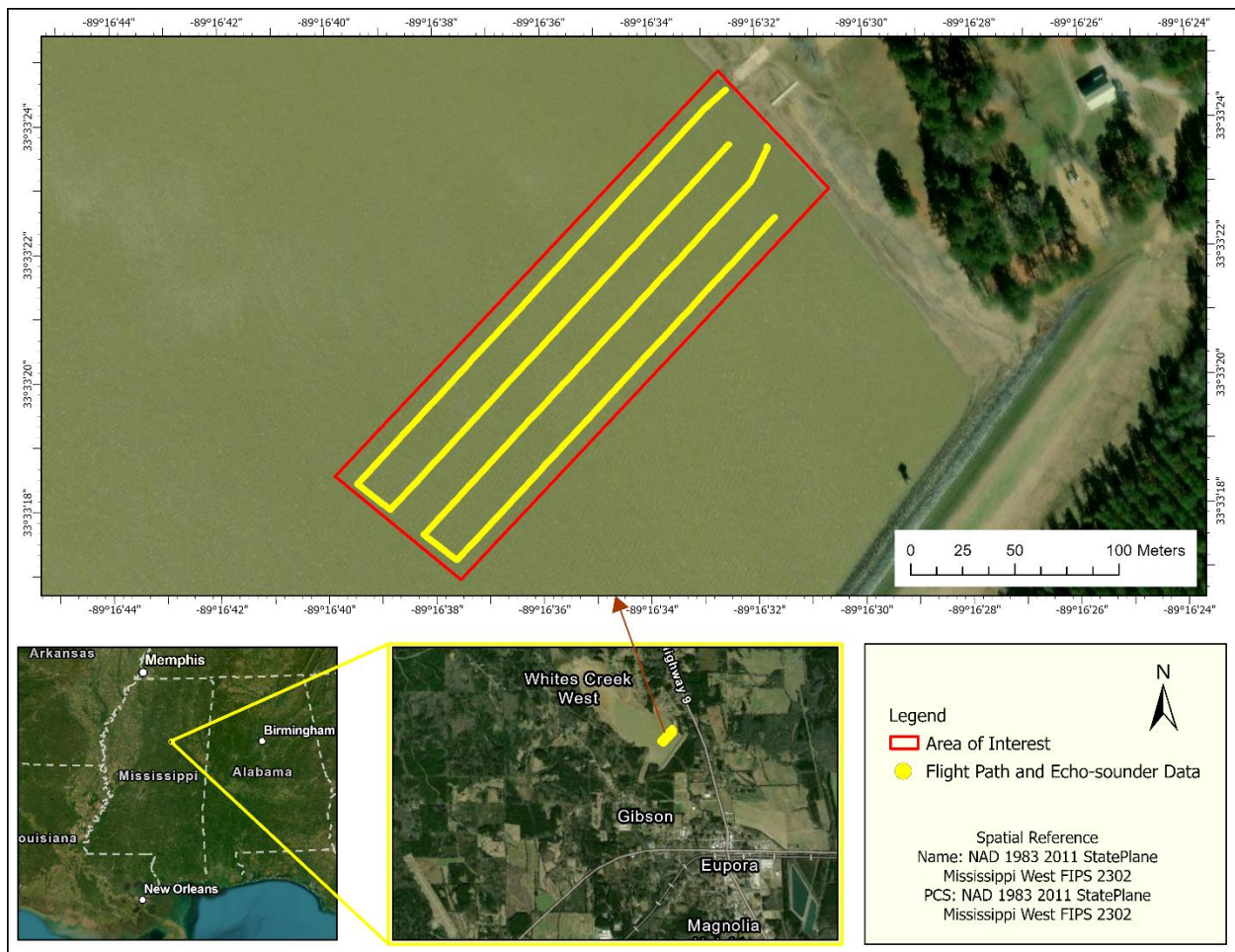


**Figure 29: UAS-echo sounder data collection at White's Creek Lake**

Field data collection at White's Creek Lake in Mississippi was executed with a flight path interval of 10 meters, necessitating 40 minutes to complete data collection for 5.04 acres. The complete distance of the flight path (1014.86 meters) was traversed utilizing two sets of fully charged batteries.



**Figure 30: Data collection day at White's Creek Lake**

The procedure involved careful planning of flight parameters, real-time monitoring during data collection, and post-processing to produce accurate lakebed maps. The environmental conditions were ideal: calm water surfaces facilitated a stable setting for UAS operations, allowing for two continuous flight sessions and guaranteeing high-quality echo sounder data. Minimal wind and wave activity diminished interference, thereby augmenting mission success. All equipment operated as anticipated, and the gathered data seemed coherent and dependable.

**Table 2: Collected UAS-echo sounder data of each location and flight line coverage length**

Serial No.	Location	Total length of the flight path (Meter)	Average flight path coverage using one single set of fully charged batteries (Meter)	Total flight required considering 40% remaining battery life	Actual total flight required considering 40% remaining battery life	Flight line spacing (Meter)	Total area covered (Acre)	Actual time required (minute)
1	Bay Springs Lake	1660.13	550	3.02	3	20	7.04	60
2	(DREC), MSU	1519.47	550	2.76	3	5	1.67	60
3	Grand Bay and Middle Bay, MS	3577.38	550	6.50	6	10	15.42	120
4	North Farm, Starkville	643.11	550	1.17	1.25	10	1.46	30
5	Tombigbee River	1868.49	550	3.40	3.5	20	8.11	70
6	White's Creek Lake	1014.86	550	1.85	2	10	5.04	40

We manually recorded the flight time and data collection parameters for each location, determining that an average flight path coverage of 550 meters is achievable per fully charged battery. The above table summarizes key metrics, including the average flight path coverage using one single set of fully charged batteries (Meter), the Total flight required considering 40% remaining battery life, and the actual total flight required considering 40% remaining battery life. These values help estimate the time and resources needed to survey specific waterbodies,

factoring in battery limitations and project requirements. For instance, locations like Bay Springs Lake (DREC) or Tombigbee River White's Creek Lake show varying flight counts and coverage areas, enabling tailored planning for efficient data collection.

## **Gradient of use cases**

The North Carolina Department of Transportation (NCDOT) has the potential to leverage UAS-echo sounder technology to transform future operations, including environmental monitoring (tracking ecosystems and sediment shifts), precision dredging (optimizing sediment removal in waterways), and proactive reservoir management (preventing urban flooding through sedimentation analysis). Advanced hydrographic surveys have the potential to improve navigational safety for bridges and ports. Additionally, applications such as submerged search and recovery, coastal erosion research, and archaeological site mapping would broaden NCDOT's responsibilities in protecting public safety, enhancing infrastructure resilience, and preserving cultural heritage. This approach would also contribute to cost reduction and minimize environmental impacts through informed decision-making based on data. A more detailed discussion is given below.

### **Environmental Monitoring and Research**

UAS-echo sounders serve as remarkably efficient instruments for the observation and delineation of aquatic ecosystems, especially in environments that present significant challenges or dangers, rendering conventional human-led surveys unfeasible or perilous. These systems demonstrate exceptional proficiency in delineating shallow, dynamic ecosystems, including lakes, rivers, and coastal zones, while delivering accurate data regarding underwater topography. Furthermore, they facilitate ongoing monitoring of essential environmental transformations, encompassing variations in water depth and sediment accumulation trends over time, thereby aiding in the informed stewardship of aquatic resources and initiatives aimed at enhancing coastal resilience.

### **Hydrographic Surveys**

Drone-based hydrographic survey systems offer significant benefits in various environments, especially in difficult conditions where conventional methods may struggle. They demonstrate exceptional proficiency in effectively mapping small, confined water bodies such as lakes, ponds, and reservoirs, addressing the challenges posed by the impracticality of boat-based surveys in these locations. Drones can operate safely in hazardous environments, including areas of contamination, or other risks, thereby mitigating potential dangers to human crews. These systems facilitate systematic depth monitoring of shipping lanes, inland waterways, and canals, identifying sediment accumulation that may lead to hazardous shallowing and ensuring navigational safety for vessels. Drones enhance the scope and safety of hydrographic data collection through the integration of precision, adaptability, and risk mitigation.

### **Dredging Operations**

UAS-echo sounders can be highly effective in supporting dredging projects by enabling accurate pre- and post-dredging surveys, which are critical for verifying the extent of sediment removal and ensuring compliance with project specifications and environmental regulations. These systems generate high-resolution bathymetric data before dredging to establish baseline conditions and after operations to confirm targeted volumes of material have been extracted, minimizing risks of over-dredging or incomplete removal while enhancing operational efficiency, cost-effectiveness, and environmental accountability.

### **Community Reservoir Maintenance**

High-resolution bathymetric data is essential for effective urban water reservoir management, facilitating targeted sediment removal in retention ponds and small-scale reservoirs. This ensures that these systems maintain their intended flood control capacity and support healthy aquatic ecosystems. By systematically tracking sedimentation patterns using UAS-echo sounders or similar technologies, municipalities can obtain actionable insights to proactively schedule dredging interventions, preventing potential threats to infrastructure resilience or ecological balance. This data-driven strategy not only protects stormwater management systems from capacity loss but also harmonizes operational efficiency with environmental stewardship, reducing flood risks while preserving habitat integrity in urban settings.

### **Search and Recovery Operations**

UAS-echo sounder utilizing single-beam technology can detect submerged objects, including debris or infrastructure, in aquatic settings. However, the detection of smaller objects is frequently constrained by the resolution of the acquired data. Operators can enhance detection capabilities by refining data collection strategies, such as modifying the spacing between flight lines. This method facilitates customization to optimize survey coverage and detail resolution, ensuring the system is adapted to the target object's dimensions and the project's particular specifications.

### **Port and Harbor Management:**

Periodic assessments of shipping routes and dock zones to ensure navigational safety. Expedited evaluations of sediment accumulation facilitate the optimization of dredging schedules.

### **Scientific Research**

UAS-echo sounder can facilitate diverse scientific pursuits, particularly in the examination of underwater geomorphology.



**Mapping submerged archaeological sites**

UAS-echo sounder technology has created new opportunities for underwater mapping and research by providing a blend of accessibility, safety, and efficiency across various applications. The enhancements underscore urban water infrastructure, transportation networks, and port administration while preserving consistency with the original framework.

**Task 3: implement end-to-end data pre- and post-processing workflows for site data collected and construct an implementation practicality envelope that defines what is and is not feasible and accomplishable with the request technology from an applied perspective by area of application (planning, modeling and mapping, and monitoring)**

### **Delta Research and Extension Center (DREC) of Mississippi State University (MSU):**

In this phase, we used the catfish pond for the accuracy assessment and validation of the UAS-echo-sounder sensor. Following the successful accuracy assessment, we tested additional locations and collected data under various environmental conditions. Finally, we conducted an analysis, documented the outcomes and observations, and provided recommendations along with the challenges we encountered during the data collection.

#### **Initial UAS-echo-sounder data cleaning and correction with the eye4hydromagic software**

The eye4hydromagic software echogram editor is an effective tool for preliminary data cleansing in this hydrographic survey. It enables users to visualize and eliminate sounding errors directly from the echogram, which illustrates the correlation between time and depth. Users can cleanse the data by employing a range filter to eliminate out-of-range measurements, manually identifying and discarding spikes or erroneous data points, and utilizing integrated smoothing algorithms like median and mean filtering to mitigate noise. This procedure mitigates measurement errors, zero-depth readings, and other discrepancies that may compromise the accuracy of the survey outcomes. By integrating these techniques, one can effectively cleanse the raw data and make it ready for subsequent processing and analysis.

A few steps need to be followed for the initial cleaning of the UAS-echo-sounder data. Cleaning UAS-echo sounder data entails the meticulous refinement of raw depth measurements. This procedure aims to eliminate noise, errors, and artifacts that may arise from sensor inaccuracies or varying environmental conditions. The Eye4hydromagic software echogram editor is an effective tool for preliminary data cleansing in this hydrographic survey. It enables users to visualize and eliminate sounding errors directly from the echogram, which illustrates the correlation between time and depth. An echogram is a graphical representation of the data collected by an echo sounder.

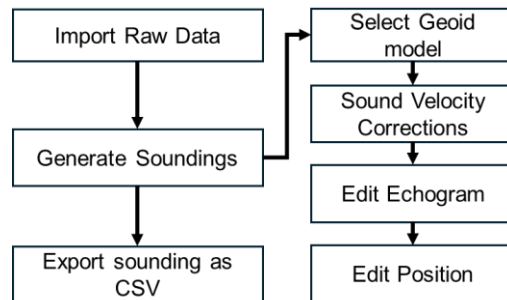
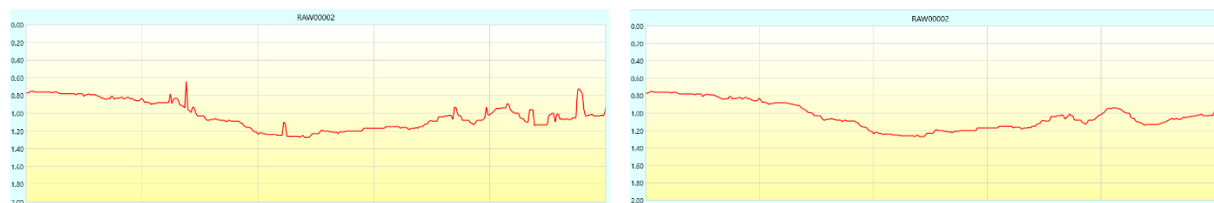


**Figure 31: Initial UAS-echo sounder data cleaning workflow using Eye4hydromagic software**

In the context of initial data cleaning of UAS-echo sounder data, the preliminary cleaning phase encompasses several steps (Fig. 16). After importing raw data, we generated soundings from it. To generate soundings, it is essential to select an appropriate Geoid model, which serves to rectify discrepancies in the Earth's surface. Next, we applied sound velocity corrections as needed, particularly in saline aquatic environments where variations in salinity and temperature can influence sound propagation. Then, it is essential to meticulously edit the echogram to eliminate any spikes and errors that may compromise the integrity of the depth profiles. Lastly, one must also refine the raw data position to make sure we have considered the correct datasets along the flight path and mission planning. These steps must be meticulously followed to ensure the accuracy and reliability of the bathymetric data obtained through the UAS-echo sounder. After implementing the pre-processing steps, we exported the soundings as CSV and used it for further analysis (Figure 3).



Raw reflected sound pulse data before data cleaning

Reflected sound pulse data post-data cleaning

**Figure 32: Editing the echogram to eliminate any spikes and errors**

## Export and Integration

Export Cleaned Data: Save corrected datasets in standardized formats (.csv) for integration with GIS platforms (e.g., ArcGIS Pro) or hydrodynamic models.

All the steps are discussed in the training video ([NCDOT deliverables 2025\SPH Documentation and training\Video recordings\UgCS SkyHub-ECT400 Echosounder Training\\_Day 2\\_01-10-23\\_Recording](#)). Initial cleaning is one of the most crucial steps for

ensuring high-quality, usable data. After exporting the data it is necessary to rename and save the file. It helps to import the CSV in the ArcGIS project environment.

We discussed data export in Hydromagic and importing to ArcGIS environment steps in more detail manner in Appendix 1 including visuals and screenshots.

#### **2.4.2 Preparing the UAS-echo sounder and *in-situ* data for accuracy assessment**

After cleaning the echo-sounding data, we assess each sounding point's elevation value. As the study site is a shallow water environment, we only considered high-frequency (200 kHz) collected elevation values acquired by the echosounder. We ensured that for both datasets, the ground truth LiDAR data and echo-sounder have the same Projected Coordinate System: NAD 1983 (2011) State Plane Mississippi West FIPS 2302 (Meters) and Vertical Coordinate System: NAVD88 height - Geoid18 (Meters). NAD 1983 and Geoid 18 ensure constant vertical referencing over both datasets, as a result, it improves the quality of comparative assessment. Finally, an exact methodology was employed to facilitate a significant comparison between echo-sounder and LiDAR data. The analysis focused on determining the search radius of 5 cm. This methodology facilitated a direct and precise comparison between the two datasets, significantly reducing spatial discrepancies and ensuring that only the most relevant LiDAR points were selected for comparison.

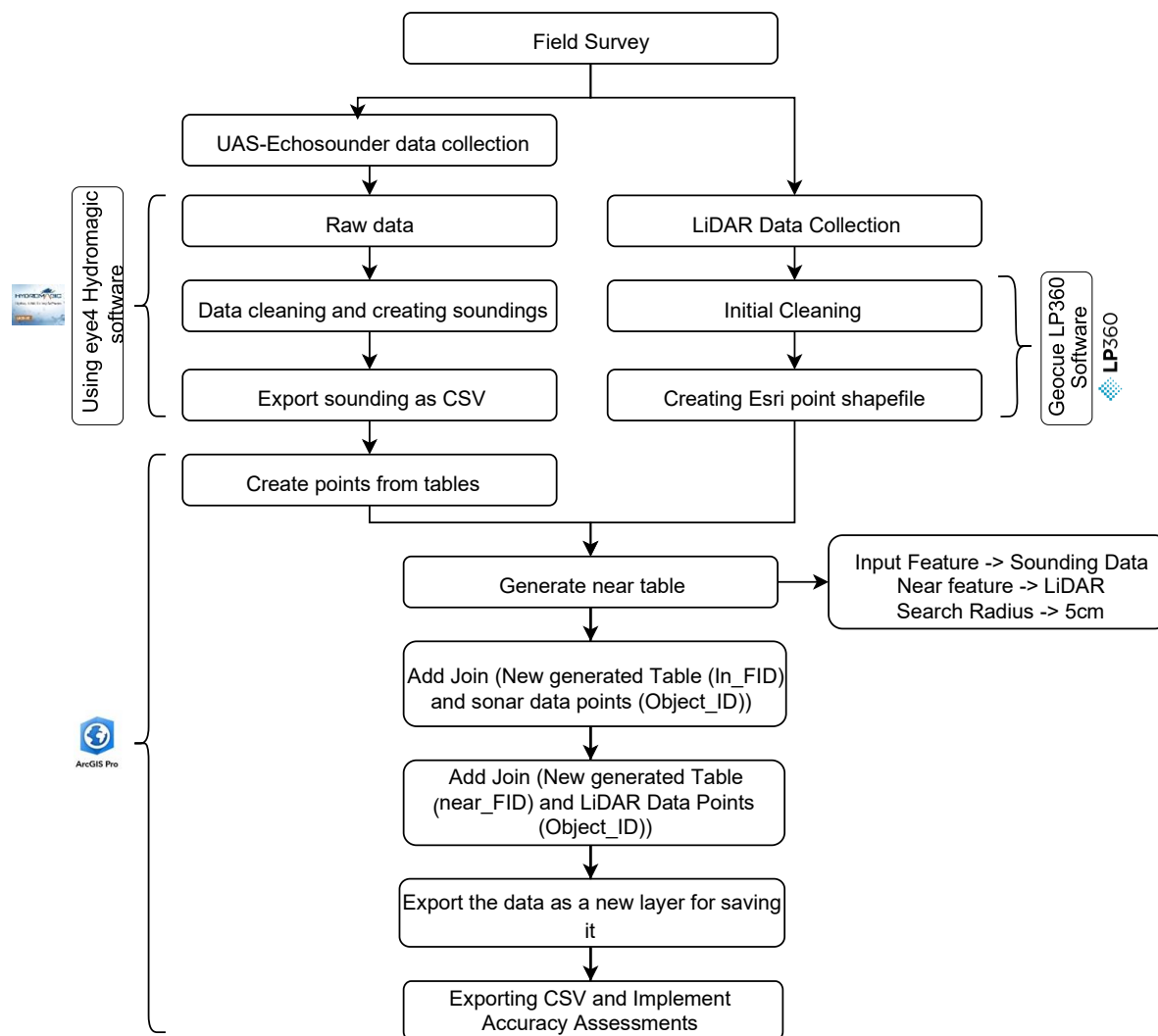


**Figure 33: Flowchart of UAS-echo sounder and LiDAR data integration process for field surveys using geospatial techniques.**

The diagram in Figure 31 shows the procedure for integrating UAS-echo sounder and LiDAR data for field surveys utilizing geospatial software. The process initiates with the collection of data from both UAS-echo sounder and LiDAR systems. The UAS-echo sounder data is subjected to cleaning and conversion into soundings, subsequently exported as CSV files. Concurrently, the LiDAR data is first cleaned and transformed into an Esri point shapefile utilizing LP360 software. Both datasets are utilized to construct points from tables, which are subsequently processed to produce a near table. This adjacent table enables the integration of sonar data points with LiDAR data points based on horizontal proximity (within a 5 cm radius). Finally, the consolidated data is exported as a new layer for additional analysis, culminating in CSV export and accuracy evaluation.

### 2.4.3 Data preparation for interpolation performance analysis

After the accuracy assessment of the echo-sounder data against *in-situ* reference data, several interpolation techniques were run.

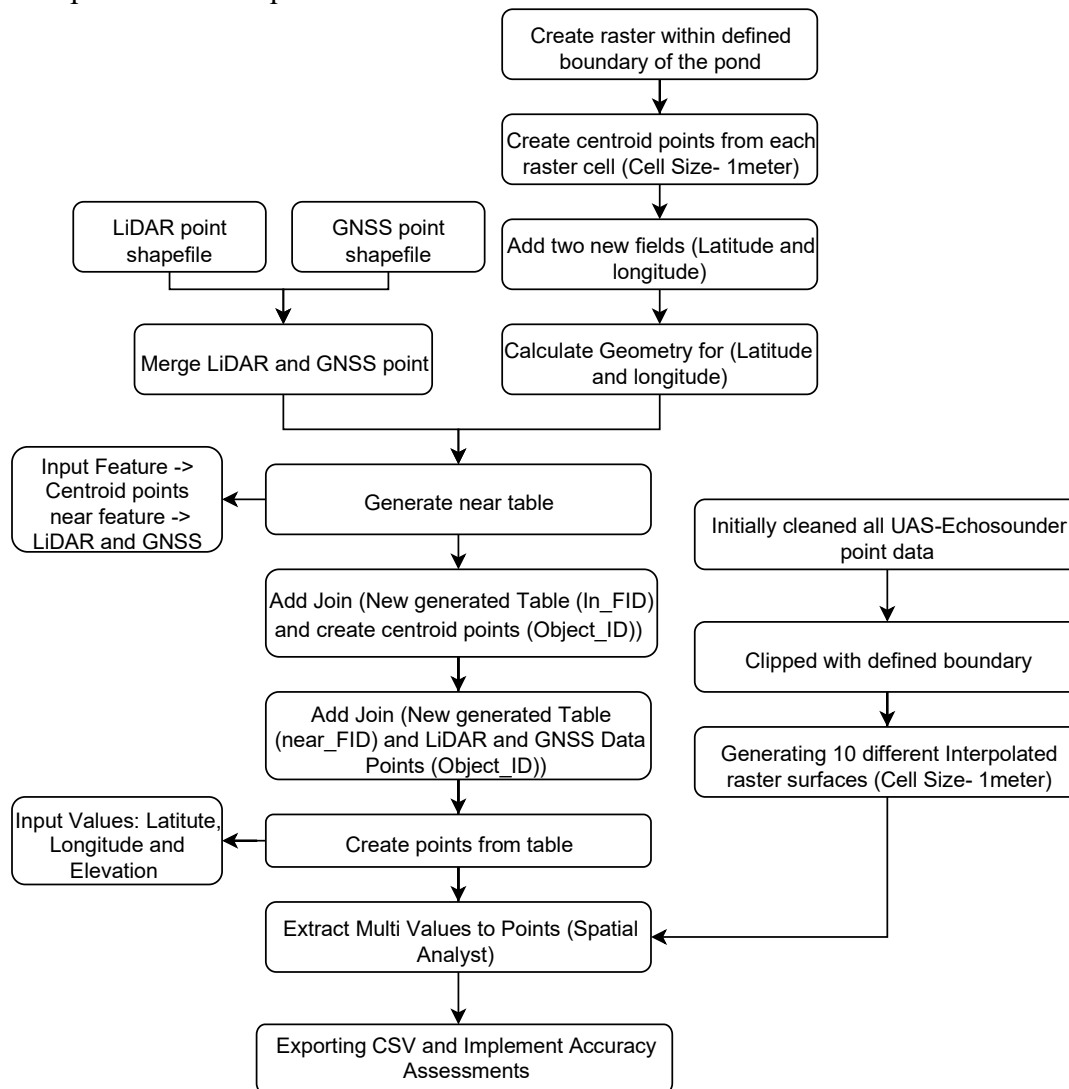


**Figure 34: Workflow of integrating LiDAR and GNSS values with interpolated raster surface using Echo-sounder data and accuracy assessment.**

The workflow diagram outlines a procedure for generating and examining geospatial data relevant to a pond. The process begins with the creation of a 1-meter resolution raster surface within the pond's specified boundary, subsequently generating centroid points from each raster cell. Two new fields for latitude and longitude have been incorporated, and their geometry has been computed. Next, the LiDAR and GNSS point shapefiles are merged, and the resulting centroid points serve as input features for the generation of a near table. This adjacent table enables the integration of sonar data points with LiDAR data points based on proximity (within a 75 cm radius). GNSS points, on the other hand, were in a unique situation because they were spread out. The centroided points were positioned approximately 0.75 meters from the corner of

each 1-meter resolution square-shaped cell. So, a search radius within 75 cm has been considered for the nearest table generation. This strategy meets two goals: it ensures that UAS-echo sounder data generated interpolated centroid raster values will be compared with GNSS data, and it follows IHO guidelines for checking the accuracy of echo-sounder data. This makes the combined dataset better overall in terms of quality and reliability. Concurrently, initially cleaned UAS-echo sounder point data has been clipped to the specified boundary, producing ten distinct interpolated raster surfaces with a 1-meter cell resolution. The next step was to incorporate joins between the generated tables and the LiDAR/GNSS data points. Points are generated from the table utilizing latitude, longitude, and elevation data. Finally, multi-values are extracted to points through spatial analysis, resulting in the exportation of data to CSV format and the execution of an accuracy assessment. In total, we found a comparable 5237 centroid points for accuracy assessment.

#### **2.4.4 Data selection and experimentation with sample points**

The UAS-echo sounder system has an option to selectively activate the echo-sounder at designated intervals along the flight trajectory, rather than continuously towing through the water. This technique is called grasshopper mode and offers several benefits including obstacle avoidance, precise point measurement, and adaptation to challenging environments. We explored the effectiveness of this mode by sampling data at specific intervals. We implemented two flight line spacing configurations: 5 meters and 10 meters. Along these flight lines, we tested data points at varying intervals of 5, 10, 20, and 30 meters. Using a systematic approach, we sampled data, applied interpolation to create continuous bathymetric surfaces, and tested the results for accuracy, determining the optimal balance between flight line spacing and data point frequency to achieve high-quality maps and maximize survey efficiency.



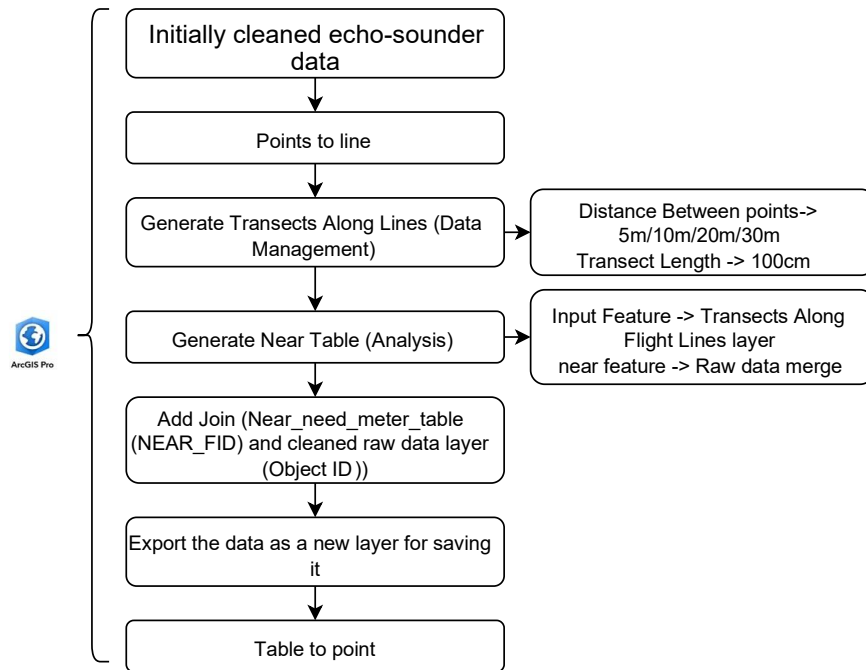


**Figure 35: Data sampling workflow and accuracy assessment**

The first step is to import initially cleaned echo-sounder data to the ArcGIS pro project environment. The next step involves generating lines from these points. Then transects are established along these lines, ensuring that the distance between the transect is defined and the transect length is 100 cm (matter of choice). A near table is generated through analysis, where the sounding data joins to create the near feature, while the input feature consists of the transects along the lines layer. The cleaned-sounding data layer (Object ID) and the near table (NEAR\_FID) subsequently joined operationally. The data is exported as a new layer for subsequent storage. The table is ultimately converted back to points utilizing latitude and longitude coordinates, thereby completing the process. Concurrently, sampled UAS-echo sounder point data has been clipped to the specified boundary, producing ten distinct interpolated raster surfaces with a 1-meter cell resolution. Finally, multi-values are extracted to points through spatial analysis as of the workflow mentioned in Figure 6, resulting in the exportation of data to CSV format and the execution of an accuracy assessment. In total, we found a comparable 5237 Centroid points for accuracy assessment.

We used *in-situ* reference measurements derived from LiDAR and GNSS systems to evaluate the accuracy of our UAS-echo-sounding data. Three main statistical measurements were used in the validation process: standard deviation (SD), coefficient of determination ( $R^2$ ), and Root Mean Square Error (RMSE). These measures gave us a thorough assessment of the alignment between our UAS-derived data and the reference data, so enabling us to measure the dependability and precision of our UAS- echo-sounding observations.

### 3. Results

#### 3.1 Data Quality Assessment Result

After primary data cleaning, we found 11439 points for the accuracy assessment. The validity check of UAS-echo sounder data with *in-situ* LiDAR data elevation measurements produced promising results, revealing specific locations with significantly higher error values than other areas. A scatter plot and additional figures were created to provide a concise visual representation of these findings, demonstrating the spatial distribution of errors and the correlation between the two datasets. This comprehensive evaluation not only identified areas of strong accuracy assessment between UAS-echo sounder and LiDAR measurements, but it also identified regions that require additional investigation or calibration.

Table 1: Accuracy of UAS-echo-sounding data relative to in-situ LiDAR data

Data	Total number of points	Number of outliers	Points after removing outliers	Upper limit of Error Value (m)	Lower limit of Error Value	R2	RMSE (m)	RMS E (cm)	Data loss
All Points	11439	N/A	11439	N/A	N/A	72.8%	0.102	10.2	0%
3 SD (97.33%)	11439	43	11396	0.3191	-0.2266	73.6%	0.1004	10.04	0.38%
2 SD (95.45%)	11439	1140	10299	0.2282	-0.1356	86.6%	0.0659	6.59	9.97%

Table 1 shows the analysis encompassing three data scenarios: all points, data within three standard deviations (3 SD), and data within two standard deviations (2 SD). The aggregate points total consistently stands at 11,439 in all scenarios. Considering all points overall accuracy of the UAS echo-sounder sensor with a root mean square error (RMSE) of 10.2 cm and  $R^2$  value of 0.728. In the 3 SD scenario, 43 outliers are identified, resulting in 11,396 points and a negligible data loss of 0.38%. The upper and lower error value limits are 0.3191 and -0.2266, respectively, with an  $R^2$  value of 0.736 and a (RMSE) of 10.04 cm. In the 2 SD scenario, 1,140 outliers are eliminated, resulting in 10,299 points and a data loss of 9.97%. This situation demonstrates enhanced precision with an  $R^2$  value of 86.6% and a smaller RMSE of 6.59 cm. The table indicates that employing standard deviation thresholds to filter outliers improves correlation and minimizes error in echo-sounding data compared to LiDAR measurements.

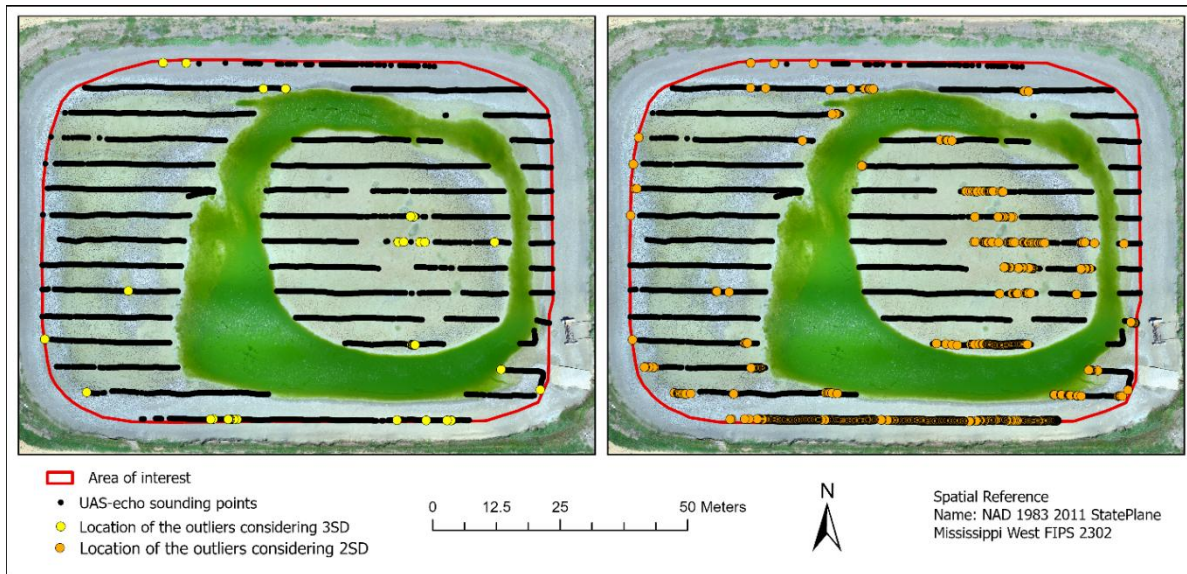


**Figure 36: Location of UAS-bathymetry data outliers plotted by (a)3 standard deviations (SD) (left) and (b)2SD (right), respectively.**

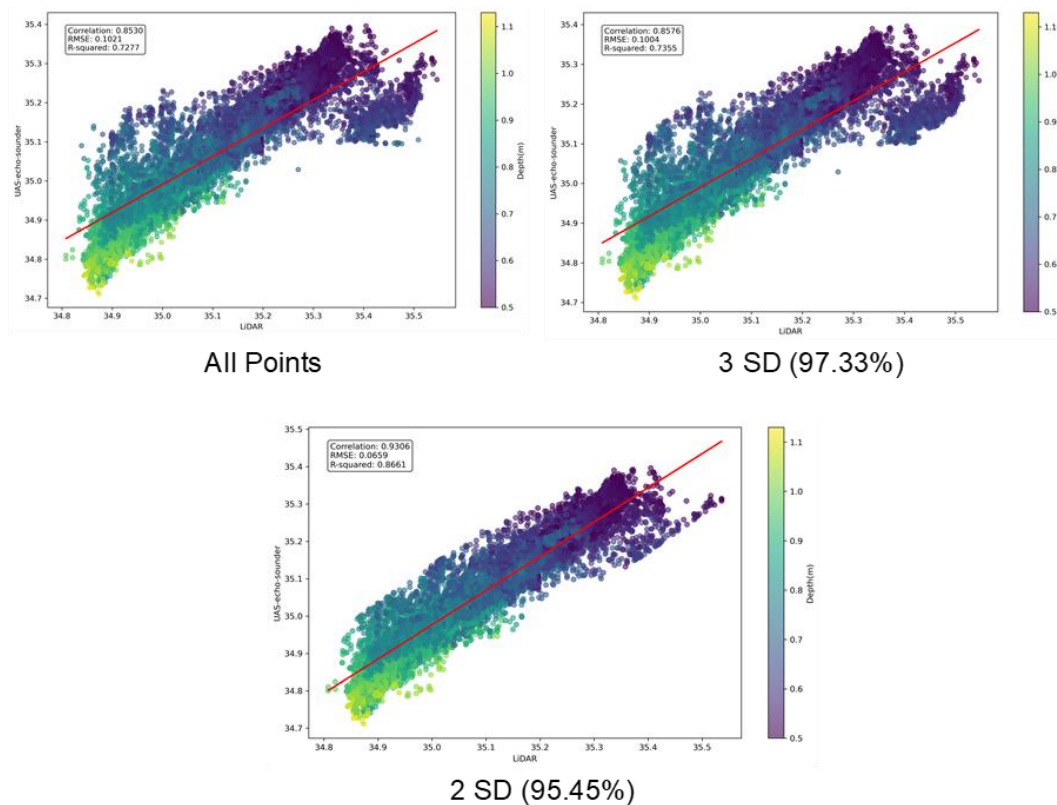


**Figure 37: Scatterplots illustrating the correlation between UAS-echo sounder bathymetric measurements and LiDAR-derived elevation data, highlighting data distribution and accuracy assessment.**

The scatter plots show the outlier's locations, and it is found that most of the locations are shallower areas (the color bar shows the depth of the waterbody) where the error values are high, alternatively in deeper regions where there is more depth there are fewer outliers.

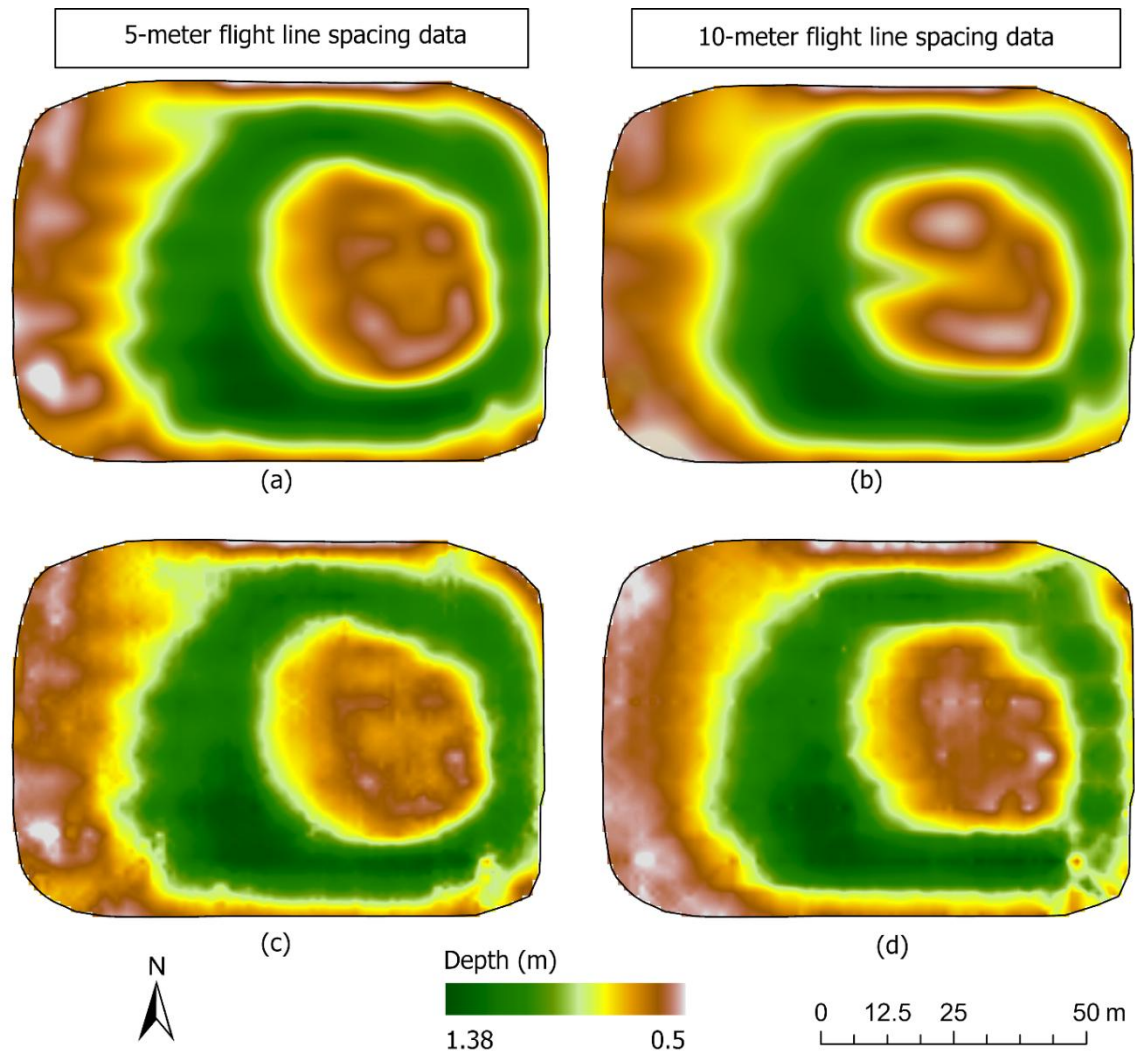
### 3.2 Interpolation Performance Analysis

Table 2: Assessing echo-sounder accuracy: comparing interpolated echo-sounder data with ground truth LiDAR and GNSS measurements

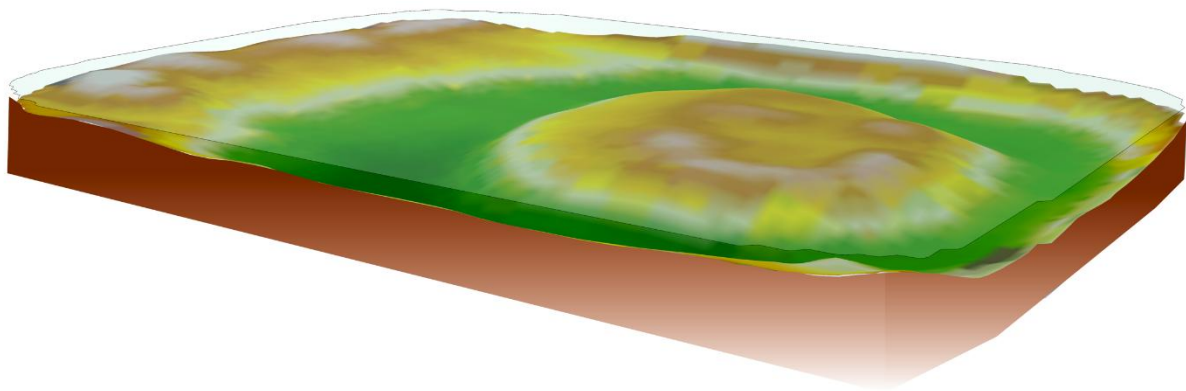
Serial no.	Independent Variable	5-meter flight line spacing		10-meter flight line spacing	
		R-squared	RMSE (cm)	R-squared	RMSE (cm)
1	IDW	78.1%	7.3	75.7%	8.1
2	RBF-CRS	80.0%	6.7	78.8%	7.1
3	RBF- IMF	78.8%	6.8	75.3%	7.5
4	RBF-MF	78.0%	7.1	78.5%	7.3
5	RBF-SWT	79.9%	6.7	78.1%	7.3
6	RBF-TPS	0.2%	-	-	-
7	OK	78.4%	7.1	78.2%	7.5
8	UK	80.3%	6.8	77.9%	7.6
9	SK	76.9%	7.5	71.1%	9.0
10	Topo to Raster	82.9%	6.3	81.5%	7.1

Table 2 shows the assessment of various interpolation techniques for echo-sounder data in comparison to ground truth LiDAR and GNSS measurements, utilizing R-squared and RMSE metrics for 5-meter and 10-meter flight line intervals. The Topo to Raster method exhibits the highest accuracy, evidenced by optimal R-squared values (82.9% for 5-meter and 81.5% for 10-meter flight line spacing) and minimal RMSE values (6.3cm for 5-meter and 7.1 cm for 10-meter spacing), signifying exceptional performance in both instances. Conversely, the “RBF\_TPS” method demonstrates bad performance, especially indicated by exceedingly high RMSE values, implying considerable inaccuracies. Alternative methods such as RBF-CRS and UK demonstrate commendable performance; however, they are surpassed by Topo to Raster.





**Figure 38: 1-meter resolution bathymetric surfaces generated using the top-performing interpolation methods for two different flight path spacing scenarios: (a)Topo to Raster (5-meter flight line spacing), (b)Topo to raster (10-meter flight line spacing), (c) Universal Kriging (UK) (5-meter flight line spacing), (d) Radial basis function - Completely regularized spline (RBF-CRS) (10-meter flight line spacing)**



**Figure 39: 3D of the Catfish Pond's bathymetric surface.**

### 3.3 Sampled data and their comparative performance analysis

In this section, several interpolation techniques have been thoroughly examined on echo-sounder data, considering two flight line spacings and data point intervals along the flight lines. We compare the effectiveness of ten different interpolation techniques for each flight line spacing, considering four different data point sampling along the flight lines, which are 5,10, 20, and 30-meter spacing along the flight lines.

By considering 5-meter flight line spacing and four different sample point spacings along the flight line, the following results (Figure 10 & Figure 11) demonstrate how varying sampling densities impact the accuracy and resolution of the collected data.

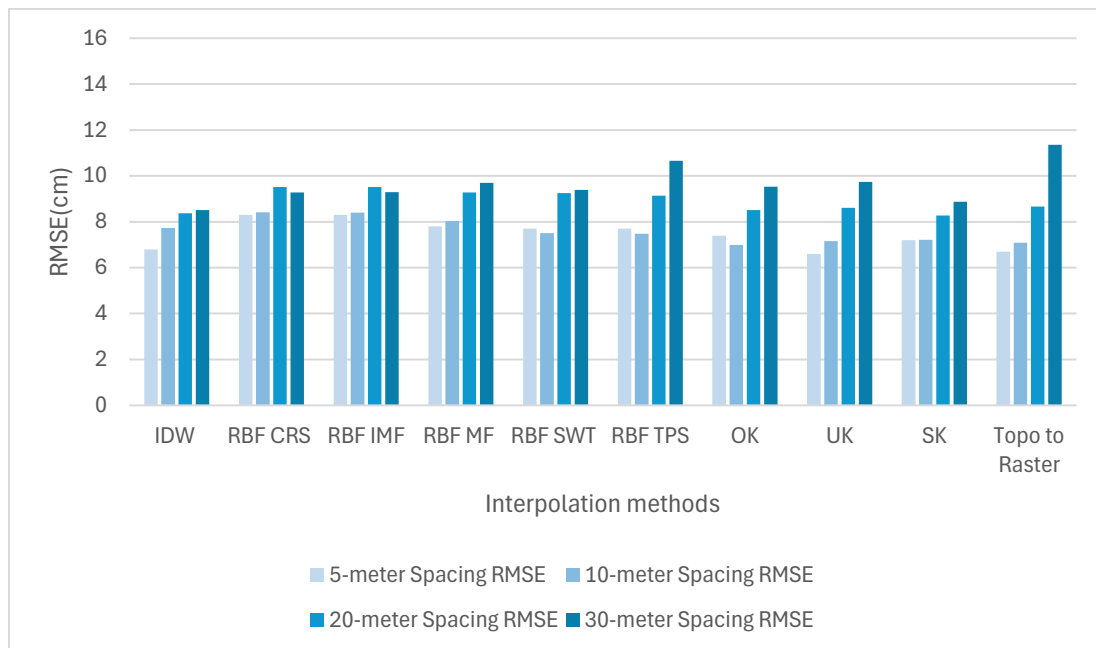


**Figure 40: Comparison of RMSE across various interpolation methods for a 5-meter flight line spacing, evaluated at four different point sampling intervals along the flight lines.**

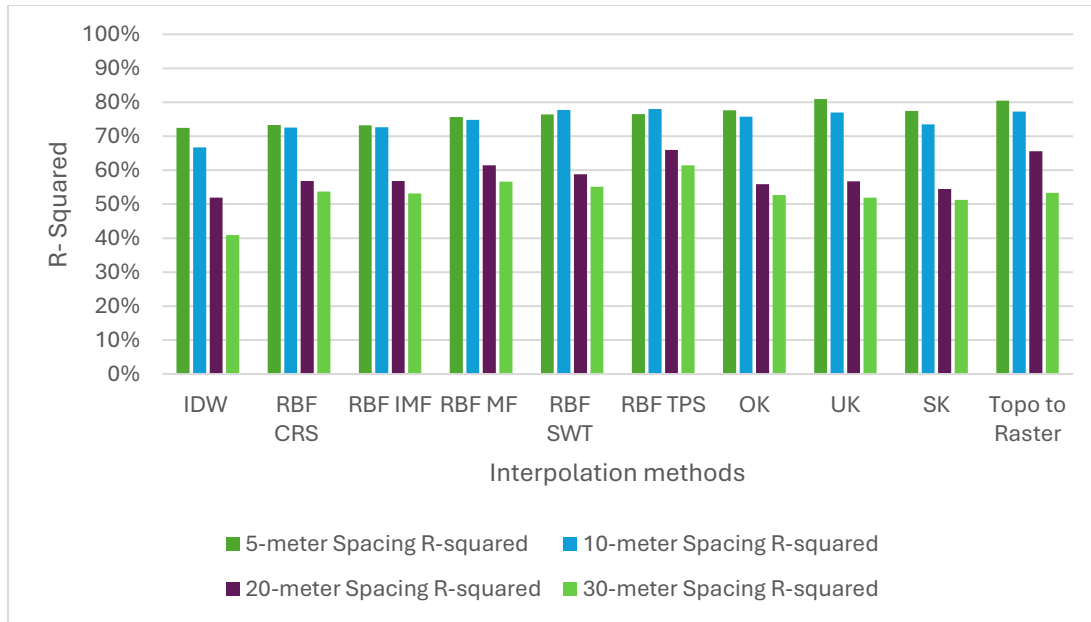


**Figure 41: Comparison of R-squared values for various interpolation methods at a 5-meter flight line spacing, assessed across four different point sampling intervals along the flight lines.**

The comparison of interpolation methods at 5-meter flight line spacings and four different point sampling along the lines. interpolation methods across different spatial resolutions reveal a consistent pattern in both RMSE and R-squared values. The RMSE values show an increasing trend as spacing increases from 5m to 30m, with Topo to raster exhibiting the highest RMSE values (reaching 11.356 at 30m spacing), while OK and UK methods demonstrate the lowest RMSE values around 7.4 and 6.6 at 5m spacing respectively. Similarly, the R-squared values display a decreasing trend as spacing increases, with the highest values observed at 5m spacing and the lowest at 30m sample point spacing. All interpolation methods (IDW, RBF variants, and Kriging methods) consistently perform better at finer resolutions (5m spacing), with performance degrading as the spacing increases, particularly between 5m and 20m intervals, while Kriging methods (OK, UK) maintain relatively superior performance across all spatial resolutions compared to other techniques. Universal Kriging at 5m point spacing achieved the best performance with an R-squared of 81% and RMSE of 6.6 cm.

By considering 10-meter flight line spacing and four different sample point spacings along the flight line, the following results (Figure 12 & Figure 13) demonstrate how varying sampling densities impact the accuracy and resolution of the collected data.

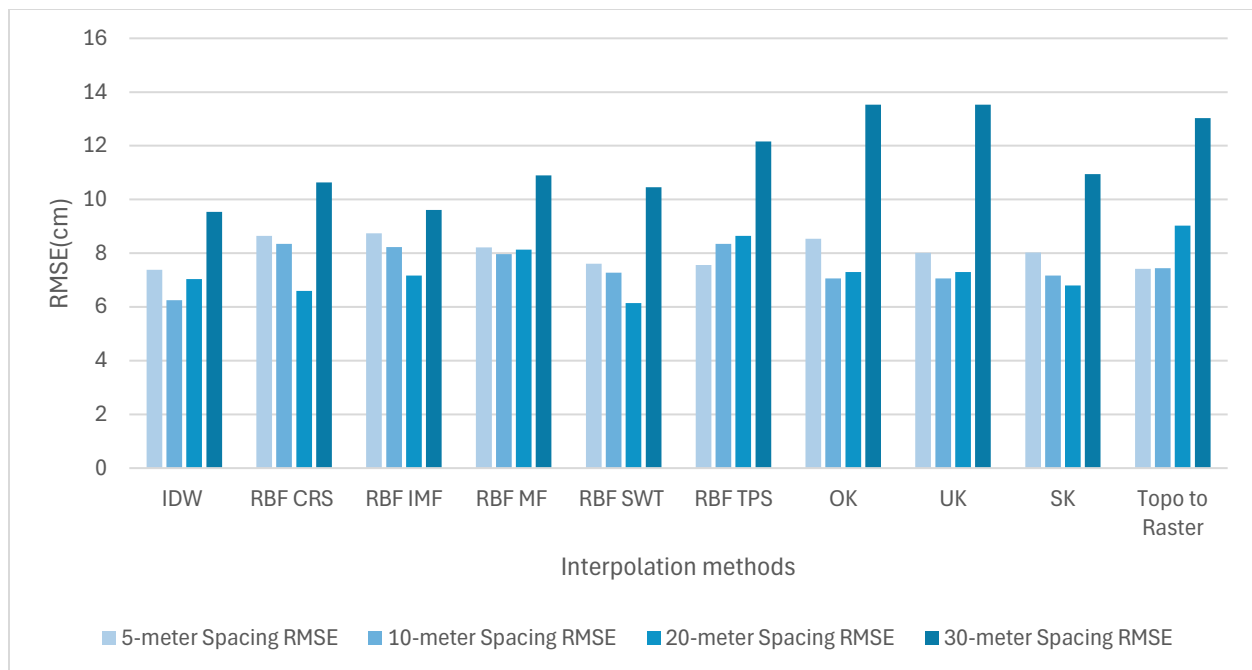


**Figure 42: Comparison of RMSE across various interpolation methods at a 10-meter flight line spacing, evaluated at four different point sampling intervals along the flight lines.**

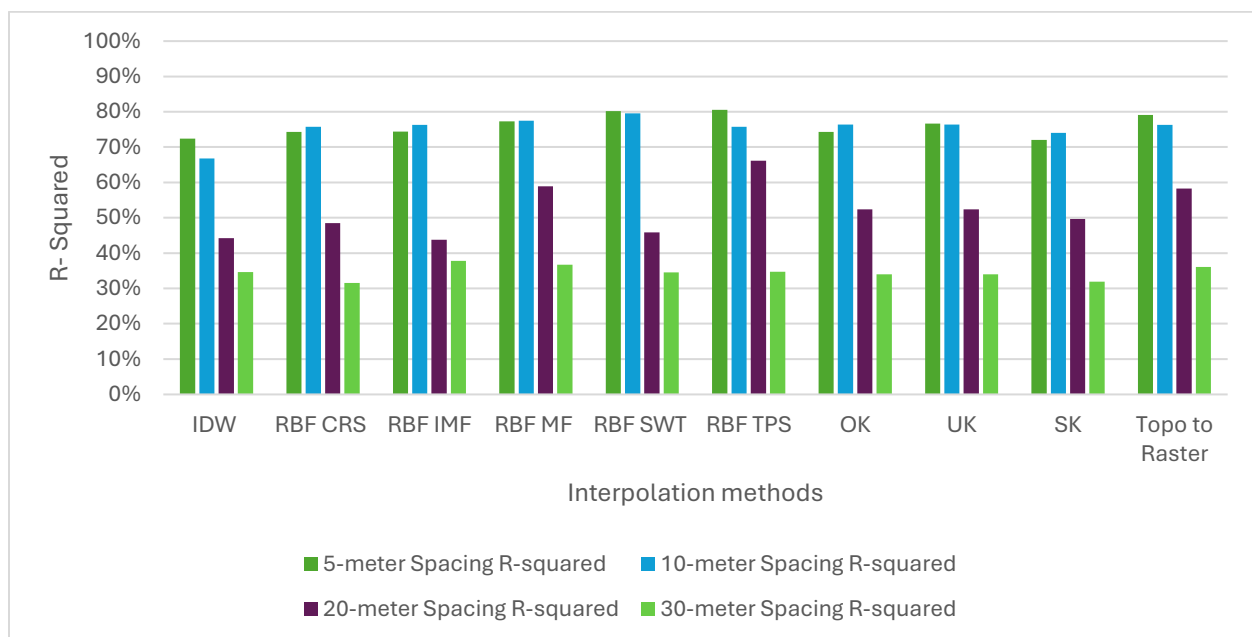


**Figure 43: Comparison of R-squared values for various interpolation methods at a 10-meter flight line spacing, assessed across four different point sampling intervals along the flight lines.**

The study shows that using 10-meter flight spacing produces lower R-squared values and greater RMSE (Root Mean Square Error), so it represents less accuracy and dependability in the



bathymetric data. Although 10 or 20-meter sample point spacing can sampling points have lower RMSE, the R-squared values for 20-meter spacing are low, so it questions the dependability of the bathymetric surface data collected at this distance.

5-meter or 10-meter spacing sample points are better for more accurate and dependable data collecting since they balance RMSE (around 7 to 8 cm) with higher R-squared values (more than 70%). These spacings therefore provide a better representation of the actual bathymetric surface, so guaranteeing more consistent findings for use in analysis and decision-making.

In Appendix 2 we include the top 10 interpolation methods for all different scenarios and the Python scripts used for accuracy assessment.

### **Observations:**

The evaluation of UAS-echo sounder data against *in-situ* LiDAR and GNSS measurements produced encouraging findings. The root mean square error (RMSE) of 10.20 cm, along with an R-squared value of 72.8% for the entire dataset, suggests a significant accuracy of the UAS-echo sounder data. Focusing on 95.45% of the data, which is contained within two standard deviations, resulted in an RMSE improvement to 6.59 cm, and the R-squared value increased to 86.6%. This enhancement suggests that even with outliers present, most data points demonstrate a significant level of accuracy, particularly in deeper regions where error values are reduced. The increase in errors observed in shallower regions can be linked to various factors including water surface reflections, sensor limitations, or environmental conditions, indicating a need for further examination. The evaluation of interpolation methods indicates that Topo to Raster demonstrates superior performance, attributed to its ability to produce hydrologically accurate surfaces, which is particularly beneficial for bathymetric data. Alternative techniques, including Universal Kriging (UK) and Radial Basis Function with Completely Regularized Spline (RBF-CRS), exhibited notable effectiveness; however, they did not surpass the performance of Topo to Raster. The study investigated the impact of different sampling intervals along flight lines on the precision of the data collected. The use of 5-meter and 10-meter sampling intervals along flight lines demonstrates an effective equilibrium between data density and survey methods. The RMSE values observed ranged from 6.6 cm to 8.1 cm, while R-squared values consistently surpassed 70%. Larger sampling intervals, such as 20-meter and 30-meter, resulted in a significant reduction in data accuracy, especially reflected in the R-squared values, which fell below 70%. This indicates that although larger intervals can enhance survey efficiency, they undermine the reliability of the data, particularly in intricate or varied underwater environments. Increasing line and point spacing enhances the performance of Universal Kriging (UK) and Radial Basis Function (RBF) methods. The UK employs spatial autocorrelation and deterministic trend components to estimate values in areas with limited data, successfully identifying global patterns via variogram analysis (Cressie, 2015). RBF methods create smooth surfaces by precisely intersecting measured points, maintaining accuracy despite the presence of limited

scattered data (Hardy, 1990). In contrast to Topo to Raster, which emphasizes hydrological accuracy, RBF aims to reduce surface curvature, rendering it appropriate for uses such as pollution modeling or elevation mapping where a smooth surface is essential (Buhmann, 2000).

These findings, in addition to being technically validated, have the potential to bring about significant change for global challenges. Accurate shallow water bathymetry data plays a crucial role in environmental monitoring. It can track debris and plastic accumulation in urban lakes (Chen et al., 2024; Hoffman & Hittinger, 2017; Nava et al., 2023) and supports climate adaptation by analyzing sedimentation in flood-prone deltas (Dunn et al., 2023). Accurate depth maps play a vital role in managing water resources. They help estimate reservoir capacities, which is especially important for drought resilience in dry areas. UAS-echosounder data can be essential for accurately characterizing reservoir depths, sediment distribution, and potential hypoxic zones, which are critical factors affecting phosphorus release dynamics during seasonal stratification (Lv et al., 2024). Infrastructure planning can greatly benefit from affordable surveys of hazardous sites. UAS-echo sounders improve infrastructure resilience by allowing for surveys of high-risk areas, such as unstable riverbanks, where traditional methods may not be feasible. To adapt to climate changes, it's important to regularly monitor shallow water bodies, as they are key indicators of changes in water systems (Salimi et al., 2021). This monitoring can help shape adaptive policies that support the goals of sustainable water management outlined in SDG 6 (Bandala, 2024). This study is the very first novel approach to assess UAS-echo sounder systems across various parameters, providing a replicable framework for high-resolution, cost-efficient bathymetric mapping. This study presents the inaugural integrative framework that optimizes the synergy between UAS and echo-sounding technology for bathymetric mapping, enhancing mission design and processing workflows to maximize cost-effectiveness and accuracy. No previous research has accomplished this technological integration or exhibited its capacity to address significant deficiencies in scalable, highly accurate underwater depth measurement.

### **Recommendations:**

For reliable bathymetric continuous surface creation and UAS-echosounder surveys in shallow waters, prioritize  $\leq 10$ -meter sampling intervals to maintain accuracy (RMSE: 6.6–8.1 cm;  $R^2 > 70\%$ ) and avoid intervals  $> 20$  meters, which degrade performance in complex terrains.

**Challenges:** Although UAS-mounted single-beam echosounder technology allows effective bathymetric data collecting, its inherent limitations should be recognized. With dense survey patterns, it achieves a maximum bathymetric surface resolution of 1-2 meters as a single-beam system. It restricts its capacity to resolve fine-scale underwater features relative to high-resolution multibeam systems. Direct comparisons between UAS-derived datasets and established single-beam or multibeam bathymetric surveys should be prioritized in future studies to rigorously evaluate vertical accuracy, spatial consistency, and operational trade-offs, including cost and coverage efficiency. While guiding improvements in sensor integration, georeferencing,

and data processing systems to bridge resolution gaps with conventional methods, such benchmarking would clarify the technology's fit for specific applications.

### Field Data Analysis for Bay Springs Lake:

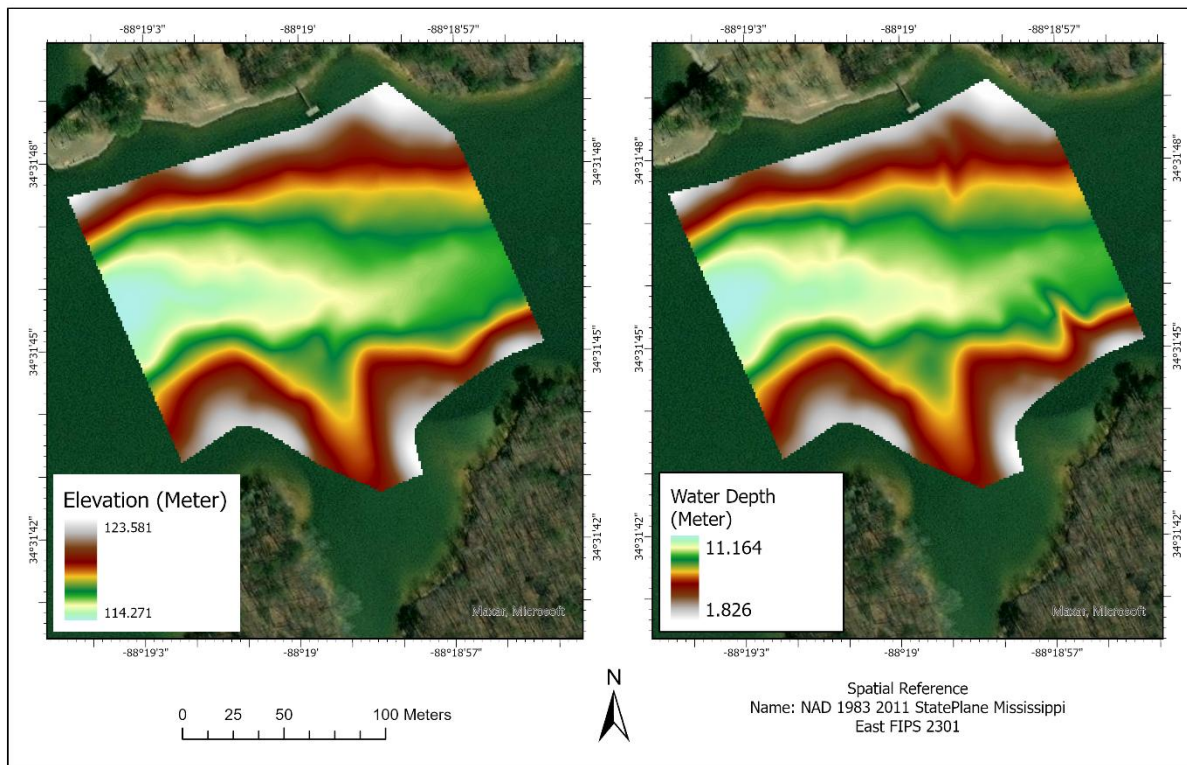


**Figure 44: Bathymetric surface of Bay Springs Lake using UAS-echo sounder's continuous mode data collection**

#### Observations:

We generated two different elevation models using two distinct variables from high-frequency UAS-echo sounder data: one is the elevation data, and the other is the corrected water depth. The dataset was highly consistent, requiring very little data cleaning as only a few instances of noise were found. According to our findings, the deeper the water, the better the data quality. The minimum depth measured was 1.826 meters, and the maximum depth was 11.164 meters at this site.

#### Recommendations:

Ensure that the UAS-RTK system is activated during the data collection process. It is important to note that water depth can vary due to factors such as tides and currents, whereas the elevation of the underwater surface remains constant over time. Therefore, for future operations such as dredging, analyzing sediment transportation, or monitoring changes in underwater surface

elevation, the UAS-echo sounder collected elevation data can be used as a consistent reference for comparison.

### Challenges:

During data collection time we faced a problem, and it was with the configuration file of Sky Hub. Make sure according to the training video everything is set to the optimum settings and save them before flying the sensor.

### Field Data Analysis for Grand Bay and Middle Bay, MS:

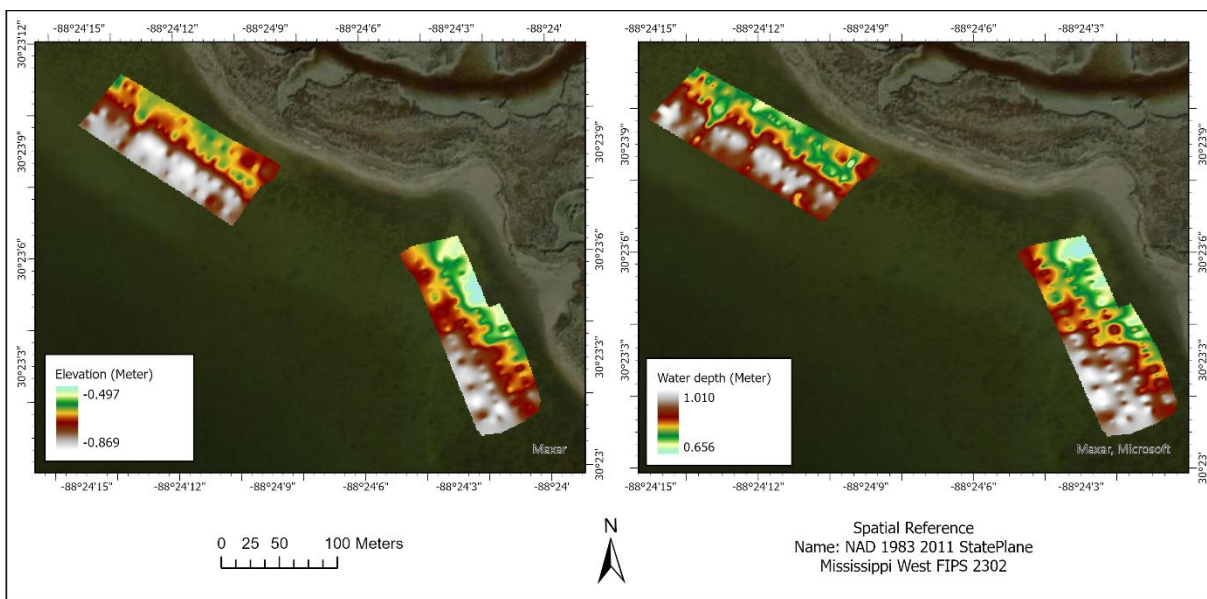


**Figure 45: Bathymetric surface of Middle Bay using UAS-echo sounder's continuous mode data collection**

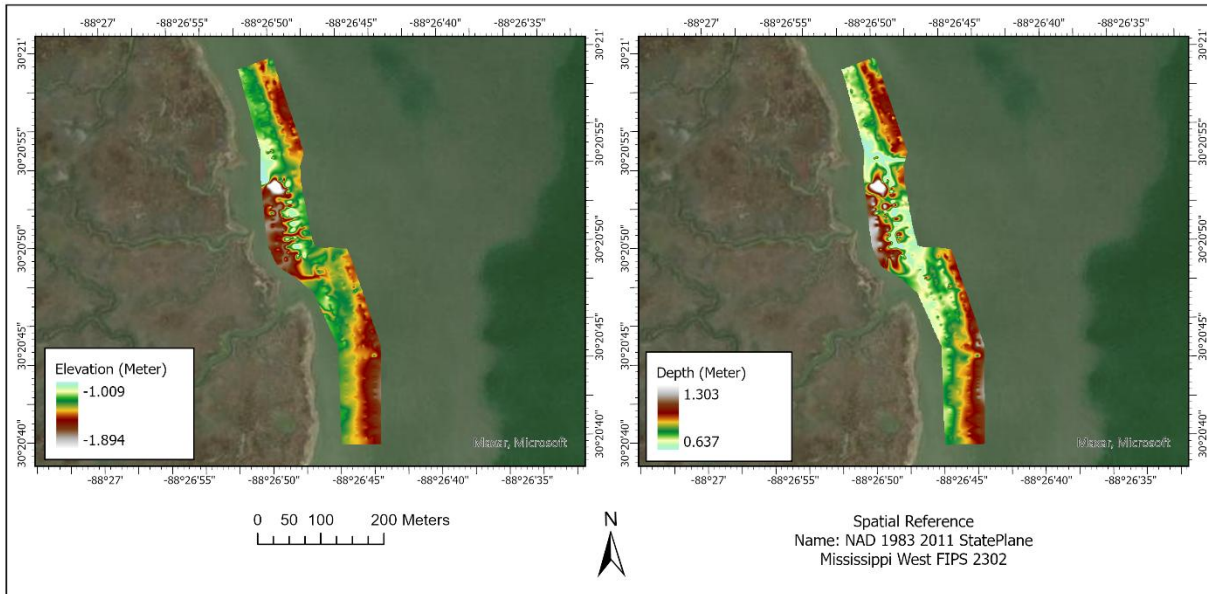


**Figure 46: Bathymetric surface of Grand Bay using UAS-echo sounder's continuous mode data collection**

### Observations:

The data quality for Grand Bay and Middle Bay was predominantly reliable; however, coverage was restricted to nearshore areas, presumably due to operational limitations of the drone, including battery life and safety protocols. Nevertheless, shallow water areas continued to display noise, necessitating specific data cleansing—similar to difficulties faced in previous analyses of catfish ponds. Notwithstanding these challenges, the sanitized dataset exhibited significant consistency, indicating efficient field methodologies and effective noise-filtering techniques.

Differences observed between bed elevations (0.885 m range) and water depth (0.666 m range) are influenced by site characteristics such as dense vegetation and challenging weather conditions, which complicate sonar signal returns and post-processing corrections. These site-specific factors will be accounted for in future deployments through refined sensor calibration and enhanced pre-mission site reconnaissance.

### Recommendations:

To improve future surveys, data collection should prioritize high tide conditions to maximize coverage in shallow zones and minimize noise. Enabling Real-Time Kinematic (RTK) positioning is critical, as it provides accurate elevation measurements of the seafloor. Since water depths fluctuate with tides, pairing RTK-derived elevation data provides. Expanding spatial coverage beyond nearshore areas is also advised; this could involve deploying drones with extended range or using boat-based UAS launches to access deeper offshore regions. Such



efforts would complement existing datasets and provide a more comprehensive understanding of the study areas. Furthermore, synchronizing data collection with tidal forecasts guarantees the most effective utilization of high-tide intervals, while amalgamating RTK data with tidal models improves depth calibration.

**Challenges:**

Environmental factors, including strong currents and wind, presented considerable risks during data collection, jeopardizing drone stability and sensor precision. To alleviate these risks, surveys ought to be conducted in favorable weather conditions, and robust drones equipped with sophisticated stabilization systems may be utilized.

## Field Data Analysis for North Farm, Starkville:

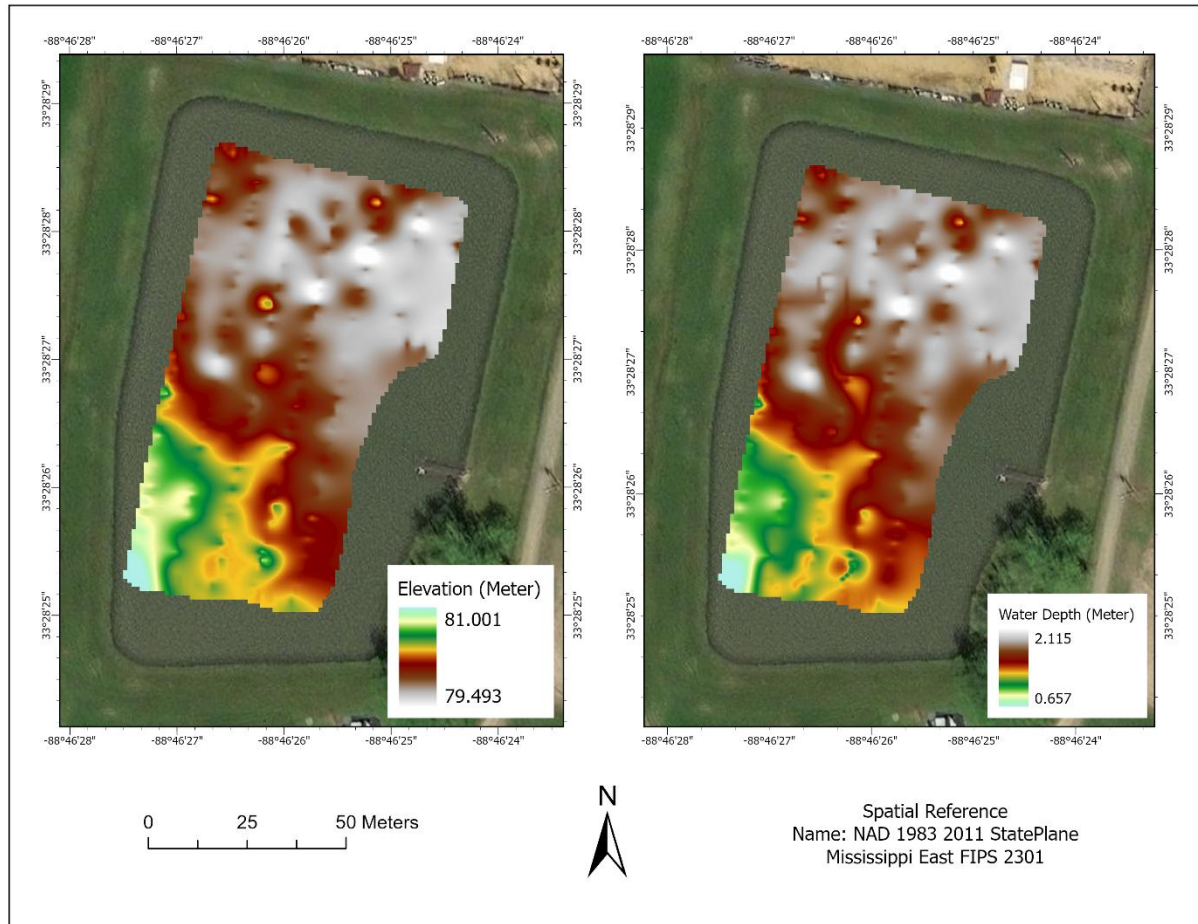


**Figure 47: Bathymetric surface of Tombigbee River using UAS-echo sounder's continuous mode data collection**

### Observations:

During our analysis, we identified a moderate level of noise in the dataset, our primary assumption is due to vegetation present in the water reservoir. To evaluate its effect, we deliberately avoided performing data cleaning on the raw data for this site. This allowed us to observe the dataset's appearance in its unprocessed form and assess the influence of the noise. This location serves as a recurring data collection site where we frequently test sensors. Typically, the site performs well during these evaluations. However, in this instance, the vegetation introduced noticeable noise along the flight line, as shown in Figure 47. This observation highlights the impact of environmental factors on data quality at this testing spot.

### Recommendations:

Thorough data cleaning is highly necessary to eliminate noise and enhance the dataset's reliability. A meticulous cleaning process ensures that the bathymetric surface is represented accurately, free from distortions caused by environmental interference.

## Challenges:

The most significant challenge at this site was the vegetation, which complicated the data-cleaning process.

## Field Data Analysis for Tombigbee River:

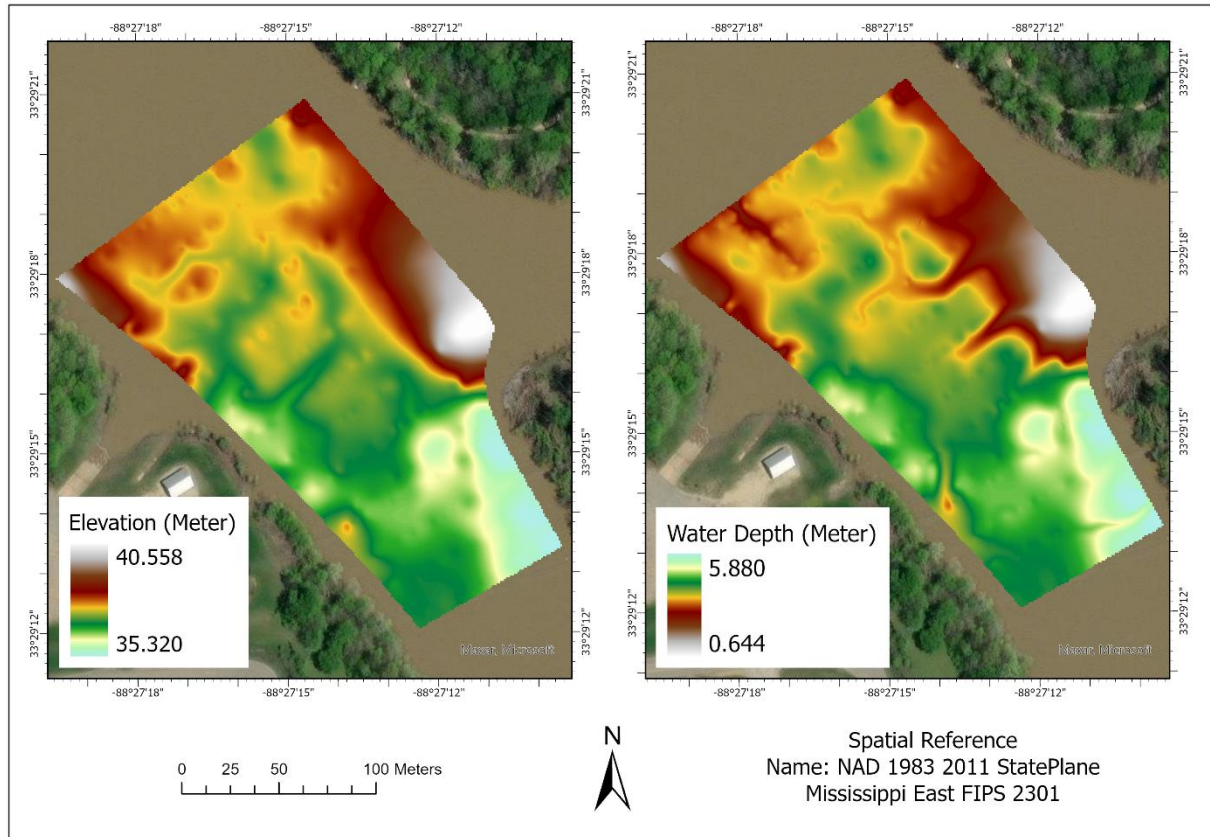


**Figure 48: Bathymetric surface of Tombigbee River using UAS-echo sounder's continuous mode data collection**

## Observations:

We tested the UAS-echo sounder on the Tombigbee River at a site characterized by the intersection of three distinct channels, possibly indicative of an anastomosed channel pattern. The survey showed depths varying from 0.644 meters to 5.880 meters. This configuration creates intricate flow dynamics, where water from different channels interacts, affecting sediment transport and deposition. Our observations revealed that the eastern channel has a shallower riverbed, likely due to reduced flow velocity in that branch. As the predominant flow is from northwest to southeast, the eastern channel may receive less of the main flow, leading to sediment accumulation.

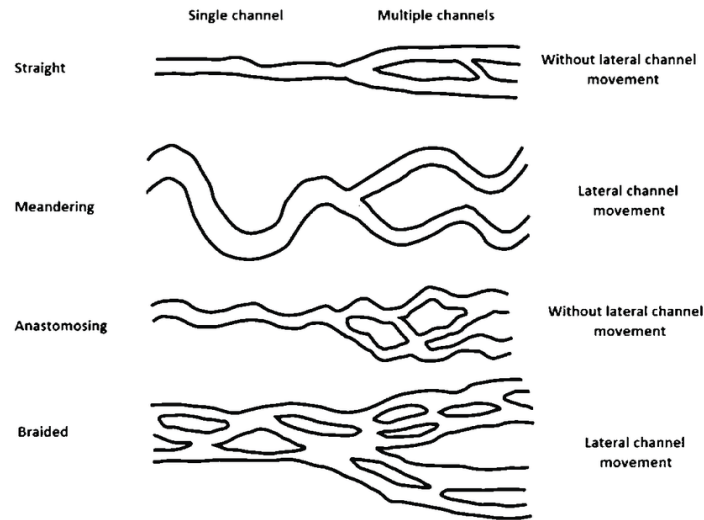


**Figure 49: River types based on their sinuosity, number of channels and lateral movement (Nichols, G., 1999. Sedimentology and Stratigraphy. Wiley-Blackwell, Oxford.)**

This phenomenon is consistent with hydrological principles governing sediment transport in multi-channel river systems, where deposition occurs in areas of lower flow energy. The overall morphology of the Tombigbee River in this region is shaped by its discharge variability, sediment load, and bank stability, all of which influence how the channels evolve.

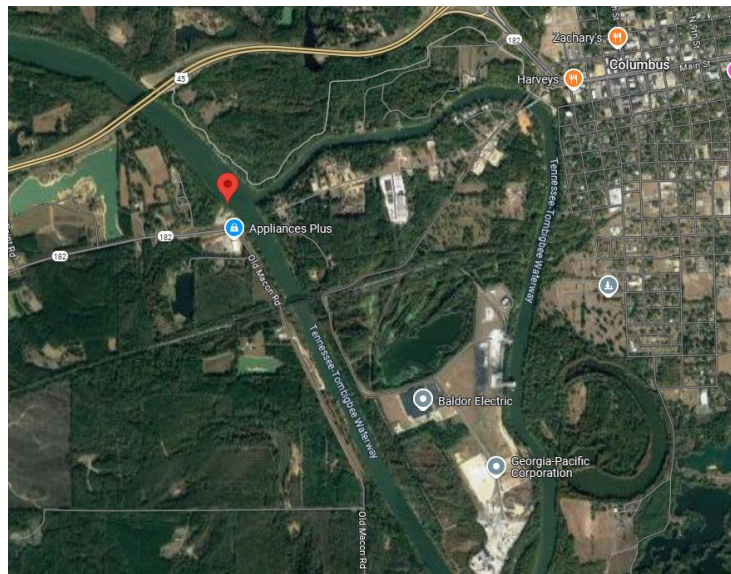


**Figure 50: Google earth image of the Tombigbee River where the data has been collected**

### Recommendations:

Make sure the UAS-RTK system is working and other safety measures for smooth and



### Challenges:

We did not face any major challenges on this site. The data collection was pretty smooth and consistent.

### Field Data Analysis for White's Creek Lake:

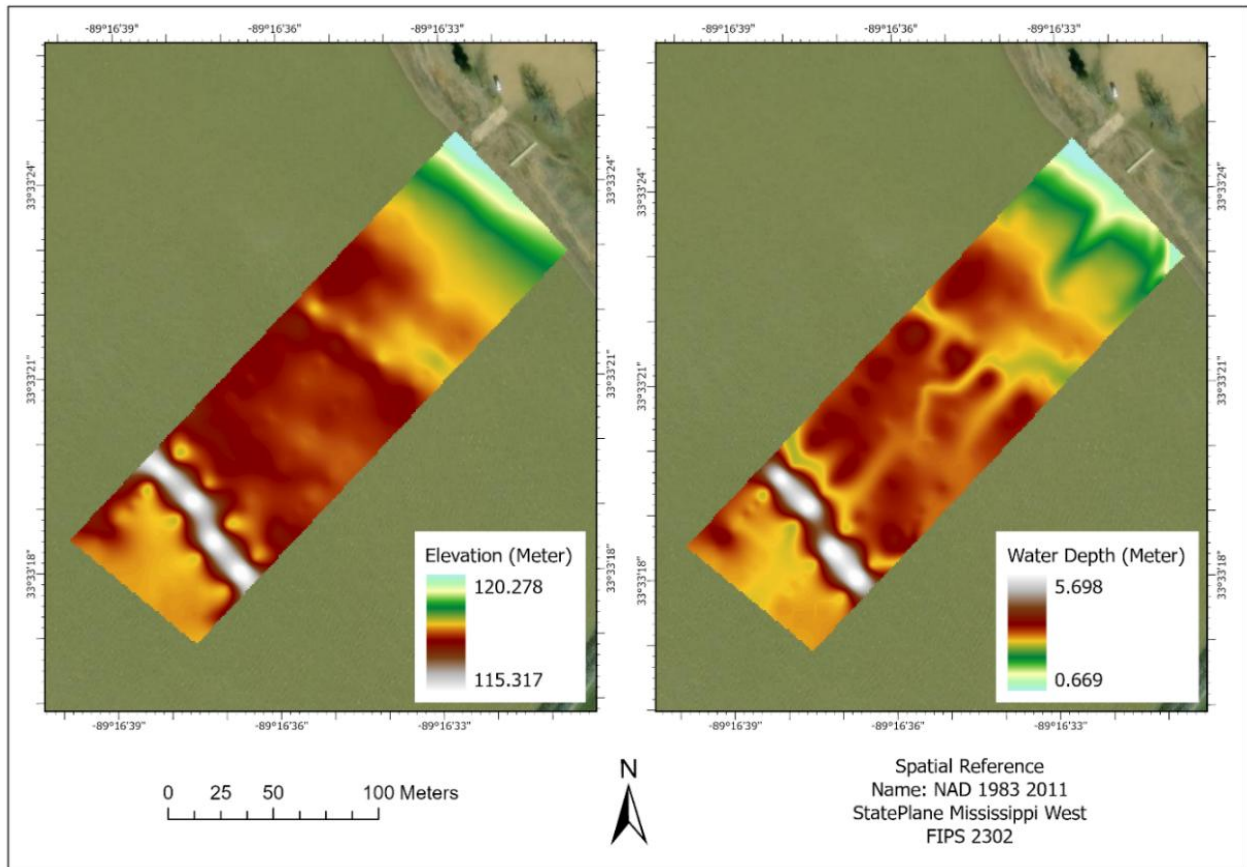


**Figure 51: Bathymetric surface of White's Creek Lake using UAS-echo sounder's continuous mode data collection**



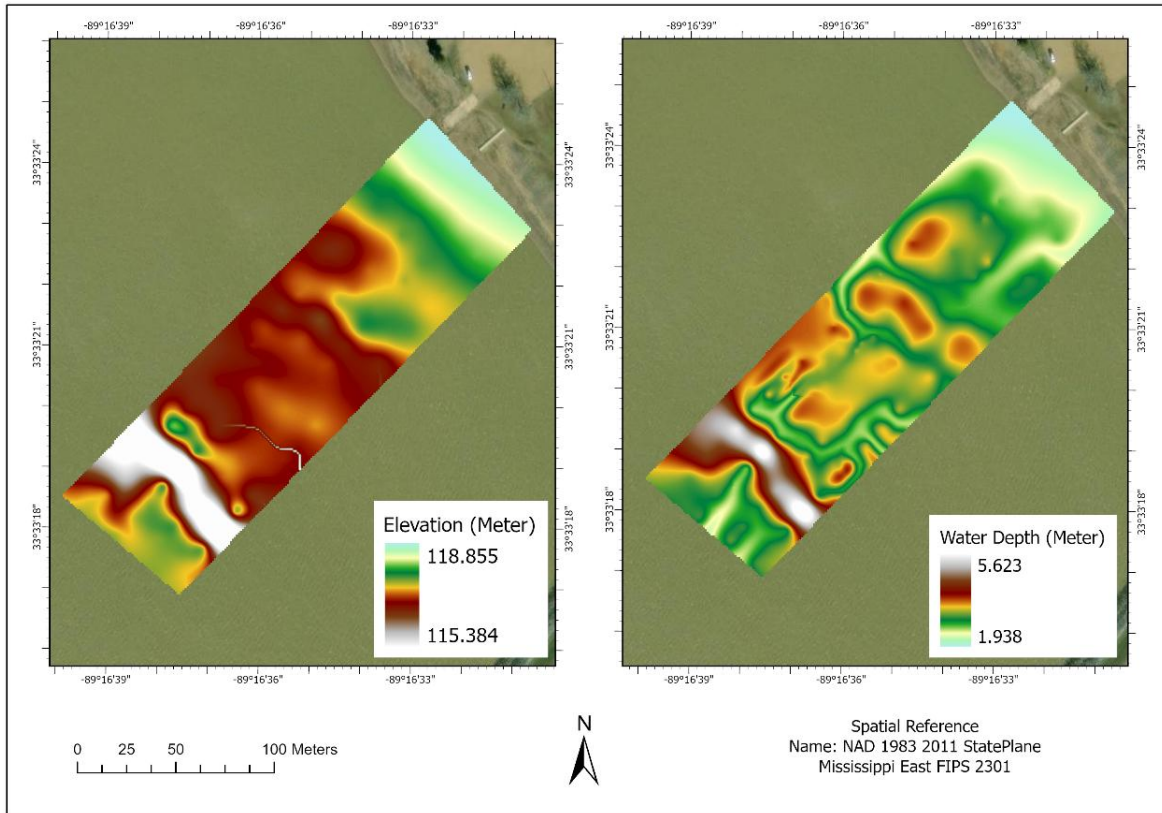


**Figure 52: Bathymetric surface of White's Creek Lake using UAS-echo sounder's grasshopper mode data collection**

### **Observations:**

We employed two data collection methods at this site: continuous mode and grasshopper mode. Our findings show that the continuous mode is far more effective for collecting detailed data compared to the grasshopper mode. For instance, when examining the figures derived from the continuous mode data, the southwestern part reveals a dammed creek and the deep channel of its old creek bed, where water once flowed. In contrast, the figures from the grasshopper mode data lack this clarity, with details of such features fading away. However, grasshopper mode elevations still have a good similarity with continuous mode data despite using a 10m by 10m sampling strategy. That said, more distancing between sampling points can lose more detailing of the data. So, it depends on the client's need and how much detail one requires. That is how one can decide what strategy one should follow for data collection. If high precision is essential, continuous mode is preferable with considerable flight line spacing like 5 meters or 10 meters, whereas grasshopper mode may suffice for a broader, less detailed overview.

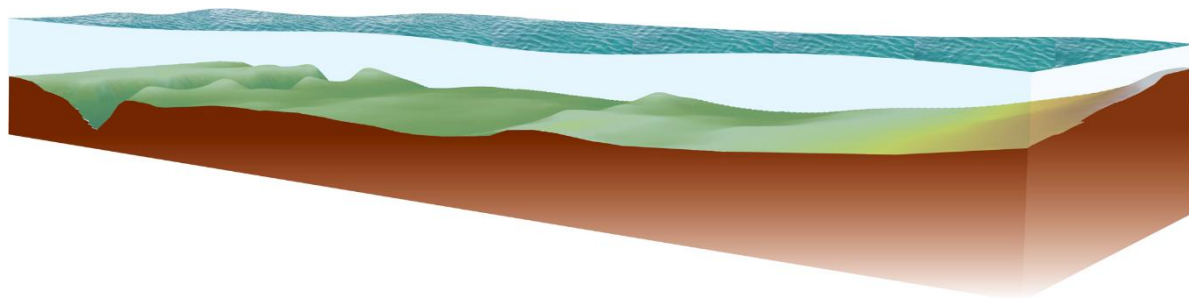


**Figure 53: 3D of the White's Creek Lake bathymetric surface.**

### **Recommendations:**

When there are no obstacles along the flight paths, it is more efficient to use continuous mode for data collection rather than grasshopper mode. During our observations using grasshopper mode, we maintained a grid pattern with 10-meter spacing between flight lines and 10-meter spacing between sampling points along each flight line. However, grasshopper mode required three full flights to survey the same area that continuous mode could cover in just two flights. This difference makes sense because, in grasshopper mode, the drone must travel to each sampling point individually, hover to dip the sensor into the water, collect data, lift the sensor out, and then move to the next fixed location to repeat the process. This stop-and-go method is naturally more time-consuming and energy-intensive. In contrast, continuous mode likely allows the drone to follow a more direct and efficient path, collecting data from multiple points with fewer interruptions, thus reducing the number of flights needed.

### **Challenges:**

We did not face any major challenges on this site. The data collection was pretty smooth and consistent.

## Real-life Use of the UAS-echo Sounder Technology for Water Volume Calculation:

For water volume calculation we choose the catfish pond at Delta Research and Extension Center (DREC) of Mississippi State University (MSU).

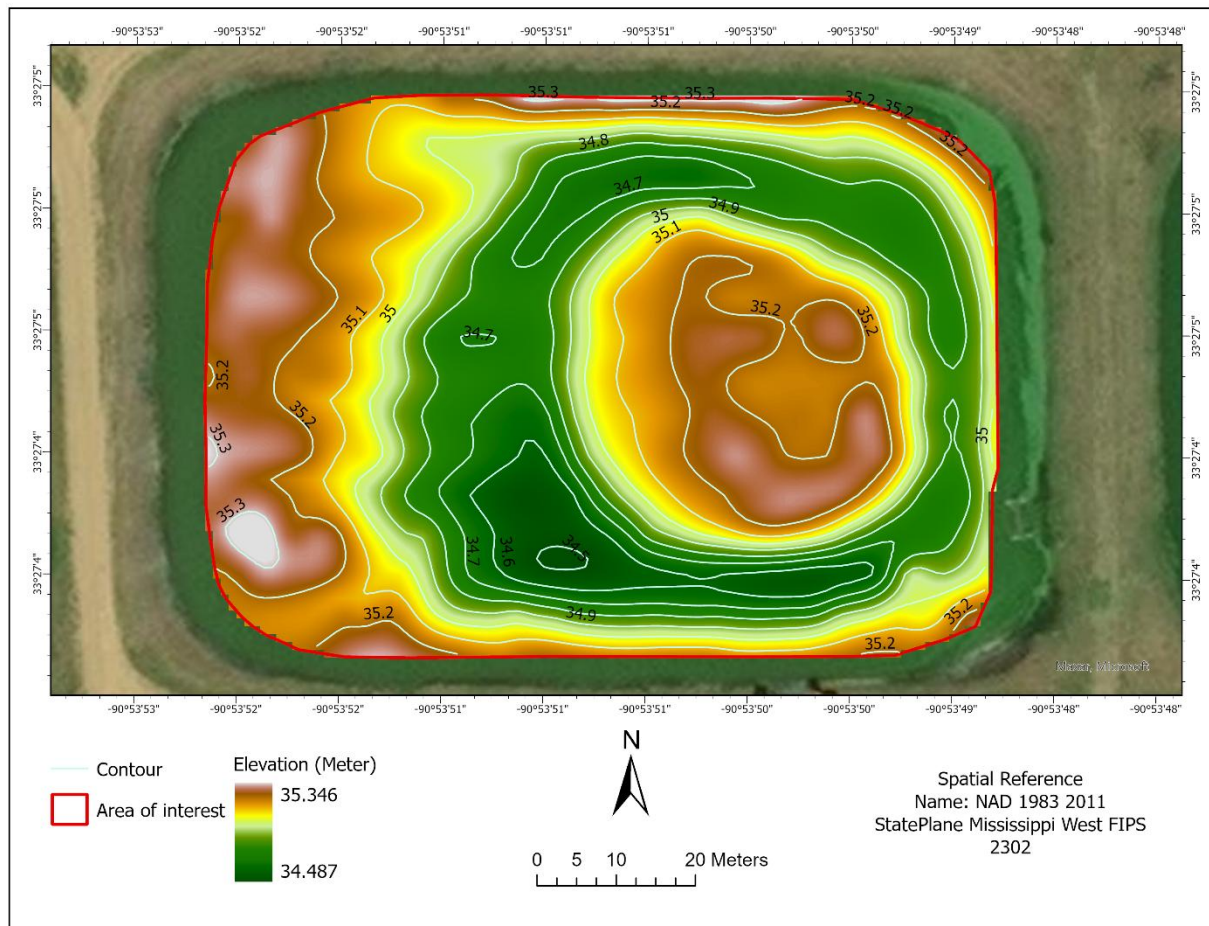


**Figure 54: Bathymetric elevation map generated using 5-meter flight spacing UAS-echo sounder data and using topoR (Topo to raster) interpolation method.**

Calculating water volume within the ArcGIS environment is a streamlined process that relies primarily on bathymetric elevation data, as depth data alone is insufficient for accurate volume estimation. In this case, a bathymetric elevation map was generated using high-resolution 5-meter flight spacing UAS-echo sounder data, followed by the application of the Topo to Raster (topoR) interpolation method to refine and interpolate the elevation surfaces. This approach ensures precise modeling of underwater terrain, enabling efficient water volume calculations by integrating elevation values across the study area, thereby leveraging ArcGIS's robust geospatial tools to transform raw data into actionable volumetric insights.

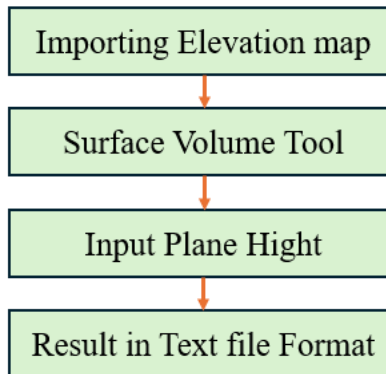


**Figure 55: water volume calculation steps in ArcGIS pro-environment.**

From Figure 54 we can see the bathymetric raster data and contour which is not mandatory to generate. In ArcGIS, in the Geoprocessing toolbox search for the surface volume tool (3D Analyst Tools/ Area and volume/ Surface volume).

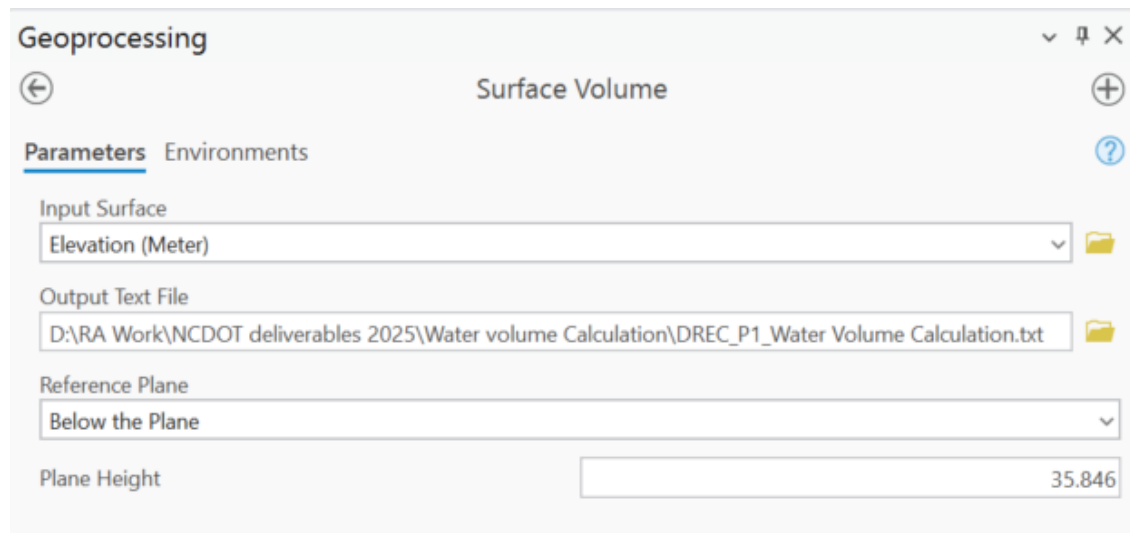
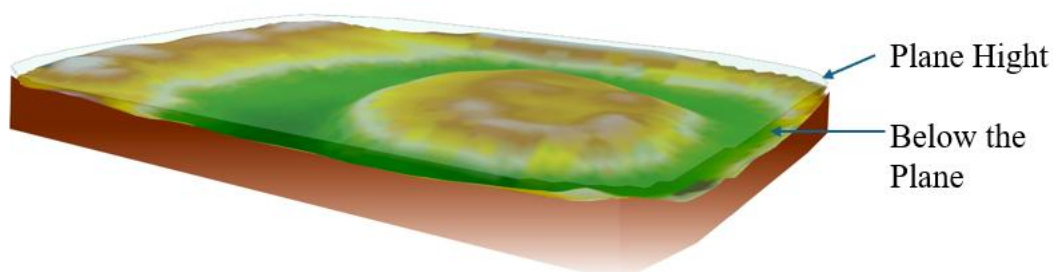


**Figure 56: Surface volume calculation tool in ArcGIS pro**

Here, the input Surface will be the bathymetric raster layer. The output result will be a text file. In our case, everything is in the metric system so the volume will be in a Cubic meter. We can always convert it to water gallons. Here plane height is an important parameter to set. Plane height is the imaginary water surface.



In our case, the plane height is set to 34.846 meters. This value is determined as follows:

Lowest Bathymetry Elevation (shallow water Depth): The shallowest measurable depth in the surveyed area corresponds to a bathymetric elevation of 35.346 meters (Figure 38). This represents the minimum water depth detectable in the system (Figure 54).

Sensor Detection Threshold: The sensor cannot record data in water shallower than 0.5 meters.

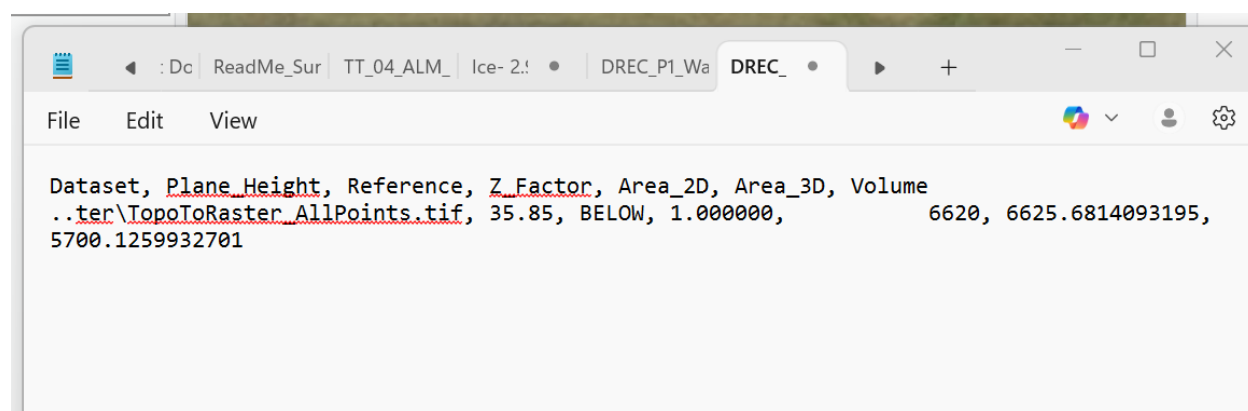
To avoid underestimating water volume, the plane height must account for both the shallowest bathymetric elevation and the sensor's detection limit. If the 0.5-meter threshold is ignored, the volume calculation would exclude water shallower than this depth. So, the plane height of the water body needs to be considered.

Thus, the plane height for the catfish pond at DREC is:

Lowest Bathymetric Elevation (35.346 m) + (0.5 m) = 35.846 m.

plane height for the catfish pond at DREC is: 118.

water volume calculation result for DEREK:



In Microsoft Excel

Dataset	Plane_Height	Reference	Z_Factor	Area_2D	Area_3D	Volume	
..ter\TopoToRaster_AllPoints.tif	35.85	BELOW	1	6620	6625.681409	5700.126	

So, the volume of the catfish pond considering the area of interest is 5700.126 Cubic meters. Still, it can be considered the most accurate approximation of the water volume calculation, not an exact water volume.

Although a fixed 'plane height' approach was used to approximate shallow fringes, future efforts will explore setting this threshold closer to the highest measured bathymetric point. This



adjustment aims to better capture shallow fringes and improve total volumetric estimates, especially in areas where direct sonar returns are not feasible due to sensor constraints

## References:

- Alvarez, L. V., Moreno, H. A., Segales, A. R., Pham, T. G., Pillar-Little, E. A., & Chilson, P. B. (2018). Merging Unmanned Aerial Systems (UAS) Imagery and Echo Soundings with an Adaptive Sampling Technique for Bathymetric Surveys. *Remote Sensing*, 10(9), Article 1362. <https://doi.org/10.3390/rs10091362>
- Arun, P. V. (2013). A comparative analysis of different DEM interpolation methods. *The Egyptian journal of remote sensing and space science*, 16(2), 133-139.
- Bandala, E. R. (2024). Sustainable Developing Goals: SDG 6 and Its Significance for Sustainable Growth. In *Circular Economy Applications for Water Security* (pp. 5-20). CRC Press.
- Bandini, F., Kooij, L., Mortensen, B. K., Caspersen, M. B., Thomsen, L. G., Olesen, D., & Bauer-Gottwein, P. (2023). Mapping inland water bathymetry with Ground Penetrating Radar (GPR) on board Unmanned Aerial Systems (UASs). *Journal of Hydrology*, 616, Article 128789. <https://doi.org/10.1016/j.jhydrol.2022.128789>
- Bandini, F., Olesen, D., Jakobsen, J., Kittel, C. M. M., Wang, S., Garcia, M., & Bauer-Gottwein, P. (2018). Technical note: Bathymetry observations of inland water bodies using a tethered single-beam sonar controlled by an unmanned aerial vehicle. *Hydrology and Earth System Sciences*, 22(8), 4165-4181. <https://doi.org/10.5194/hess-22-4165-2018>
- Bashit, M. S., & Pricope, N. (2024). The impact of topobathymetric technologies in hydrography.
- Buhmann, M. D. (2000). Radial basis functions. *Acta numerica*, 9, 1-38.
- Chen, D., Wang, P., Liu, S., Wang, R., Wu, Y., Zhu, A.-X., & Deng, C. (2024). Global patterns of lake microplastic pollution: Insights from regional human development levels. *Science of The Total Environment*, 176620.
- Cressie, N. (2015). *Statistics for spatial data*. John Wiley & Sons.
- Dunn, F., Cox, J., Scown, M., Du, H., Triyanti, A., Middelkoop, H.,...Minderhoud, P. (2023). Sedimentation-enhanced for sustainable deltas : An integrated socio-biophysical framework. *ONE EARTH*, 6(12), 1677-1691. <https://doi.org/10.1016/j.oneear.2023.11.009>
- Erena, M., Atenza, J. F., Garcia-Galiano, S., Dominguez, J. A., & Bernabe, J. M. (2019). Use of Drones for the Topo-Bathymetric Monitoring of the Reservoirs of the Segura River Basin. *Water*, 11(3), Article 445. <https://doi.org/10.3390/w11030445>
- Ferreira, I. O., & Andrade, L. C. d. (2022). Bathymetric surveys: improvements and barriers. *Hydro International*.
- Genchi, S. A., Vitale, A. J., Perillo, G. M. E., Seitz, C., & Delrieux, C. A. (2020). Mapping Topobathymetry in a Shallow Tidal Environment Using Low-Cost Technology. *Remote Sensing*, 12(9), Article 1394. <https://doi.org/10.3390/rs12091394>
- Hardy, R. L. (1990). Theory and applications of the multiquadric-biharmonic method 20 years of discovery 1968–1988. *Computers & Mathematics with Applications*, 19(8-9), 163-208.
- Hell, B., Broman, B., Jakobsson, L., Jakobsson, M., Magnusson, Å., & Wiberg, P. (2012). The Use of Bathymetric Data in Society and Science: A Review from the Baltic Sea. *Ambio*, 41(2), 138-150. <https://doi.org/10.1007/s13280-011-0192-y>
- Hoffman, M., & Hittinger, E. (2017). Inventory and transport of plastic debris in the Laurentian Great Lakes. *MARINE POLLUTION BULLETIN*, 115(1-2), 273-281. <https://doi.org/10.1016/j.marpolbul.2016.11.061>
- Jagalingam, P., Akshaya, B. J., & Hegde, A. V. (2015). Bathymetry Mapping Using Landsat 8 Satellite Imagery. *8th International Conference on Asian and Pacific Coasts (Apac 2015)*, 116, 560-566. <https://doi.org/10.1016/j.proeng.2015.08.326>

- Jawak, S. D., Vadlamani, S. S., & Luis, A. J. (2015). A synoptic review on deriving bathymetry information using remote sensing technologies: models, methods and comparisons. *Advances in remote Sensing*, 4(2), 147-162.
- Li, J. W., Knapp, D. E., Schill, S. R., Roelfsema, C., Phinn, S., Silman, M.,...Asner, G. P. (2019). Adaptive bathymetry estimation for shallow coastal waters using Planet Dove satellites. *Remote Sensing of Environment*, 232, Article 111302. <https://doi.org/10.1016/j.rse.2019.111302>
- Lv, Y., Zhang, M., & Yin, H. (2024). Phosphorus release from the sediment of a drinking water reservoir under the influence of seasonal hypoxia. *SCIENCE OF THE TOTAL ENVIRONMENT*, 917, Article 170490. <https://doi.org/10.1016/j.scitotenv.2024.170490>
- Nava, V., Chandra, S., Aherne, J., Alfonso, M., Antao-Geraldes, A., Attermeyer, K.,...Leoni, B. (2023). Plastic debris in lakes and reservoirs. *NATURE*, 619(7969), 317-+. <https://doi.org/10.1038/s41586-023-06168-4>
- Parente, C., & Vallario, A. (2019). Interpolation of Single Beam Echo Sounder Data for 3D Bathymetric Model. *International Journal of Advanced Computer Science and Applications*, 10(10), 6-13.
- Pricope, N. G., & Bashit, M. S. (2023). Emerging trends in topobathymetric LiDAR technology and mapping. *International Journal of Remote Sensing*, 44(24), 7706-7731.
- Salimi, S., Almuktar, S., & Scholz, M. (2021). Impact of climate change on wetland ecosystems: A critical review of experimental wetlands. *JOURNAL OF ENVIRONMENTAL MANAGEMENT*, 286, Article 112160. <https://doi.org/10.1016/j.jenvman.2021.112160>
- Siljeg, A., Lozic, S., & Siljeg, S. (2015). A comparison of interpolation methods on the basis of data obtained from a bathymetric survey of Lake Vrana, Croatia. *Hydrology and Earth System Sciences*, 19(8), 3653-3666. <https://doi.org/10.5194/hess-19-3653-2015>
- Sotelo-Torres, F., Alvarez, L., & Roberts, R. (2023). An Unmanned Surface Vehicle (USV): Development of an Autonomous Boat with a Sensor Integration System for Bathymetric Surveys. *SENSORS*, 23, Article 4420. <https://doi.org/10.3390/s23094420>
- Udoh, I., Ekpa, A., & Mbat, J. (2022). Optimizing Single Beam Data for Bathymetric Analysis. *SSRG International Journal of Geoinformatics and Geological Science*, 9(3), 10-24.
- Wölfl, A., Snaith, H., Amirebrahimi, S., Devey, C., Dorschel, B., Ferrini, V.,...Wigley, R. (2019). Seafloor Mapping - The Challenge of a Truly Global Ocean Bathymetry. *FRONTIERS IN MARINE SCIENCE*, 6, Article 283. <https://doi.org/10.3389/fmars.2019.00283>
- Yao, F., Minear, J., Rajagopalan, B., Wang, C., Yang, K., & Livneh, B. (2023). Estimating Reservoir Sedimentation Rates and Storage Capacity Losses Using High-Resolution Sentinel-2 Satellite and Water Level Data. *GEOPHYSICAL RESEARCH LETTERS*, 50, Article e2023GL103524. <https://doi.org/10.1029/2023GL103524>

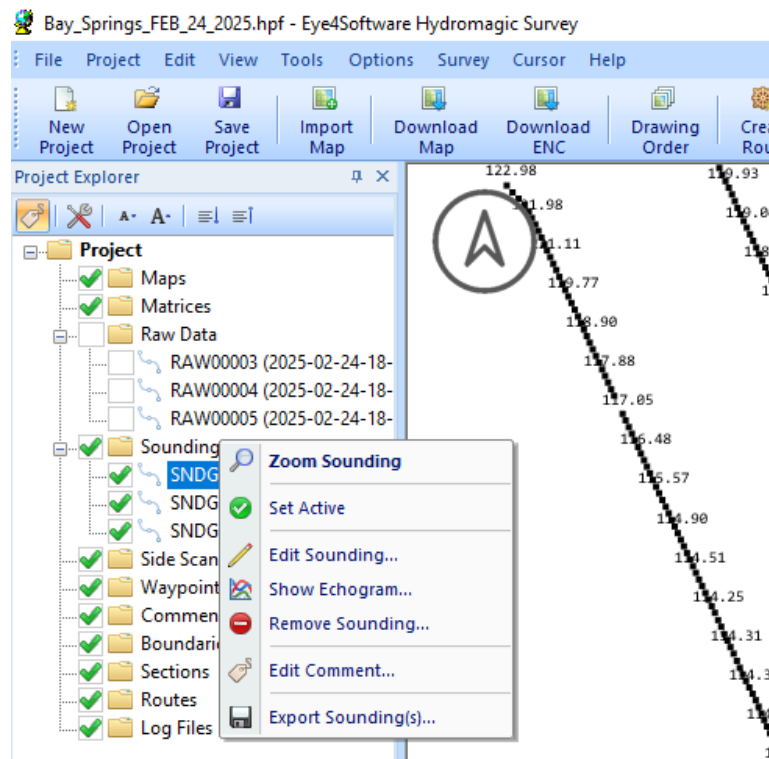
# Mississippi State University Appendices

## APPENDIX 1:

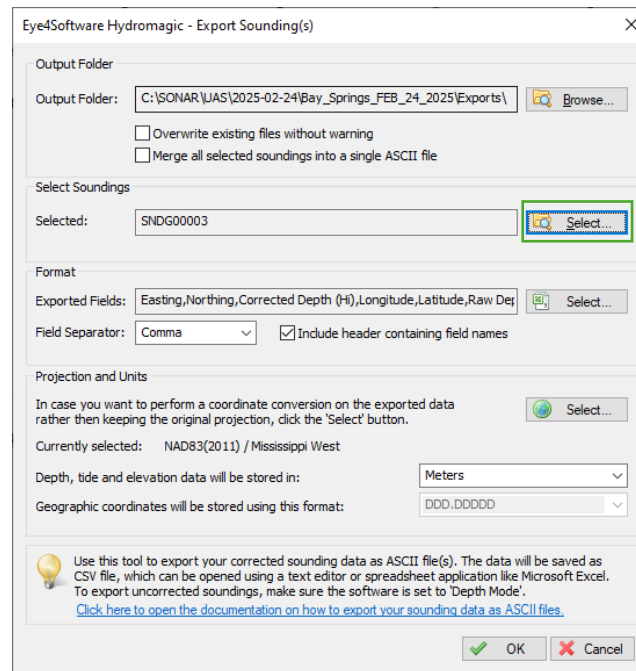
Primary data cleaning is performed using Eye4Software Hydromagic, which is clearly described in the training video (UgCS SkyHub-ECT400 Echosounder Training\_Day 2\_01-10-23\_Recording.mp4)

Here we are going to cover how to export the soundings and make is useable in the AcrGIS environment which is not covered in the training video.

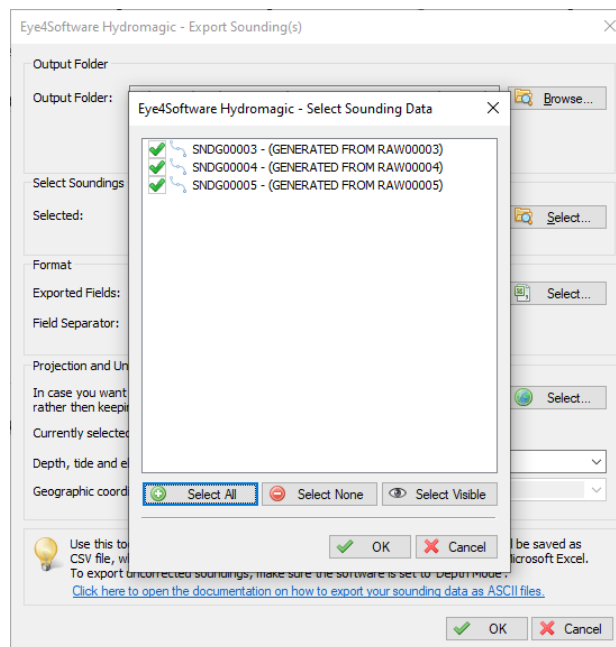
So after creating the soundings we have right right-click on any of the soundings layers and click on the export soundings.



Now the following window will show up browse the location where you want to save the data and click on the select soundings. There is an option called merging all the soundings into a single ASCII file. If you check the file there will be one single merged file from many different soundings files. It is better to check it as it will help to import all the data to the ArcGIS project environment using that one exported file and there will be no need to merge many different files in ArcGIS.

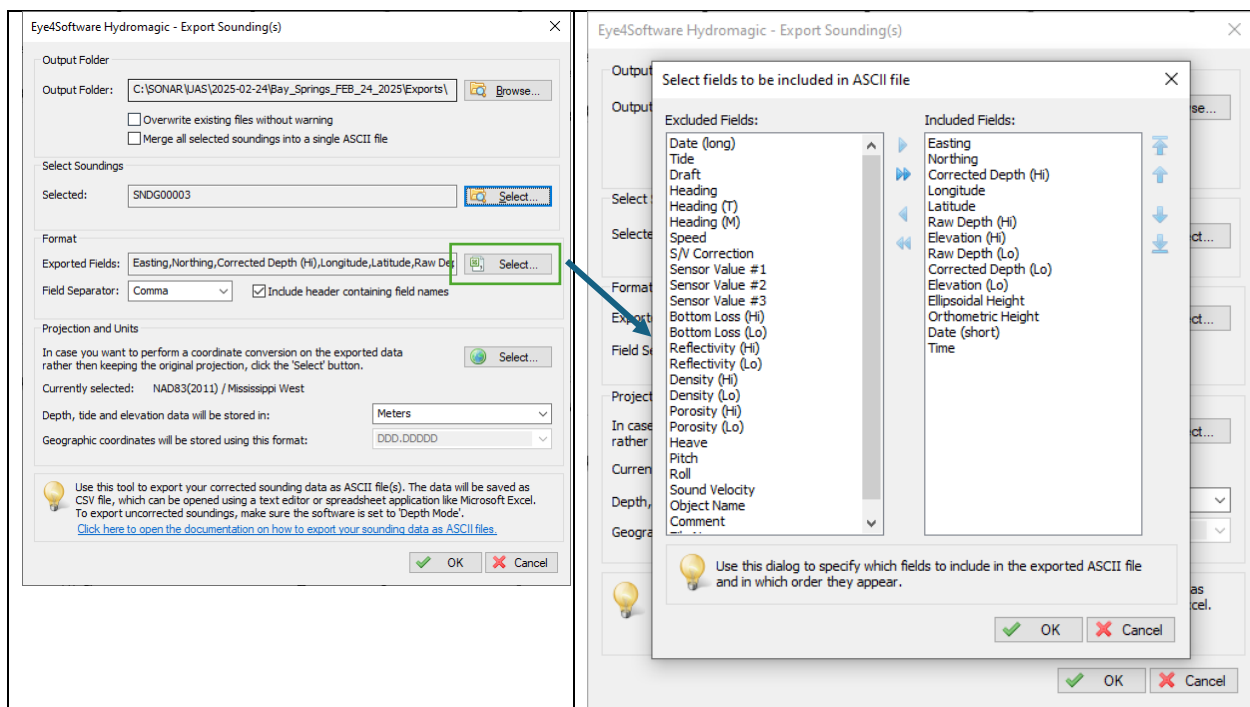


Select all the soundings or the soundings you want to be exported-

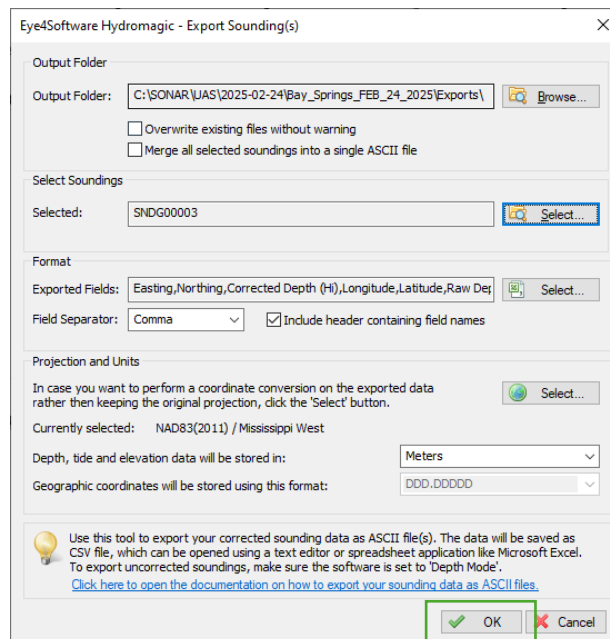




Finally, now click on the exported fields and select the data field you want to see in your data set.

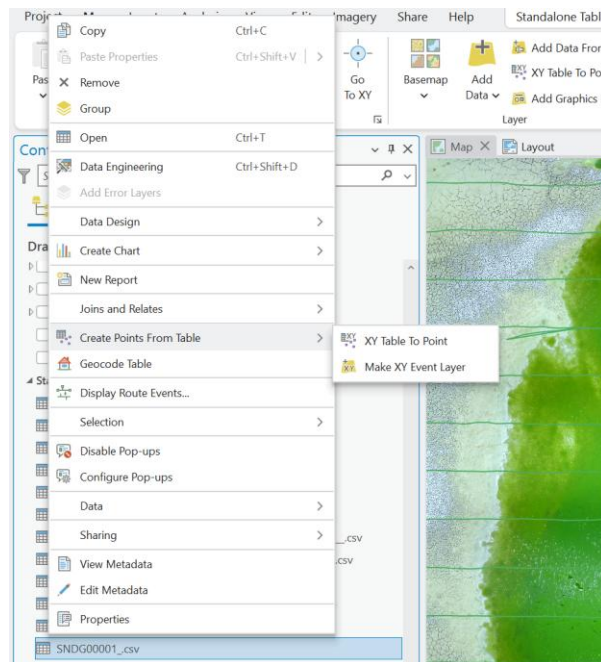


Finally, click ok and the sounding CSV file will be exported to the designated location.

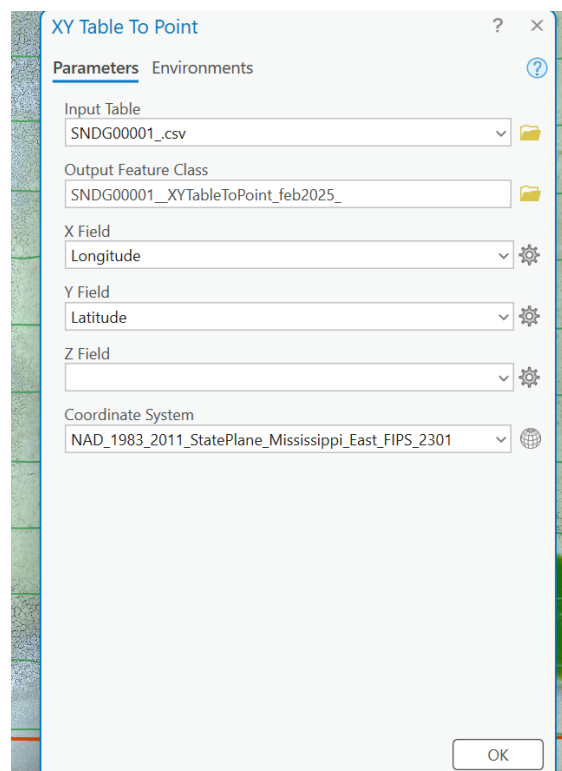


Finally, it is recommended to open the CSV file and rename it and save it.

After that saved and renamed CSV can be imported into the ArcGIS environment and right click on the file and create points from table and select XY to point.



Then, the following window will show up. Select the X field as Longitude and the Y field as latitude and select the proper projected coordinate system. And finally, click ok. The soundings will be imported.



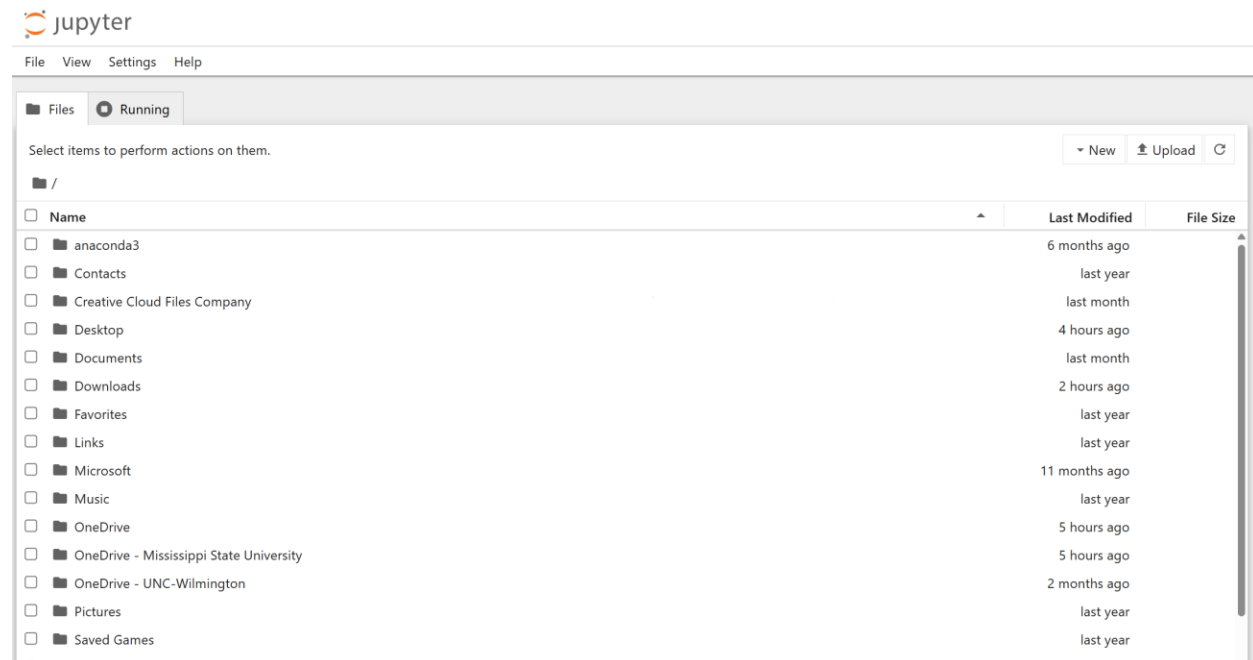
## APPENDIX 2:

After exporting the data there will be only two columns for accuracy assessment one is UAS-echosounder data (“Elevation\_\_Hi” in our case), and the other one is the nearest *in-situ* LiDAR data (“Z” in our case).

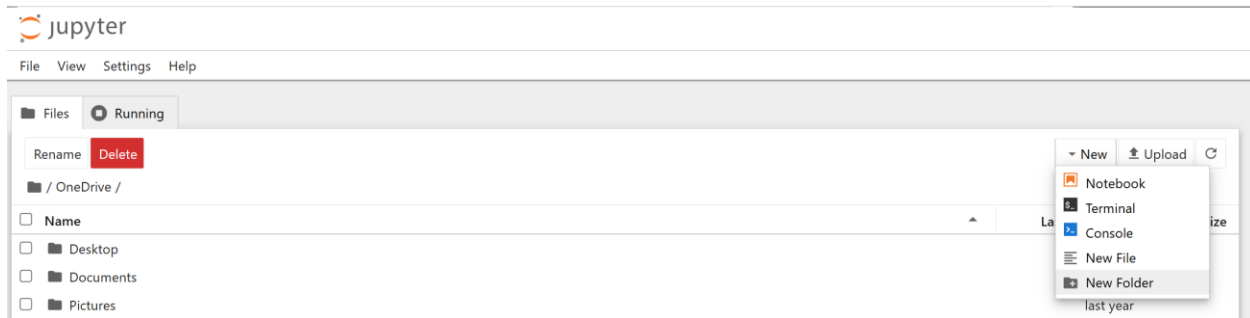
	Z	Elevation__Hi_
3037	35.275	35.231
441	35.386	35.156
7225	34.853	34.800
10897	34.908	34.908
9680	35.083	34.986

Figure: Sample of the accuracy assessment datasets

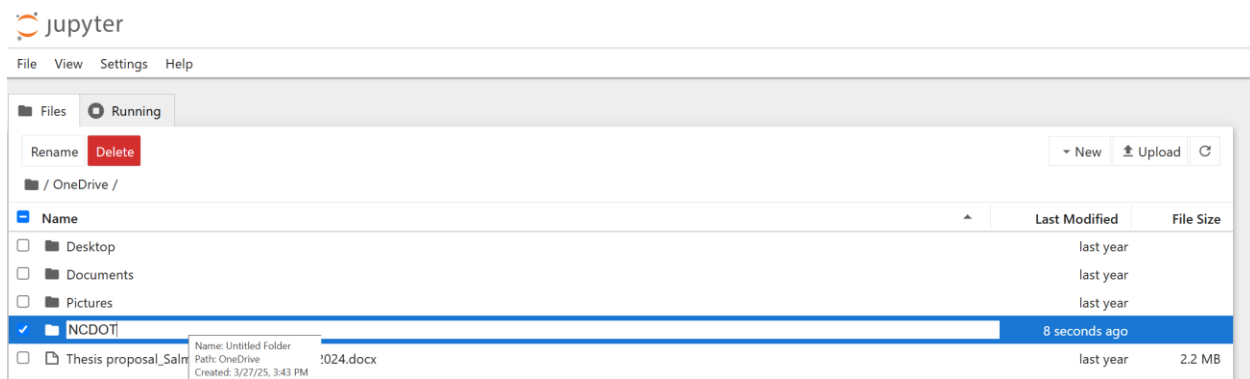
Now for acca accuracy assessment, we have used the Anaconda python environment and Jupyter Notebook for data analysis. For the installation process and launching to the Jupyter Notebook, the YouTube video can be followed ([https://www.youtube.com/watch?v=WOK9HeB-OmY&ab\\_channel=TheCodeCity](https://www.youtube.com/watch?v=WOK9HeB-OmY&ab_channel=TheCodeCity)) published by The Code City. After that, we will see an interface like that which is Jupyter Notebook Library and we can create our file directory.



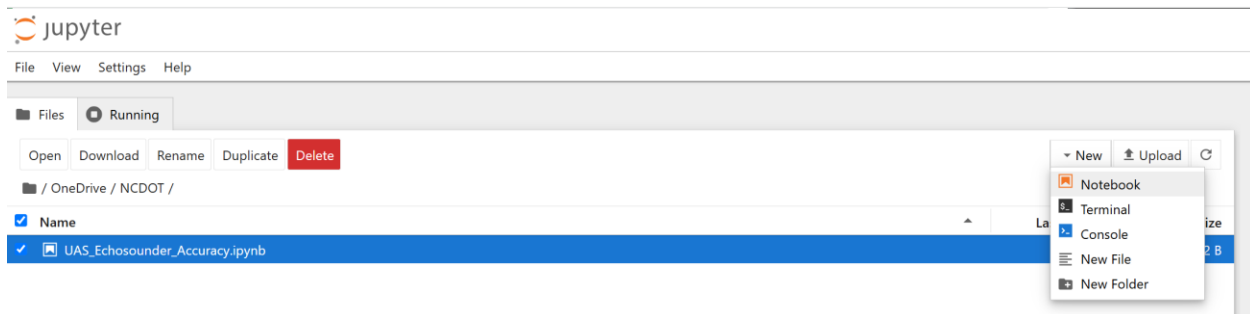
One can choose one drive for data storage and then create a new folder.



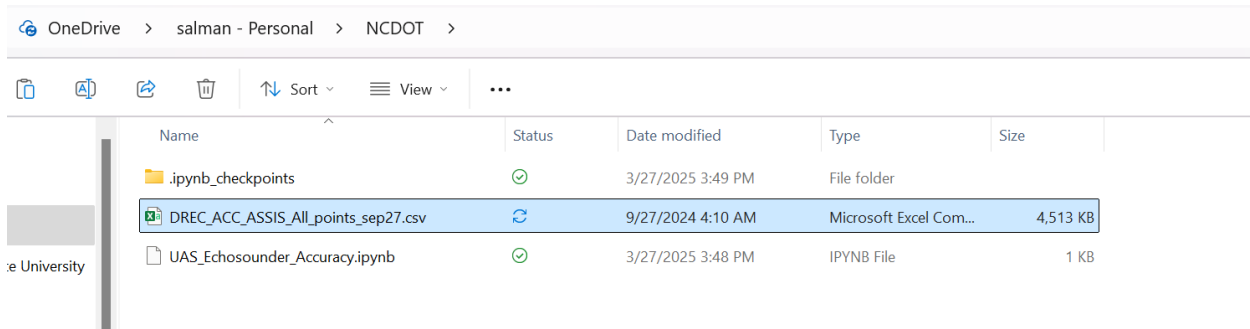
Rename it



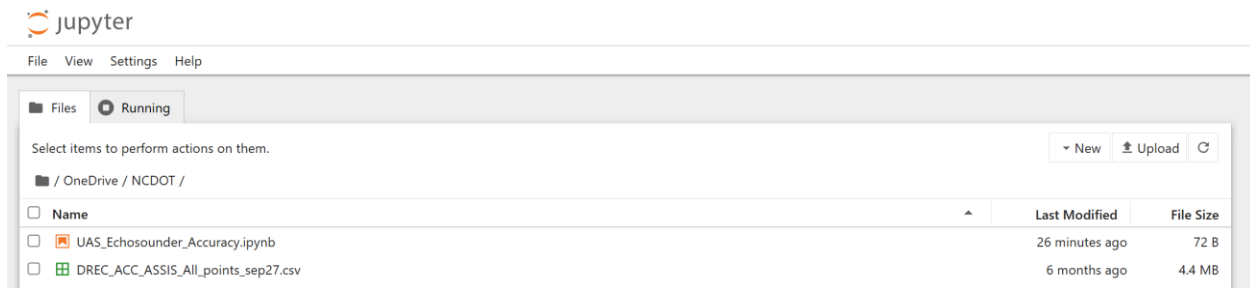
Within the folder create a new notebook and rename it according to your choice.



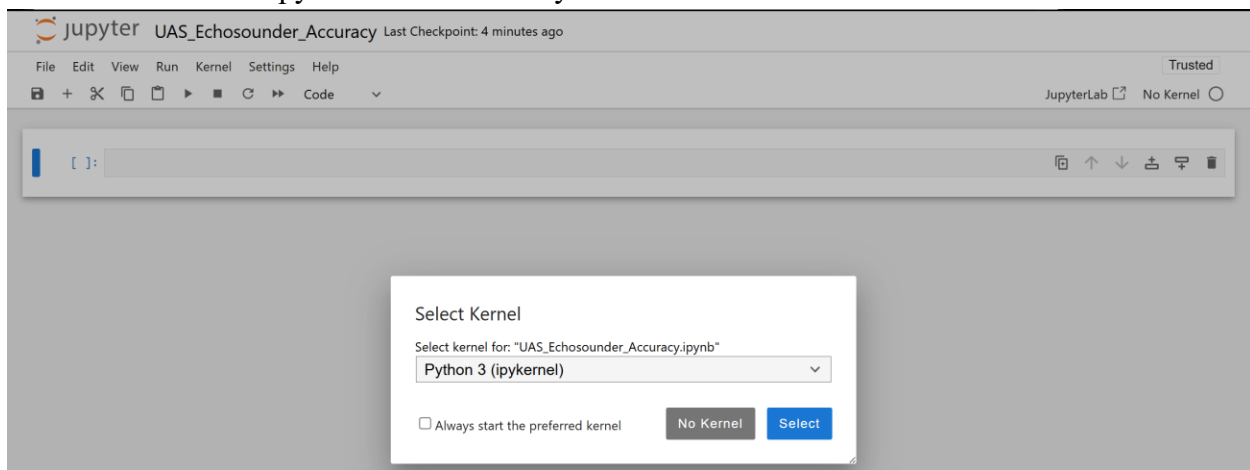
Now copy the CSV file to the same directory



Now reload the browser and it will show up in the directory.



Double-click to the .ipynb file and select Python 3.



Then we need to install different libraries like pandas and matplotlib and some more. And it is very crucial for the automation of the process. To install those libraries check the video ([https://www.youtube.com/watch?v=Fl8QzmoKYfg&ab\\_channel=TheCodeCity](https://www.youtube.com/watch?v=Fl8QzmoKYfg&ab_channel=TheCodeCity)). After downloading and installing those libraries now you can import the libraries and import the libraries and give them an alias (short name) for easier use in your code.

**For instance:**

1. import **pandas**
  - This loads the Pandas library, which is a powerful tool for data manipulation and analysis in Python.
2. as **pd**
  - This assigns the alias pd to the Pandas library, so you can refer to it using pd instead of typing pandas every time.



Finally, the following code is used for calculating RMSE and R-Squared value through Ordinary least squares (OLS) Regression.

```
[1]: import pandas as pd
import statsmodels.api as sm
import matplotlib.pyplot as plt
import seaborn as sns
df=pd.read_csv(r"DREC_ACC_ASSIS_All_points_sep27.csv")
df=df[['Z', 'Elevation__Hi_']]
x=df['Z']
y=df['Elevation__Hi_']
X = sm.add_constant(x)
model = sm.OLS(y,X)
results = model.fit()
print(results.summary())
from scipy.stats import pearsonr

# correlation
print(pearsonr(x, y))
from sklearn.metrics import mean_absolute_error, mean_squared_error, r2_score
from math import sqrt
msr=sqrt(mean_squared_error(x, y))
print(f" RMSE : {msr}")
```

The codes are available as .ipynb file at (NCDOT deliverables 2025\Codes\Echo sounder Accuracy assessment)

The results look like the following-

```
=====
                        OLS Regression Results
=====
Dep. Variable:          Elevation__Hi_   R-squared:                0.728
Model:                  OLS             Adj. R-squared:          0.728
Method:                 Least Squares    F-statistic:             3.056e+04
Date:                   Thu, 27 Mar 2025  Prob (F-statistic):      0.00
Time:                   12:21:25         Log-Likelihood:          13133.
No. Observations:      11439            AIC:                   -2.626e+04
Df Residuals:           11437            BIC:                   -2.625e+04
Df Model:                1
Covariance Type:        nonrobust
=====
               coef      std err          t      P>|t|      [0.025      0.975]
-----
const         9.7904      0.145      67.657      0.000      9.507      10.074
Z              0.7200      0.004     174.815      0.000      0.712      0.728
=====
Omnibus:                 69.510   Durbin-Watson:           0.154
Prob(Omnibus):            0.000   Jarque-Bera (JB):         60.039
Skew:                    -0.123   Prob(JB):                 9.18e-14
Kurtosis:                 2.745   Cond. No.                  7.09e+03
=====

Notes:
[1] Standard Errors assume that the covariance matrix of the errors is correctly specified.
[2] The condition number is large, 7.09e+03. This might indicate that there are
strong multicollinearity or other numerical problems.
PearsonRResult(statistic=0.8530374661476068, pvalue=0.0)
RMSE : 0.10205494167287112
```

Similarly, we find out the outliers for 2SD and 3SD and calculate the accuracy excluding the outliers. The codes are available as .ipynb file at (NCDOT deliverables 2025\Codes\Echo sounder Accuracy assessment)

The second phase of the accuracy assessment of different interpolation methods considers 5-meter and 10-meter flight line spacing and UAS-echosounder collected all cleaned raw data.

The following code is being used, and we also rank the interpolation methods according to their performance.

The code (.ipynb file) and the data set can be found at –

1. NCDOT deliverables 2025\Codes\Using Sampling point method Accuracy assessment\_5\_Meter\_flight\_line spacing
2. NCDOT deliverables 2025\Codes\Using Sampling point method Accuracy assessment\_10\_Meter\_flight\_line spacing

In the third phase experimenting with sampling points the following code is being used, and we also rank the interpolation methods according to their performance.

The code (.ipynb file) and the data set can be found at –

1. NCDOT deliverables 2025\Codes\Using Sampling point method Accuracy assessment\_5\_Meter\_flight\_line spacing
2. NCDOT deliverables 2025\Codes\Using Sampling point method Accuracy assessment\_10\_Meter\_flight\_line spacing

## Chapter 2 – Appalachian State University Work

### Executive Summary

This report from Appalachian State University presents the findings of a bathymetric survey conducted at three key sites: Wards Mill reach of the Watauga River, Rhodhiss Lake, and Price Lake. The study aimed to assess changes in streambed and lakebed topography, evaluate the accuracy and cost-effectiveness of various bathymetric surveying methods, and identify the most suitable techniques for different environmental conditions.

**Wards Mill Dam in Sugar Grove, NC:** The survey at the Wards Mill reach of the Watauga River, conducted approximately 1.5 years after the removal of the Wards Mill Dam, revealed significant changes in streambed composition, with increased sediment deposition and shifts in bed elevation. Structure-from-Motion (SfM) photogrammetry, when corrected with linear adjustments, demonstrated a Root Mean Square Error (RMSE) of 0.33 feet (0.1 m), showing strong alignment with total station data ( $r = 0.94$ ,  $p = 2.5e-10$ ). While SfM provided high accuracy in shallow and clear water conditions, its performance was limited by turbidity and complex bed features. Sonar-based methods proved more effective in deeper and turbid waters but incurred higher operational costs.

**Rhodhiss Lake in Morganton, NC:** At Rhodhiss Lake near Huffman Bridge, sonar-based surveying was the primary method used due to the greater depth and low visibility of the lakebed. The survey achieved consistent depth measurements with an RMSE of 1.74 feet (0.53 m), confirming the reliability of sonar in deep and turbid conditions. SfM photogrammetry was not viable due to limited water clarity. The results underscore the suitability of sonar-based methods for large, deep water bodies where visibility constraints limit optical techniques.

**Price Lake in Blowing Rock, NC:** Surveying at Price Lake involved both sonar-based methods and SfM photogrammetry. While SfM captured high-resolution data in shallow and clear water areas, sonar was essential for mapping deeper sections where water clarity was poor. The combined use of both methods resulted in comprehensive lakebed coverage with an overall RMSE of 1.01 feet (0.31 m). The findings highlight the advantages of integrating sonar and photogrammetry to improve accuracy across varying depths and water clarity conditions. A follow-up study was planned to collect additional data; however, parkway closures following Hurricane Helene prevented the team from conducting further surveys. Although the team anticipated returning this year to gather more data, administrative changes prevented the necessary permits from being secured for a flight.

The study demonstrates the effectiveness of combining sonar-based methods and SfM photogrammetry to optimize data accuracy and coverage across different environmental settings. Recommendations include adopting a hybrid surveying approach tailored to site-specific conditions, balancing cost, accuracy, and operational feasibility. Future research should investigate the impact of seasonal variations and long-term sediment transport on streambed and lakebed morphology, as well as assess how these changes may affect infrastructure stability and resilience.

## Introduction

Dams across the entire U.S. have been taken down in increasing numbers in the past decade as they have filled with sediment, and become unsafe or inefficient (Bellmore et al. 2017; Connor et al. 2015). After a dam is removed, there is usually an acute release of water and sediments from the previous impoundment downstream, which could rapidly alter the downstream channel, due to the redistribution of the sediment and the damage to the shoreline (Doyle et al. 2002). In addition, long-term soil erosion and sediment scour could occur on the riverbed and on the two banks of the upstream area, which was previously submerged by the high-level water in the impoundment and is then revealed to air after dam removal. Both processes above will significantly change the bathymetry of the up- and down-stream river channel.

Traditionally, the monitoring and assessing of dam removal impacts on stream geomorphology, bathymetry, and bank soil erosion requires temporally frequent *in-situ* surveys (e.g., cross-sectional and longitudinal surveys) on the up- and down- stream before and after dam removal. These temporally frequent surveys require a lot of manpower and cost a great amount of time. The advent of Unmanned Aerial Vehicles (UAVs) offers a new approach that can be used to efficiently monitor soil erosion and bathymetric changes caused by dam removal and save significant time and money. However, few dam removal efforts have incorporated this newly emerged technology, and significant information and technology gaps still exist in planning, mapping, and assessment.

Ward's Mill Dam, a 130-foot-long, 20-foot-high rock and concrete dam, was built in 1890 and impounded the Watauga River downstream in Valle Crucis, NC (about six miles downstream). The dam was used for hydroelectricity to power a sawmill and to provide electricity for local homes in the valley, but it has been inactive since 2016 and has become a significant blockage on the Watauga River for aquatic species migration and public recreational activities, such as kayaking and canoeing. Watauga County, therefore, decided to remove the dam on May 12 - 14, 2021.

This project first aims to take advantage of the recent removal of Ward's Mill Dam (Figure 1), located on the Watauga River in Western North Carolina. We would like to compare UAV-based pre/post-removal data on the erosion/sediment transport regime to develop a better understanding of how southern appalachian river systems like the Watauga will respond to the removal of dams of similar type and size, which are common throughout southern Appalachia. In particular, we are interested in the river's bathymetric response to dam removal.

UAV-based echo sounder sonar sensors provide a versatile, accurate, and cost-effective solution for bathymetric data collection, particularly in areas where traditional methods may be challenging or less efficient. They are well-suited for monitoring changes over time, such as after dam removal, and can be integrated with other sensors to improve the quality and scope of data

collection for various water bodies. The accuracy of UAV-based data, including sonar data and optical data will be first assessed. Then, the collected data will be used to detect the changes that occurred to the banks and riverbeds after dam removal. In addition, the possibility of combining different UAV-based sensors for the survey of topography and bathymetry of different waterbodies will be evaluated. We are particularly interested in evaluating the applicability of UAV-based sonar for a broader range of areas.



**Figure 57: Ward's Mill Dam – facing upstream (left: pre-removal, right: post-removal).**

## Research Objectives

The main objective of this project is to evaluate and investigate the applicability of UAV-based Sonar for the bathymetry of waterbodies with different levels of water clarity. Specifically, this research is aimed to:

- 1) Refine the set of standard procedures developed by this research team for collecting UAV-based remote sensing data (e.g., surface elevation and bathymetric maps),
- 2) Evaluate the accuracy of UAV-based remote sensing data by comparing with the *in-situ* survey data produced by total stations, and
- 3) Assess the bathymetric changes along the river channel and the soil erosion on the up- and down-stream banks after dam removal through monitoring the elevation, shoreline, and water depth changes.

We aim to accomplish this by investigating the following specific research questions:

- 1) How can UAV technology be implemented as an easy and quick tool to capture the changes of up- and down- stream banks and water depth after dam removal? What is the best time interval for UAV-based data collection?
- 2) What is the accuracy of UAV-based remote sensing data? Is UAV technology reliable for the monitoring of dam removal-induced soil erosion and bathymetric changes?



- 3) How can UAV data be efficiently analyzed using geographic information systems (GIS) to extract the information on soil erosion/riverbed scouring? What is the rate of soil erosion/riverbed scouring on Watauga River after the dam was removed?
- 4) How can the information on soil erosion and bathymetric changes assist with the mission of reviving the communities adjacent to the removed dam and guide public recreational activities (e.g., kayaking) in that area?
- 5) Is UAV-based Sonar reliable for retrieving bathymetric information of waterbodies with different levels of water clarity located in Western North Carolina?

In this proposed project, we plan to adopt a UAV-based Sonar system for the retrieval of river bathymetry (i.e., topography of riverbeds). With the advancement of UAV technology, bathymetric mapping with UAV-based Sonar systems becomes feasible. In this proposed project, we aim to evaluate the capability of UAV-based sonar and assess the possibility of combining UAV-based SFM and bathymetry Sonar for the monitoring of soil erosion and riverbed scouring after dam removal. To monitor the short-term and long-term changes, we plan to collect the UAV-based remote sensing data every month for two years. In addition, to evaluate the applicability of UAV-based Sonar over waterbodies with different levels of water clarity (or turbidity), we plan to collect data for two other lakes, including 1) Price Lake on Blue Ridge Parkway and 2) Rhodhiss Lake near Huffman Bridge, NC. Price Lake has a high level of water clarity while Rhodhiss Lake has a low level of water clarity (high turbidity) as shown in Figure 2.

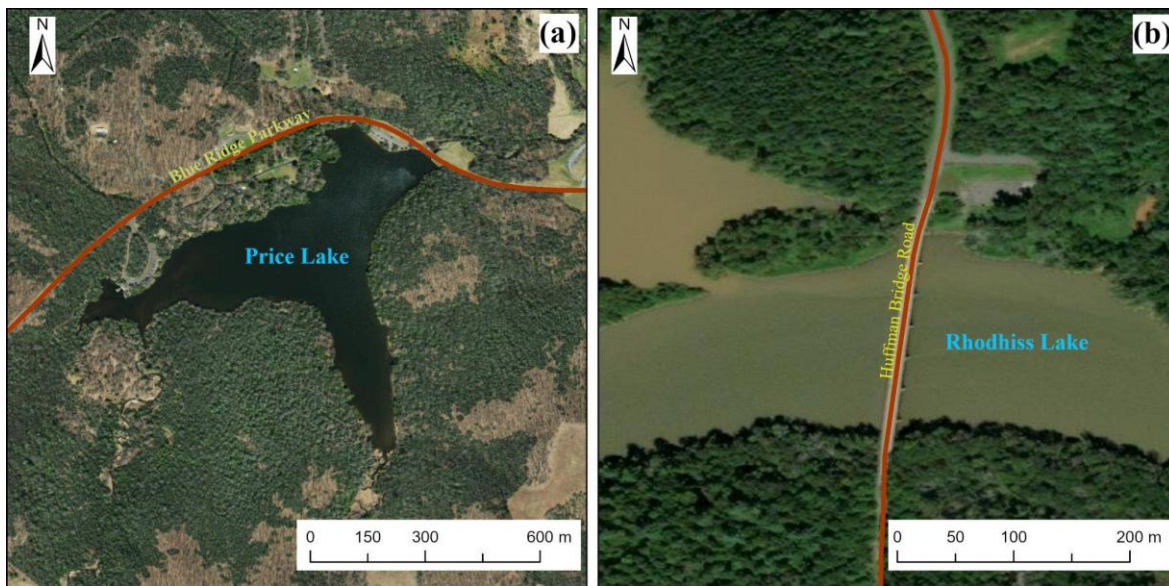


**Figure 58: Two more testing sites (left: Price Lake, right: Rhodhiss Lake).**

The specific steps are as follows:

- 1) Refine our current standard procedures of data collection based on preliminary results and previous experience.

- 2) Collect UAV imagery data for the up- and down-stream of Ward's Mill Dam every month for one year.
- 3) Generate orthophotos, DEMs, and bathymetric maps.
- 4) Evaluate the accuracy of UAV-based remote sensing data by comparing it with data obtained from conventional field surveys (e.g., cross-sectional surveys).
- 5) Combine the data generated by the two different technologies for more detailed and accurate mapping of river bathymetry.
- 6) Identify dam removal impacts on channel morphology (e.g., soil erosion/riverbed scour) by comparing the orthophotos, DEMs, and bathymetric data collected at different dates.
- 7) Evaluate the applicability of UAV-based Sonar with different levels of water clarity.
- 8) Publish and disseminate research outcomes.

### Significance of Proposed Work

Traditional surveys (e.g., cross-sectional and longitudinal surveys) to monitor and assess the impact of dam removal on river bathymetry and soil erosion/scour are labor-intensive and time-consuming. The advent of UAVs offers a new approach that can be used to efficiently monitor soil erosion and bathymetric changes caused by dam removal. In recent years, sonar sensors have been used to collect data on underwater topography. However, this technology has limitations with how accurately it can make measurements. Part of the significance of this proposed study will be to create a site-specific evaluation for the viability of this and other methods for obtaining underwater topography. The proposed research project will provide a set of standard procedures to improve the accuracy of topographic/bathymetric data collection using UAVs. This will help better understand southern Appalachian river systems' bathymetric response to dam removal.

In addition, this research will offer a great opportunity to evaluate the possibility of combining different UAV-based sensors for the survey of topography and bathymetry of different water bodies. Prospective users must understand the capabilities and constraints associated with various types of remote sensing to ensure efficient use of these evolving technologies. We firmly believe that the proposed study will be an excellent starting point to expand the applicability of UAV-based systems for the bathymetry of waterbodies to larger scales.

The use of UAV technology in dam removal projects and soil/bathymetric monitoring has direct connections to NCDOT's mission to develop sustainable communities. It will provide valuable insights into the influences of construction projects on river systems and offer guidance for the balance of sustainable development and environmental protection.

## Ward Mill Dam Results

### Streambed Bathymetric Survey and Impact of Hurricane Helene

Accurate streambed bathymetric data are essential for a wide range of hydrologic research applications. Traditionally, data collection has relied on methods such as manual cross-sections, sonar, and, more recently, aerial lidar sensors. However, in shallow or high-gradient streams, sonar may be impractical, while manual surveys struggle to capture continuous streambed surfaces effectively. Conventional aerial topographic-bathymetric surveying provides high accuracy but often requires resource-intensive methods, leading to significant costs and labor demands. Additionally, the use of large sensors necessitates equally large aerial systems, posing challenges for surveying steep, narrow, or forested waterways.

The Wards Mill reach of the Watauga River in Western North Carolina serves as the focal point of this investigation. Approximately 1.5 years post-dam removal, this area exhibits a diverse streambed composition, featuring sand, cobbles, and boulders. This diversity makes it an ideal location for testing new bathymetric surveying methods. Figure 3 displays cross-section data, with observed total station data serving as the benchmark against which Structure-from-Motion (SfM)-derived model data is compared. After applying a linear correction, the Root Mean Square Error (RMSE) of the model dataset was 0.33 feet (0.1 m), demonstrating strong agreement between modeled and observed data ( $r = 0.94$ ,  $p = 2.5e-10$ ). However, smoothing effects are evident, particularly in regions with rapid elevation changes.

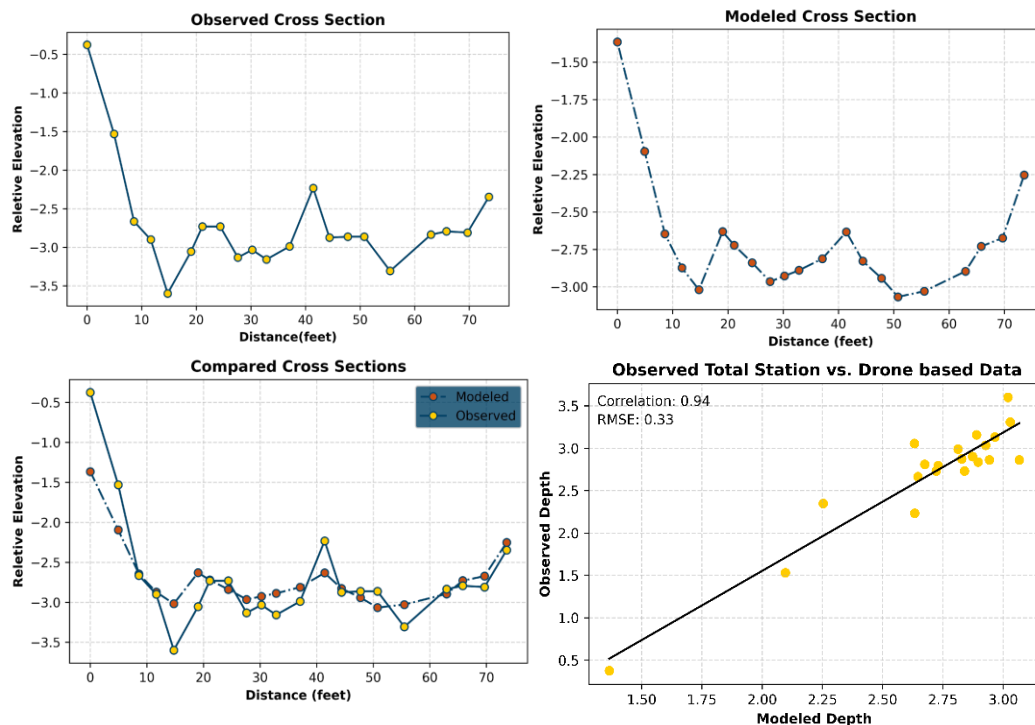
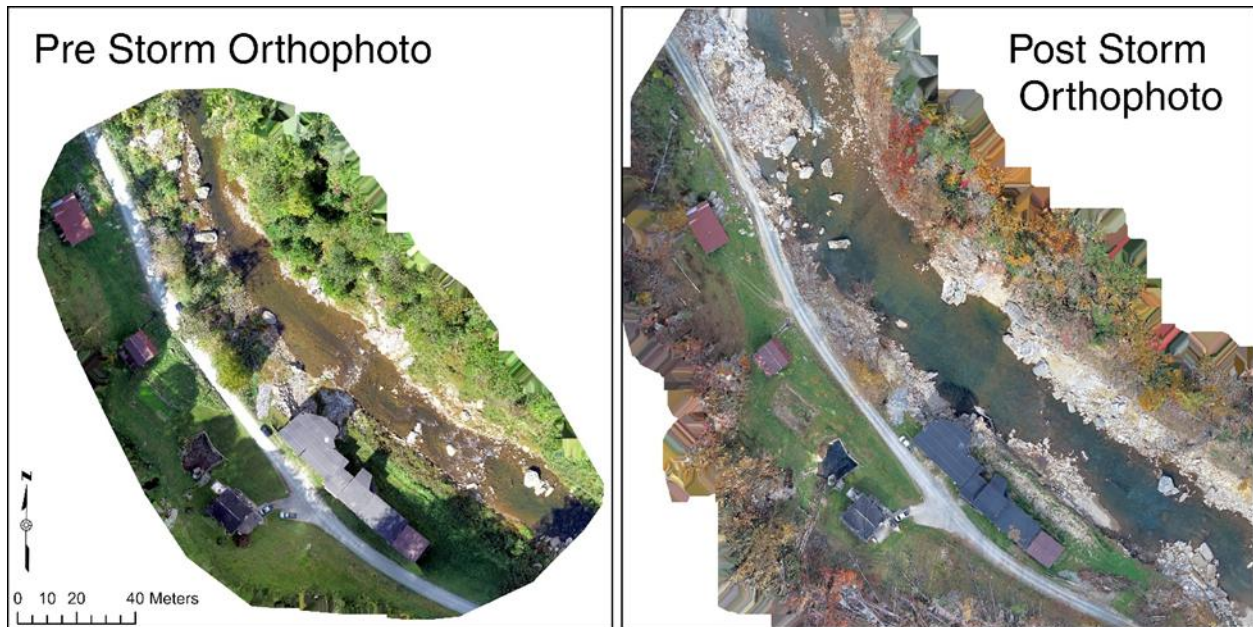


Figure 59: Cross-section data analysis



## Hurricane Helene: A Natural Experiment

Following the initial proof-of-concept study, Hurricane Helene provided an unexpected opportunity to assess the geomorphic impacts of extreme weather on the streambed. To capture these changes, a second aerial survey was conducted using a Phantom 4 RTK drone. The post-storm orthophoto (Figure 4) revealed substantial geomorphic transformations in the streambed.



**Figure 60: Storm damage overview**

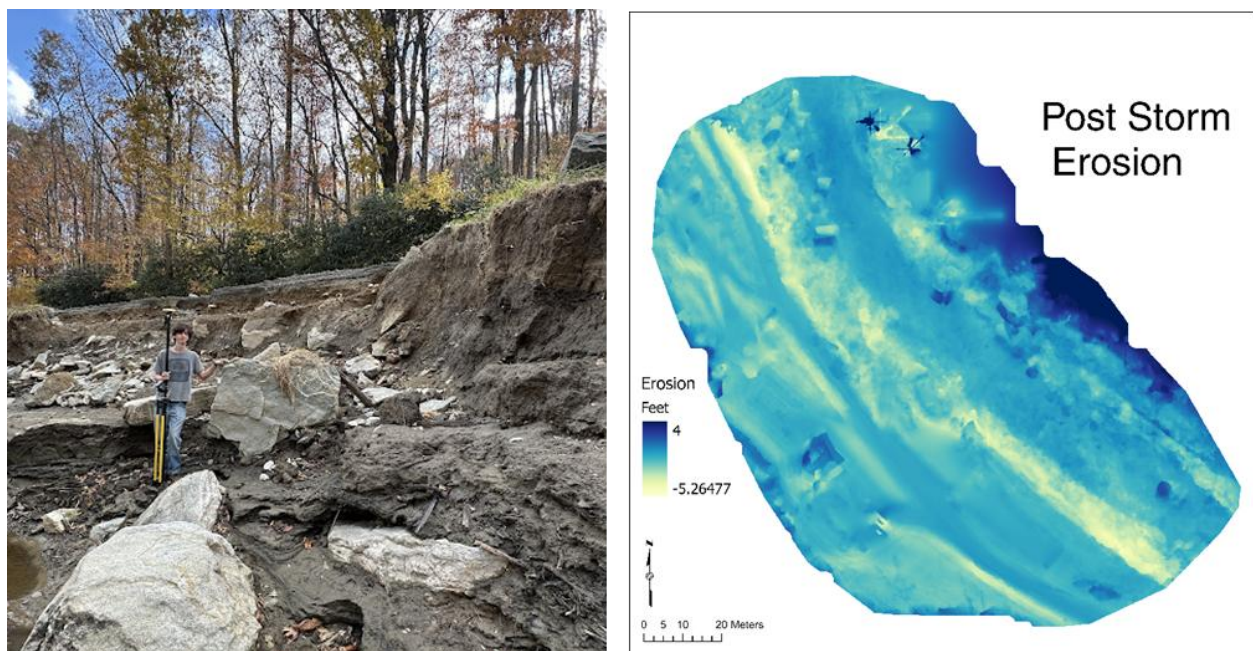


**Figure 61: Bank erosion and GCP collection (left), Erosion and deposition from Helene (right)**

Ground control points (GCPs) were collected during this flight (Figure 5), and the data was georeferenced accordingly. A differencing operation was performed to identify areas of erosion and deposition. The results (Figure 5) indicate extensive erosion along the streambanks, with channel widening exceeding 100% in multiple areas. Erosion depths exceeding 4 meters were observed, leading to an estimated total erosion volume of 8,424 cubic meters over a 200-meter stretch of the river.

## Rhodhiss Lake near Huffman Bridge in Morganton, NC Results

### **Data Collection at Rhodhiss Lake near Huffman Bridge:**

In the last quarter, the App State team made significant progress toward achieving our project goals. A key milestone was the acquisition of the SkyHub and Echo Sounder, which enabled us to begin evaluating UAV-based sonar systems for bathymetric surveying and bridge scour monitoring. This equipment acquisition marked a crucial step in advancing our research capabilities.

Following the acquisition, the team completed virtual training provided by SPH Engineering in early July, which covered the operation of the SkyHub, Echo Sounder, UGCS Custom Payload Manager (CPM), and Hydromagic processing software. After our training, we conducted several test flights and training scenarios at App State Duck Pond, where we developed a data collection protocol (Figure 6). These exercises were invaluable for refining our operational skills and gaining familiarity with the new equipment in real-world conditions. Additionally, the team completed further data collection using an RTK-enabled drone to develop Structure-from-Motion (SfM) topobathy models for a pre-dam removal survey on the Shulls Mill section of the Watauga River.



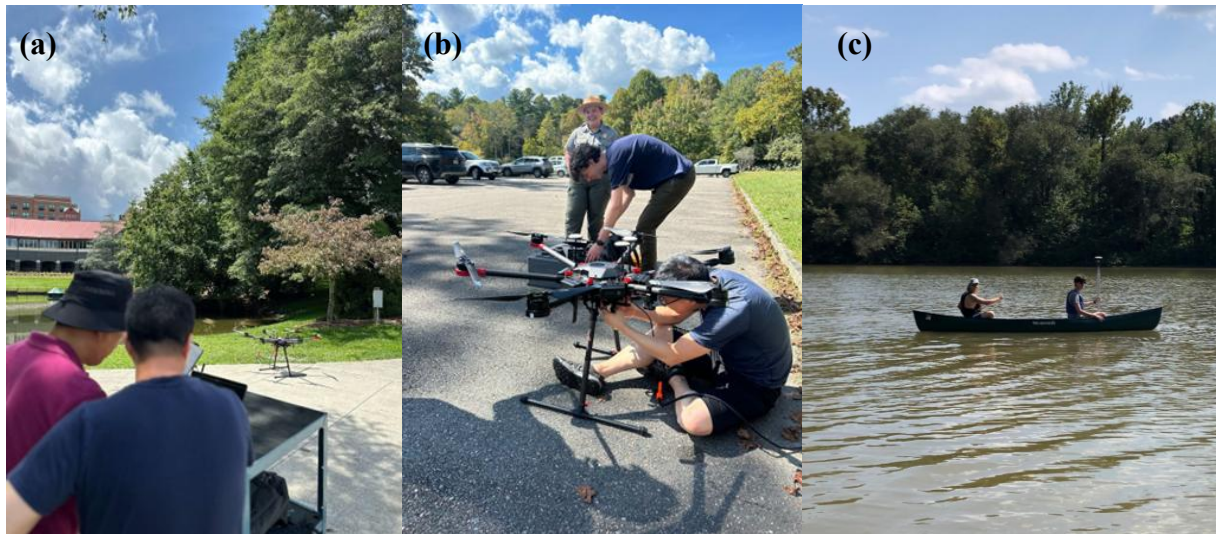


**Figure 62: (a) test flights and training scenarios at App State Duck Pond. (b) collect echo sounder data at Rhodhiss Lake. (c) collect ground truth data with a canoe at Rhodhiss Lake.**

The App State UAV team collected data at Rhodhiss Lake near Huffman Bridge, NC (see Figure 7) on 8/22/2024. The team used the Matrice 600 Pro equipped with the SPH ECT 400S single-frequency echo sounder to collect bathymetric data from the lake bed. The data was collected in 2 flights, the first flight ran along a pre-made route as indicated by the back-and-forth lines in Figure 8a, while the second flight was flown manually under the bridge to collect information on the bridge footers. The UAV flew at a fixed speed of 0.8 m/s, as recommended by SPH, to reduce the sensor angle. With this flight speed, the sampling distance is about 0.1 m along the flight routes. After the drone flights, ground-truth water depth was randomly collected at 29 points in a canoe with a 25 ft rod and a Differential-GPS (Trimble DA-2) fixed to the top of the rod, as shown in Figure 8b. The water depth at each point was measured to the accuracy of 1/10 ft. This manually collected data set was then used to assess the accuracy of the UAV-based echo sounder data.

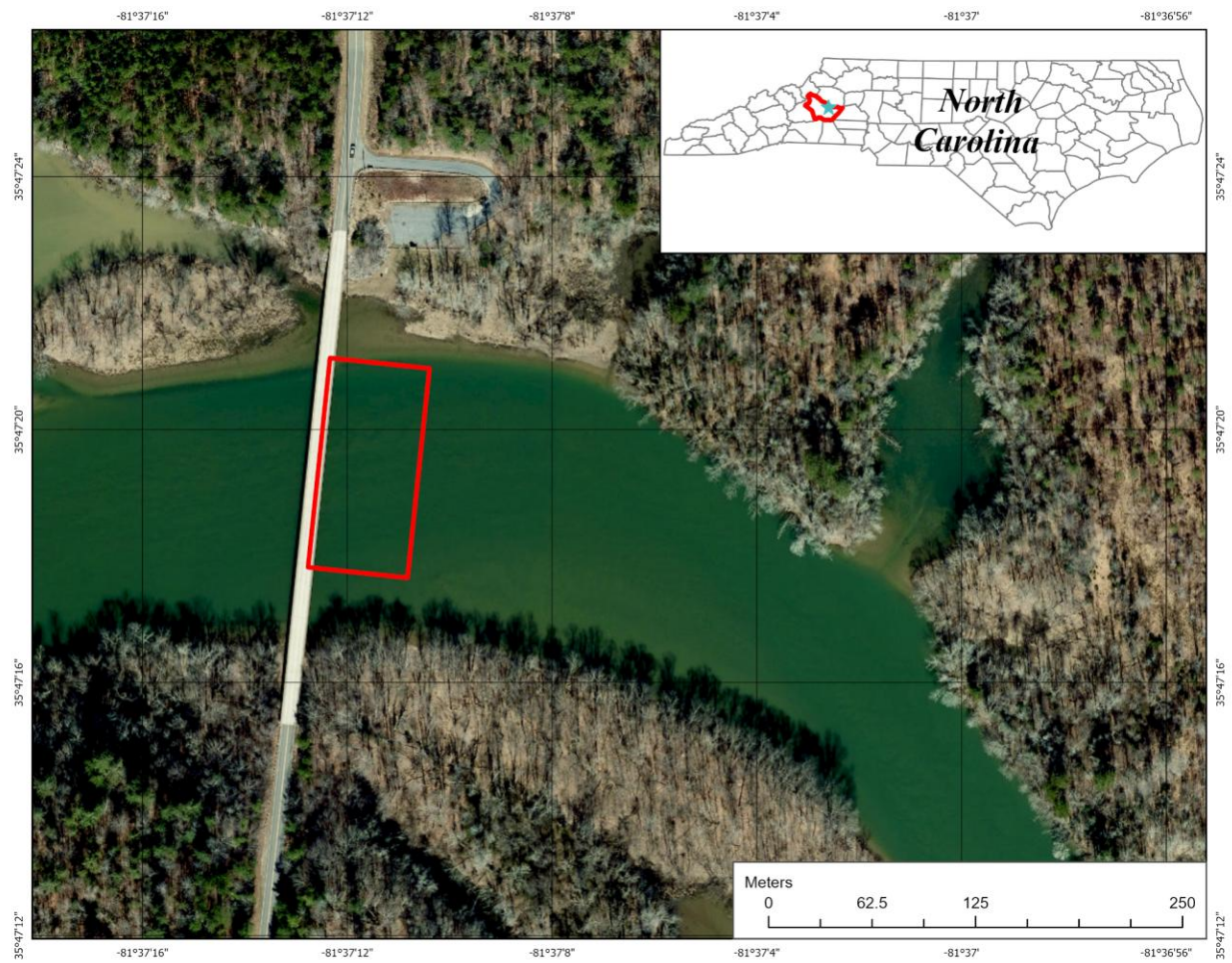


**Figure 63: Study Location**

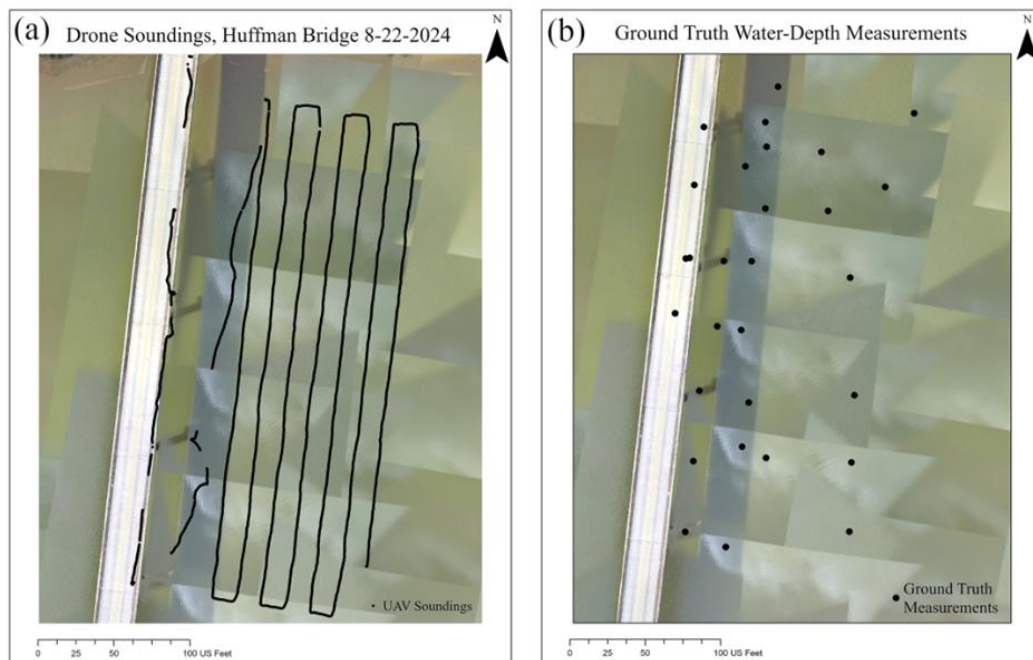


**Figure 64: (a) Bathymetric data collected by drone-based echo sounder, (b) ground truth depth measurements.**

### **Data Processing:**

The echo sounder data was processed in Eye4Software Hydromagic to remove outliers and to generate the bathymetric raster map for the downstream area of Huffman Bridge. The bathymetric map was generated by interpolating the UAV echo sounder data with the Delaunay triangulation algorithm. The spatial resolution is set to 1 ft (about 30 cm). As shown in Figure 9, the area in the middle of the lake covered by the UAV flight routes has much better details as compared to the areas close to the banks on the upper and lower sides (shown in red in Figure 9).

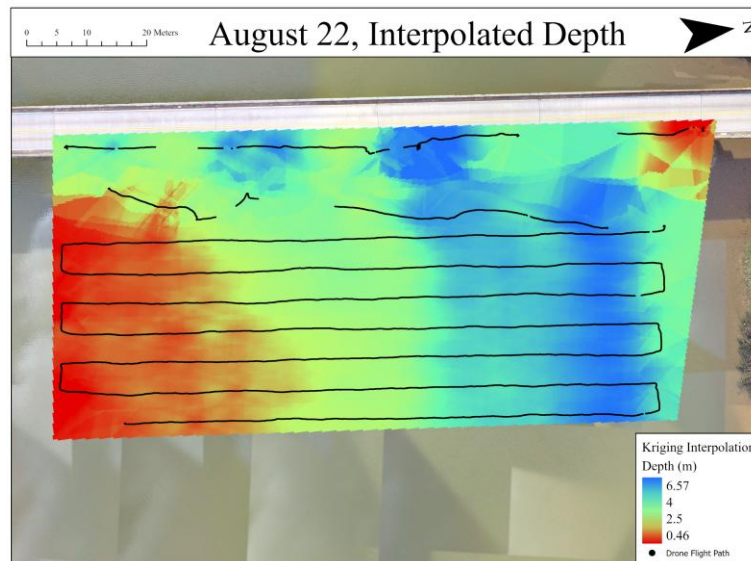


**Figure 65: Interpolated depth matrix from UAV based echo sounder.**

### **Accuracy Assessment:**

The interpolated bathymetric raster map was loaded into ArcGIS Pro for accuracy assessment. The raster values (interpolated water depth) at the ground-truth sampling points were extracted and exported to Excel. The raster values were then compared to the ground-truth measurements to calculate the accuracy of the soundings. As shown in Figure 10, a strong correlation was observed between the interpolated water depth and the ground-truth measurements. The  $R^2$  was 0.90 and the  $RMSE$  was 0.53 m, showing a promising direction for bridge scouring monitoring.



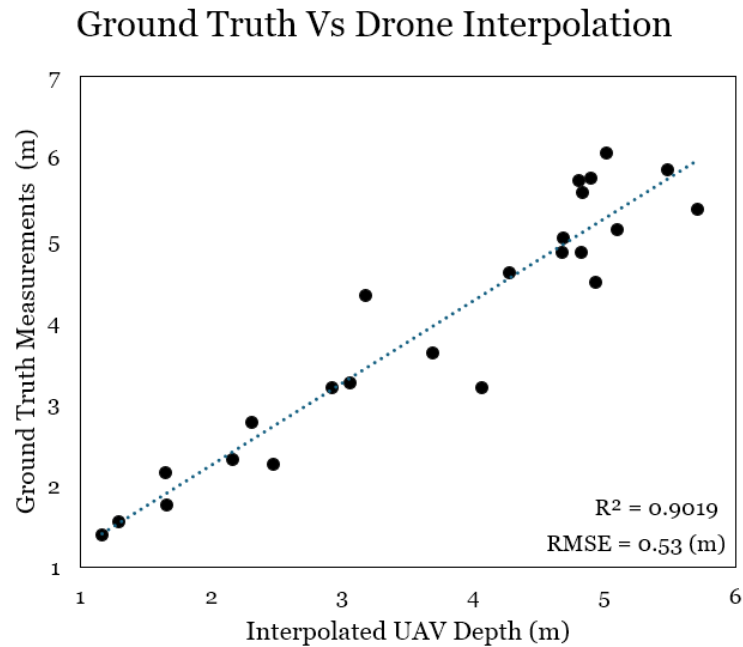


**Figure 66: Delaunay triangulation algorithm interpolation compared to the ground truth data.**

#### **Traditional Inspection Comparison:**

The bridge inspection team with Arete Engineering accompanied us to our data collection and conducted their traditional inspection. This involved them walking the length of the bridge and collecting data at and between every footer with a plumb bob. As this bridge has six-footers, that meant that the data they were using to monitor the health of this bridge only contained 12 points. Figure 11 displays the UAV depth information compared to the manual survey. These different data sets did not match that well. This is likely due to several factors, one is that the plumb bob might sink farther into the bottom than the sonar would penetrate, vegetation on the bottom, errors in the interpolated data that was extracted (not at the exact location), and potential misalignments. Even with these possibilities, the trend in the data is the same and includes a much greater amount of detail compared with traditional methods. It is worth investigating the reasons for the differences, as they could likely be easily remedied.

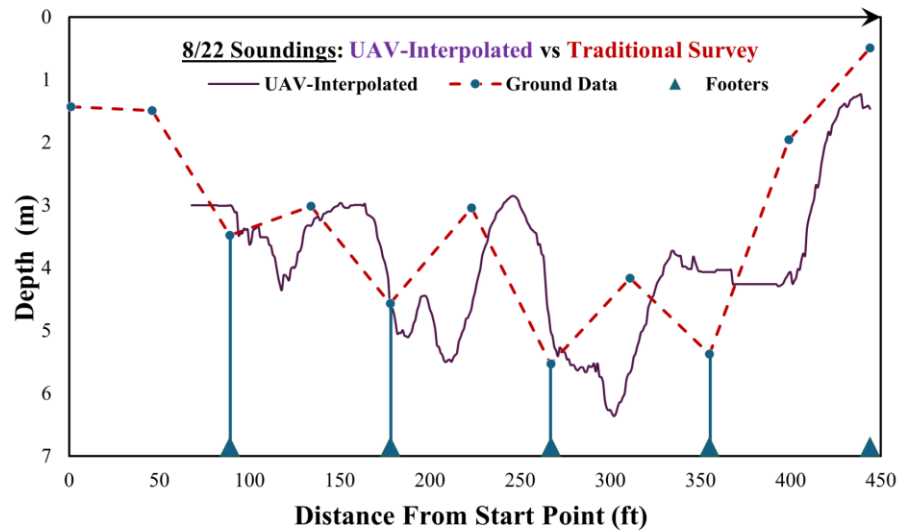


**Figure 67: Comparison between the UAV-interpolated depth and traditional survey depth**

### Post Hurricane Helene:

The data was collected in the same way as the previous collection. Using the Matrice 600 Pro with the ECT 400s Echologger (Figure 12) to collect the sonar data. The autonomous flight path was made in UgCS with the accompanying UgCS CPM to log the sonar data. The other flight was flown by Professor Alex O'Neill to collect closer to the bridge (Figure 13).



**Figure 68: M600 Pro (left), ECT 400s Echologger (right)**



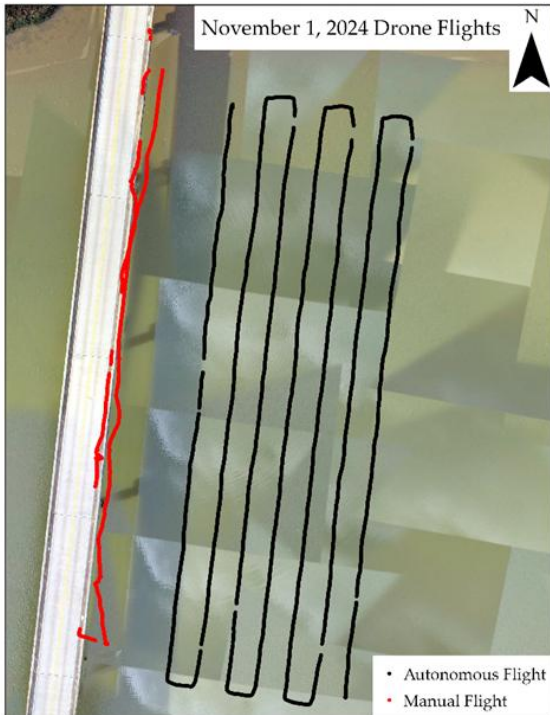


**Figure 69: Flight paths**

### Data Processing:

In much the same way, the sonar data was pulled from the Skyhub and brought into Eye4Software Hydromagic for pre-processing (Figure 14). The processing was relatively simple and subjective, essentially removing any spikes and obvious visual errors.

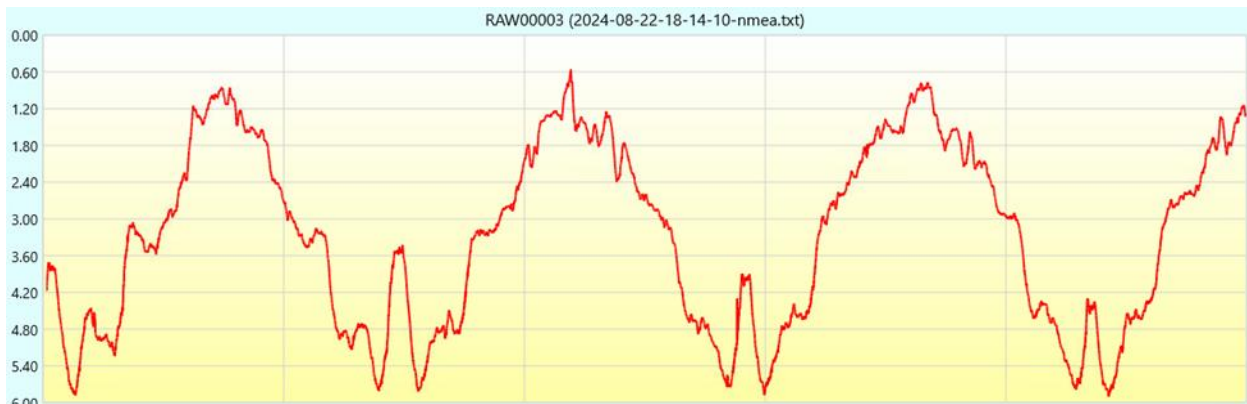


**Figure 70: Example Echogram as seen in Hydromagic Software**

To improve the control over the final products, the pre-processed data was then brought into ArcGIS Pro. This was learned after the first collection and was implemented to improve the workflow. The actual processing involved plotting the soundings with xy table to point, and then

several different interpolation methods were used to create a depth map of the surveyed areas. The universal kriging method was decided on for generating the final products (Figure 15).

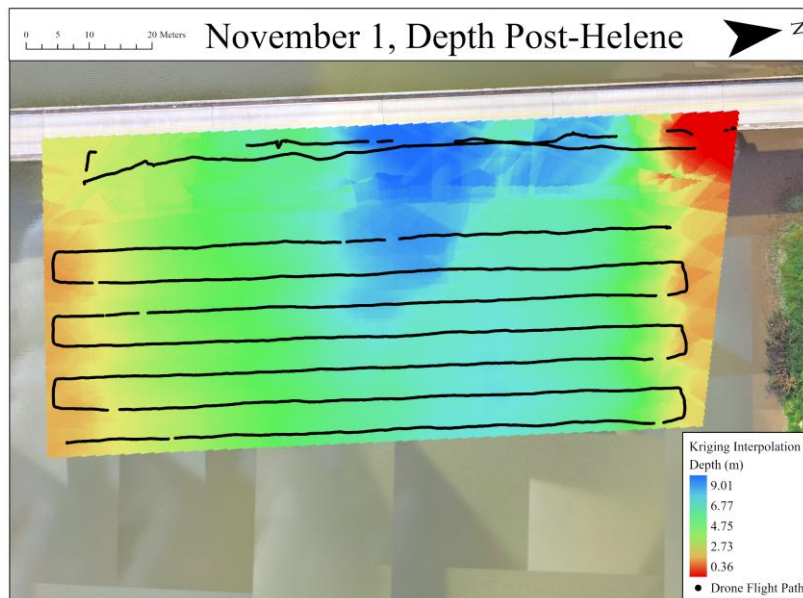


**Figure 71: Post Helene interpolated depth map.**

### Change Detection:

Utilizing the previous flight information from before Hurricane Helene allowed for the visualization of change between the dates (Figure 16). To generate the change detection raster, the 8/22 flight was brought into ArcGIS Pro to create a universal Kriging raster for consistency. The 11/1 raster was then subtracted from the 8/22 raster to display the erosion and deposition that occurred.

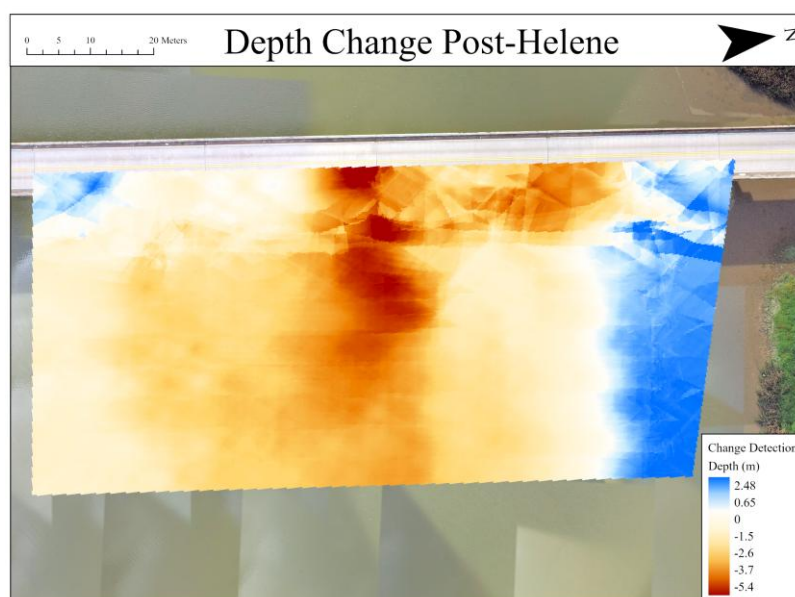


**Figure 72: Depth change after Helene, red indicates erosion and blue indicates deposition.**

### **3D Visualization:**

To further improve the visualization of the bathymetric data, 3D products were created for both 8/22 and 11/1. This was done by creating new interpolated rasters with absolute elevation included instead of depth values, this was done by taking the measurements of the water surface and subtracting the depth values from them. The rasters were then converted into Triangulated Irregular Networks (TINs) from which the TINs were converted to 3D polygons that allowed them to be viewed in 3D. These were all brought into ArcGIS Online to host and display the files. The online map can be found here

(<https://appalachian.maps.arcgis.com/apps/instant/3dviewer/index.html?appid=b51228fd2f8a4c80b61c2c8573adb456>).

Figure 17 shows the maximum depth recorded in both collections. The 3D bridge asset generated in ArcGIS Drone2Map uses images collected on 8/22 that were used to create the ortho mosaics in the background of the figures. While the model may be rough, this was due to the drone mission being focused on nadir imagery, thus not capturing information on the underside of the bridge. Maximum depth increased by 2.5m (8.2ft), with some areas eroding over 5 meters (16.4ft). The highest rate of erosion was just south of the deepest location at 5.4 meters of erosion. Figure 16 displays the detected erosion between the flights, while Figure 17 show the deepest recorded point in both collections.

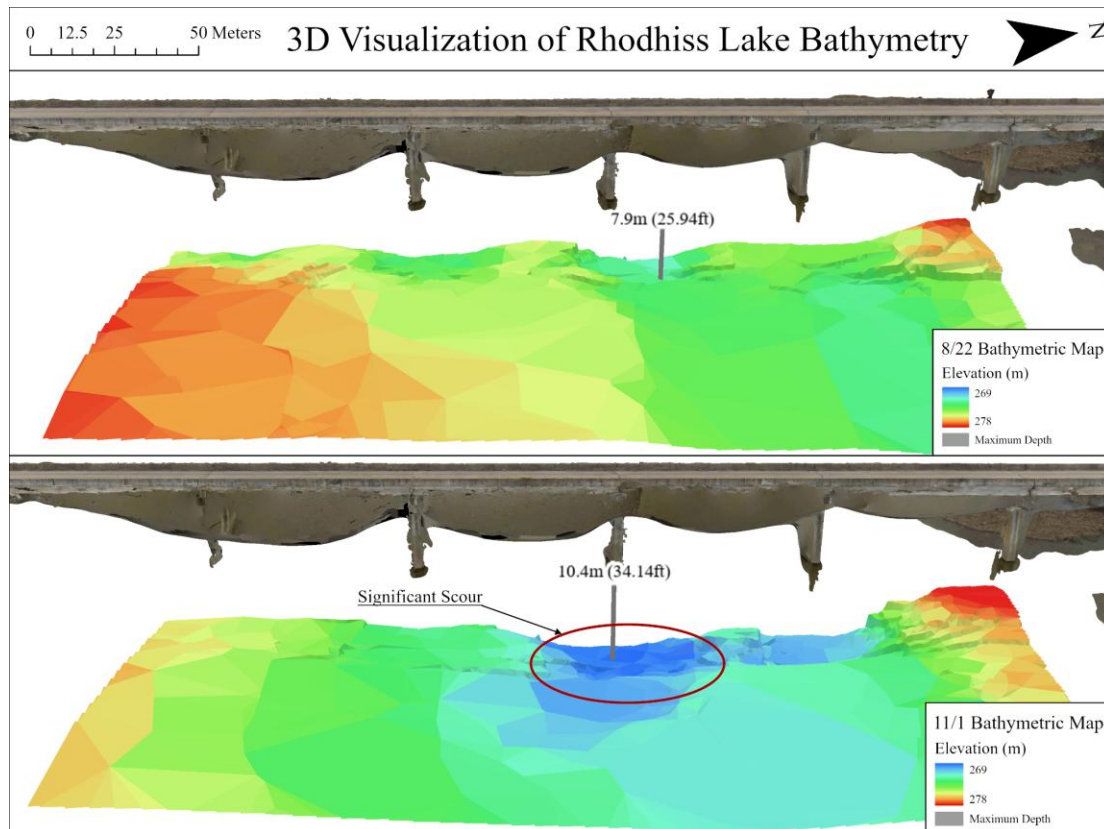


**Figure 73: Visualization of Rhodhiss bathymetry, with Huffman bridge SfM model included**

## Price Lake in Blowing Rock, NC Results

### Data Collection:

The data collection at Price Lake took place on September 20th, it consisted of a sonar flight with the M600 system and a ground truth collection from a canoe. The procedures of this data collection were the same as the previous collection at Price lake. So, the route was made in UGCS and flown autonomously, with no bridge to worry about, no manual flight was conducted. The only difference between the Price Lake collection and the Rhodhiss collection was the use of a plumb bob attached to a cloth measuring tape, compared to the rod used at Rhodhiss. This was because, before the collection, we found no data on the depth of the lake. While in the field, watching the live sonar feed in UGCS we witnessed a large amounts of spikes and erroneous readings, which is why there are points in the line in figure 18 that are more sparsers.

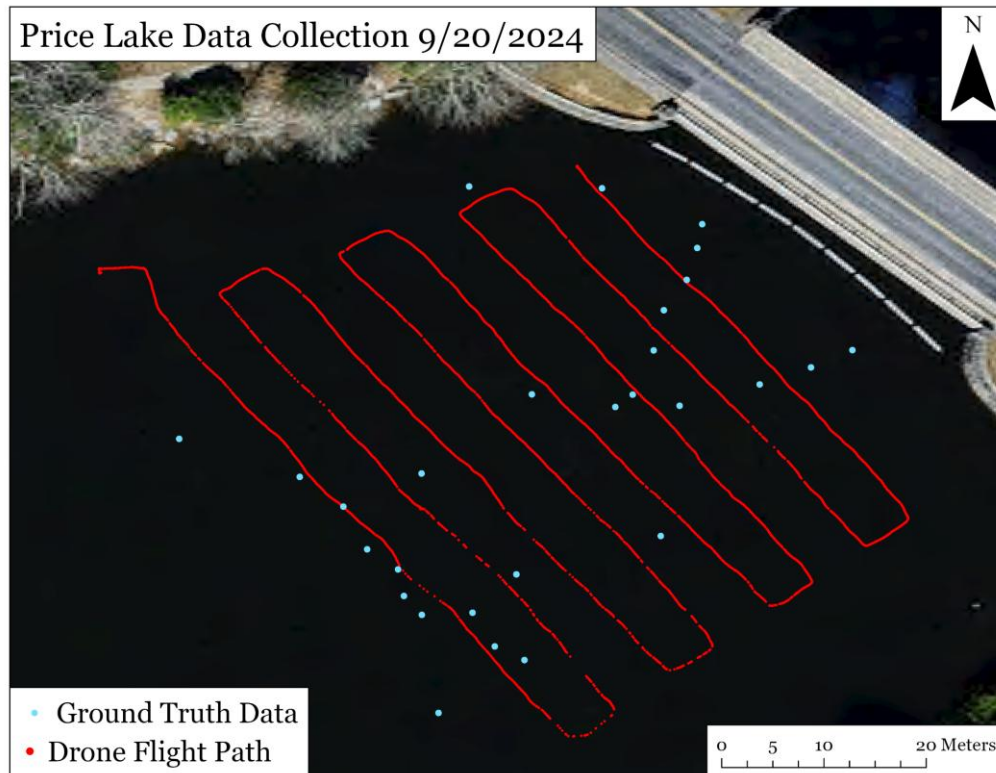


**Figure 74: Map of collected data points.**

#### **Data Processing:**

The raw sonar data was processed in Hydromagic again, and the echogram displayed none of the errors we were witnessing in the field, likely because they were being automatically removed by the software. The processed soundings were then brought into ArcGIS to be interpolated into a bathymetric map and a 3D model as shown in Figure 73, this was done the same as with the Rhodhiss Lake case study.



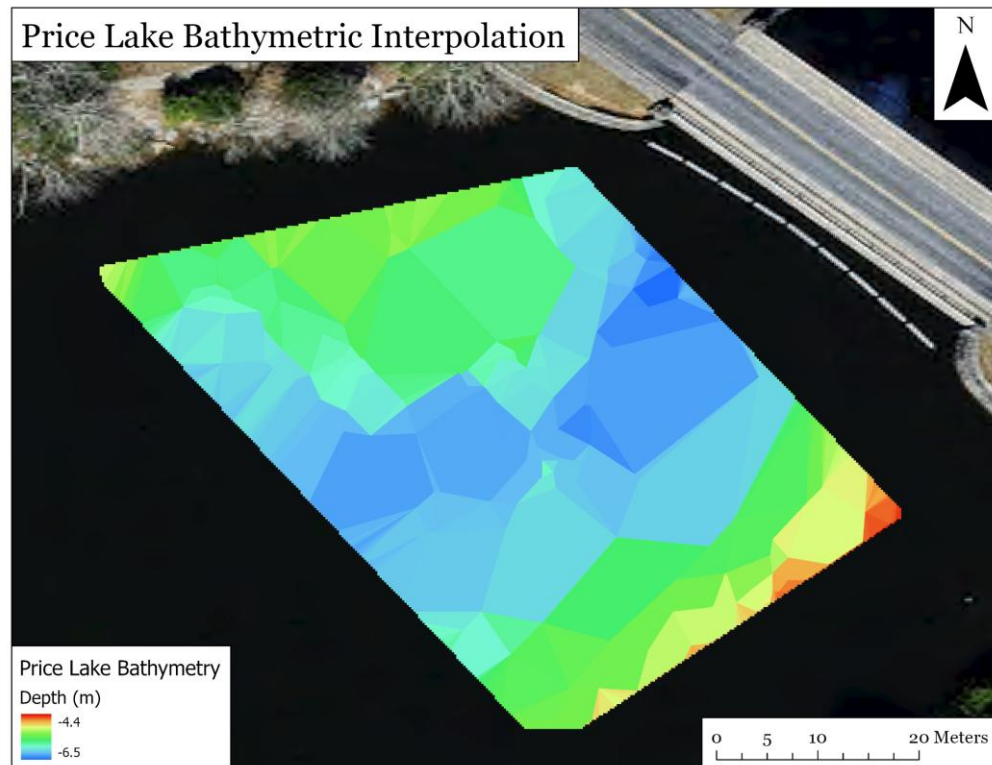


**Figure 75: Price Lake bathymetric map**

#### **Accuracy Assessment:**

Once the interpolated map was created, the ground truth points were used to extract cell values to compare against. The values were then used to calculate an R-squared value as well as the RMSE. The values of this flight were not nearly as accurate as those from Rhodhiss lake, with the R-squared being 0.5 compared to 0.9 for Rhodhiss as shown in Figure 74. This was a disappointing result but can likely be attributed to several factors. Changing from a rod to the tape, while it increased the speed of point collection, sacrificed the anchoring effect that the rod had. We also believe that the errors the sensor was getting were due to vegetation on the bottom that was not present at Rhodhiss. These combined to give worse results than we saw in the Rhodhiss Lake case study.

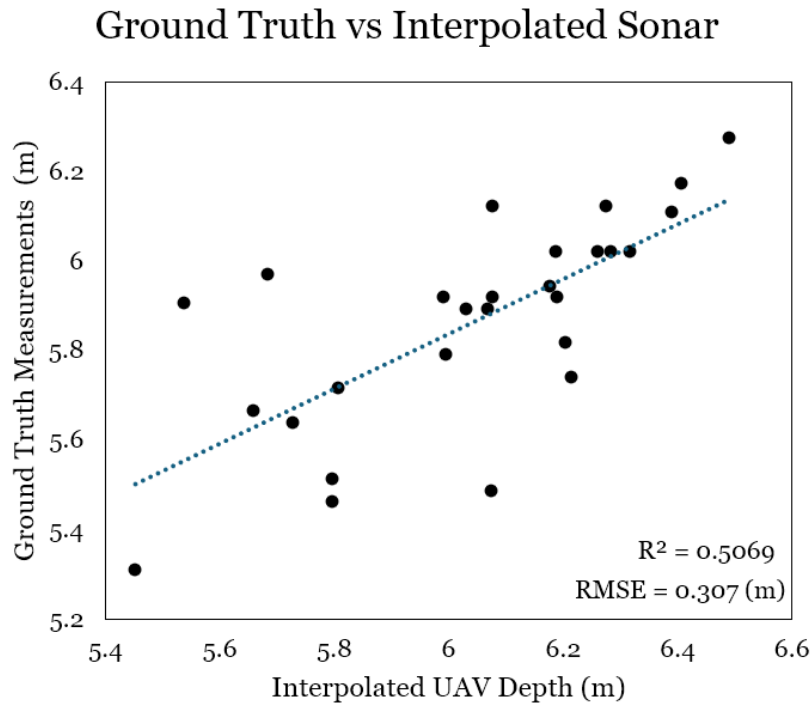


**Figure 76: Accuracy assessment**

### 3D Visualization:

The visualization was done the same as previously, with the raster being converted to a TIN to then be represented in 3D. Unlike with Rhodhiss, there was no cellular reception, and we could not fly the RTK Phantom to collect imagery to be used for SfM, which is why it is just the depth map (Figure 21).

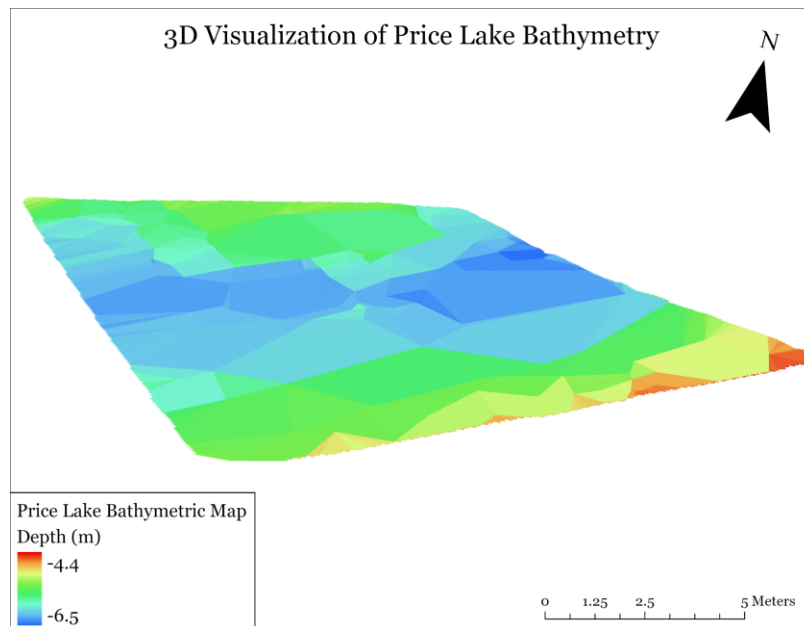


**Figure 77: 3D Visualization**

### **Return Study:**

Due to closures of the parkway following Hurricane Helene, the team was unable to return to collect more data. We anticipated going this year to collect more data, but after the administration change, we were unable to secure permits for a flight.

## **Findings and Conclusions**

The Ward Mill Dam study highlights the effectiveness of Unmanned Aerial System (UAS)-based Structure-from-Motion (SfM) photogrammetry for topo-bathymetric surveying, demonstrating a strong correlation with observed data when appropriate linear corrections are applied. However, as water depth, aeration, and turbidity increase, noise becomes more apparent in the model, especially under whitewater conditions, where the water surface is often represented as the lowest elevation. The bilinear filtering method used to reduce noise proved effective, though it tended to overly smooth the streambed profile, suggesting the need for further research to identify an optimal filtering technique. The study also suggests that incorporating a denser network of observed cross-sections in future surveys would enhance model accuracy and provide better insight into influencing variables. While the linear correction method significantly improved accuracy, further exploration is needed to refine the effects of refraction, with the potential implementation of a cell-wise correction model to reduce RMSE and enhance bathymetric precision. Overall, this method shows considerable potential for rapid and accurate storm damage assessments in drainage systems, establishing its viability as a tool for post-disaster analysis.

The data collection at Rhodhiss Lake near Huffman Bridge marked significant progress in the application of UAV-based sonar systems for bathymetric surveying and bridge scour monitoring. The team successfully utilized the Matrice 600 Pro UAV equipped with the SPH ECT 400S echo sounder to collect bathymetric data from the lake bed. The data collection protocol, refined through several test flights, demonstrated promising results in terms of accuracy, with an  $R^2$  value of 0.90 and an RMSE of 0.53 meters. This high correlation between UAV-collected data and ground-truth measurements suggests the UAV-based sonar system is effective for monitoring bathymetric changes and can be a valuable tool for bridge scour assessment.

When compared to traditional bridge inspection methods, the UAV system provided a much more detailed data set. Although there were some discrepancies between the two data sets — potentially due to sensor penetration, vegetation interference, and interpolation errors — the UAV system still demonstrated a clear advantage in terms of providing more precise and extensive data. Further investigation is needed to understand and address these differences for more accurate results.

The post-Hurricane Helene data collection revealed changes in the lake's bathymetry, with noticeable erosion and deposition around the bridge. The use of 3D visualization allowed for clearer insights into the spatial extent of these changes, showing up to 5.4 meters of erosion in some areas. This capability to detect post-disaster changes is one of the significant advantages of UAV-based sonar systems, offering rapid and accurate assessments for post-disaster monitoring.

At Price Lake, the results were less favorable, with a lower R-squared value of 0.5, indicating a decrease in accuracy compared to Rhodhiss Lake. The use of a cloth measuring tape instead of a rod and the presence of bottom vegetation likely contributed to the lower precision. Despite these challenges, the process of collecting and processing sonar data, followed by interpolation and 3D visualization, was similar to that used for Rhodhiss Lake, demonstrating that the UAV-based method is adaptable across different sites.

In conclusion, the study demonstrates the significant potential of UAV-based sonar systems for bathymetric data collection, offering detailed, accurate, and efficient mapping for both pre- and post-disaster monitoring. Future improvements in sensor calibration, data collection protocols, and error reduction techniques are necessary to enhance the system's precision and reliability in diverse environments, such as Price Lake.

## Recommendations

To improve bathymetric surveying accuracy, the filtering process should be enhanced to reduce noise and smoothing effects, especially in areas with rapid elevation changes and under whitewater conditions. Alternative interpolation methods beyond bilinear filtering should be explored to better capture streambed variability and reduce RMSE. Additionally, incorporating a denser network of observed cross-sections would enhance the accuracy of Structure-from-Motion (SfM) models and provide more detailed insights into streambed composition and dynamics.

Refining the UAV-based sonar system's performance is essential to improve data consistency and accuracy. Investigating discrepancies between UAV-based sonar data and traditional survey results, particularly sensor penetration, vegetation interference, and misalignments in interpolation, would help address potential sources of error. Optimizing flight parameters, such as altitude and speed, can minimize data gaps and improve spatial resolution in complex streambed environments. Testing different sonar frequencies or multi-frequency sonar systems may also help mitigate data loss in high-turbidity or shallow areas.

A more robust calibration and correction framework should be developed to further enhance accuracy. Implementing a cell-wise correction model to account for varying refraction effects across different water depths and streambed compositions would improve data reliability.

Establishing a standardized calibration protocol for UAV-based sonar systems would also ensure greater consistency and accuracy across different study sites.

Post-disaster monitoring and change detection could benefit from more frequent data collection in high-risk areas, which would establish a more detailed baseline for comparison after extreme weather events. Automating change detection processes within ArcGIS Pro would expedite the analysis of post-disaster erosion and deposition patterns, allowing for more rapid response and decision-making. Enhancing 3D visualization techniques by incorporating oblique imagery and integrating multi-sensor data would improve model accuracy and interpretability, especially for post-disaster assessments.

Surveying methods should be adapted to challenging conditions, such as those encountered at Price Lake. Returning to the rod-based method for ground-truth measurements would likely improve consistency and accuracy compared to the cloth measuring tape used in the initial survey. Developing protocols to address sonar signal interference from vegetation and variable streambed materials would further enhance data quality. Exploring alternative data collection strategies, such as side-scan sonar or higher-resolution LiDAR, could provide more detailed mapping in vegetated or shallow waters.

Finally, expanding UAV-based surveying to additional sites would strengthen the method's validation and applicability. Conducting additional surveys at Ward Mill Dam and Rhodhiss Lake would enable long-term monitoring of geomorphic changes and validate model performance over time. Exploring new test sites with diverse hydrologic and geomorphic conditions would help evaluate the adaptability and accuracy of UAV-based sonar systems. Collaborating with local agencies and research institutions to integrate UAV-based surveying into routine water resource management and infrastructure monitoring would further enhance the utility and impact of this technology.

## Implementation and Technology Transfer Plan

The implementation and technology transfer plan will be developed in close collaboration with the State Transportation Innovation Council (StIC) to ensure that the research findings are effectively translated into practical applications. The first step involves identifying the key research products generated from this study, including bathymetric models, change detection analysis, and UAV-based surveying protocols. These products provide valuable insights into streambed geomorphology, erosion patterns, and bridge scour, which can inform infrastructure maintenance and disaster response strategies.

The primary end users within the NCDOT would include hydrology and bridge inspection teams, as well as infrastructure maintenance and disaster response units. The bathymetric models and



change detection analysis could be integrated into existing GIS platforms used for infrastructure monitoring and water resource management. For instance, bridge inspection teams could use high-resolution bathymetric data to assess bridge scour risk more accurately, while hydrology teams could apply the change detection results to improve floodplain modeling and erosion mitigation planning.

To facilitate successful implementation, targeted training programs would be necessary. Training should focus on the operation and maintenance of UAV-based sonar systems, data processing using Hydromagic and ArcGIS Pro, and interpreting bathymetric and change detection outputs. Additionally, training sessions on calibration procedures and quality control measures would ensure consistent and accurate data collection. Cross-functional training involving both hydrology and bridge inspection teams would foster a more integrated approach to infrastructure monitoring and risk assessment.

Preliminary return on investment (ROI) and cost-benefit estimates indicate that adopting UAV-based bathymetric surveying could substantially reduce operational expenses and enhance overall efficiency. Unlike traditional survey methods, which are time-consuming and labor-intensive, UAV-based approaches provide a faster, more accurate, and cost-effective alternative. By decreasing the need for frequent manual inspections and improving the precision of scour risk assessments, long-term maintenance costs could be lowered, and costly infrastructure failures could be prevented. The ability to quickly perform post-disaster surveys would also strengthen disaster response efforts, minimizing downtime and repair costs. Additionally, reducing the need for manual inspections in hazardous or hard-to-reach areas would enhance worker safety by limiting exposure to dangerous conditions. The combined advantages of increased accuracy, lower labor demands, improved disaster response, and enhanced safety make UAV-based bathymetric surveying a highly beneficial investment.

## **Publications**

### **Conferences**

- Keefer, Q., O'Neill, A., Andrade, B., Shu, S. & Yu, O., "Evaluating UAV-based sonar for bathymetric monitoring: a case study of Huffman bridge on Rhodhiss lake before and after Hurricane Helene", NCGIS 2025, Winston Salem, NC, March 2025
- Keefer, Q., O'Neill, A., Andrade, B., Shu, S. & Yu, O., "Evaluating the applicability of UAV-based sonar for bridge substructure monitoring", NCDOT Symposium 2025, Raleigh, NC, February 2025
- O'Neill, A., Shu, S., & Yu, O. "*Topo-Bathymetric Modeling of High-Gradient Mountain Streams Utilizing UAS based Structure from Motion (SFM)*", American Association of Geographers, Honolulu, Hawi, April 2024.
- Shu, S., Yu, O., Platt, J., & Martin, D. "*UAV-based Monitoring of Soil Erosion Induced by Dam Removal*", American Geophysical Union Annual Meeting, San Francisco, CA, USA, December 2023.

### **Journal**

- Keefer, Q., Gibbs, L., Ekstrand, J. O'Neill, A., Platt, J., Shu, S., Yu, O., Martin, D. & Andrade, B. "Evaluating the Accuracy of UAV-Based Soil Erosion Monitoring at the Ward Mill Dam Removal Site in Valle Crucis, North Carolina", submitted to *Remote Sensing*.